AD

AD 666803

USAAVLABS TECHNICAL REPORT 67-69

PRELIMINARY DESIGN OF AN ADVANCED EXHAUST GAS DIVERTER

By

Albert Mierlet

December 1967

U. S. ARMY AVIATION MATERIEL LABORATORIES
FORT EUSTIS, VIRGINIA

CLEARINGHOUSE

Disclaimers

The findings in this report are not to be construed as an official Department of the Army position unless so designated by other authorized documents.

When Government drawings, specifications, or other data are used for any purpose other than in connection with a definitely related Government procurement operation, the United States Government thereby incurs no responsibility nor any obligation whatsoever; and the fact that the Government may have formulated, furnished, or in any way supplied the said drawings, specifications, or other data is not to be regarded by implication or otherwise as in any manner licensing the holder or any other person or corporation, or conveying any rights or permission, to manufacture, use, or sell any patented invention that may in any way be related thereto.

Trade names cited in this report do not constitute an official endorsement or approval of the use of such commercial hardware or software.

Disposition Instructions

Destroy this report when no longer needed. Do not return it to originator.

DEPARTMENT OF THE ARMY
U S ARMY AVIATION MATERIEL LABORATORIES
FORT EUSTIS. VIRGINIA 23604

This report has been reviewed by the US Army Aviation Materiel Laboratories and is considered to be technically sound.

The work was performed in order to advance the state of the art in gas generator exhaust diversion. The symmetrical butterfly valve diverter described herein is considered to represent a significant advancement in diverter technology. Weight, scaling, and growth data are offered as a tool for the designer.

Task 1M121401D14415
Contract DA 44-177-AMC-433(T)
USAAVLABS Technical Report 67-69
December 1967

PRELIMINARY DESIGN OF AN ADVANCED EXHAUST GAS DIVERTER

Final Report

By

Albert Mierlot

Prepared by

Solar Division of International Harvester Company
San Diego, California

for

U. S. ARMY AVIATION MATERIEL LABORATORIES
FORT EUSTIS, VIRGINIA

SUMMARY

The report contains results of a design study program for an advanced device for the diversion of high energy gas generator turbine discharge gases. Numerous concepts of such devices were initiated during the preliminary period. Evaluation of these concepts resulted in the selection of two design approaches for further design studies. One design, a basic butterfly valve, embodies significant improvements over the current type. The second design represents a unique concept which uses a rotating elbow enclosed within a housing to achieve gas flow diversion. An analysis and comparison of the two designs brought about the selection of the butterfly approach for the preparation of a final design and for the preparation of manufacturing drawings. A manufacturing plan describing the processes and methods which would be required to fabricate a prototype version of the butterfly valve is included.

TABLE OF CONTENTS

TABLE OF CONTENTS (Cont)

Page

LIST OF ILLUSTRATIONS

LIST OF ILLUSTRATIONS (Cont)

LIST OF ILLUSTRATIONS (Cont)

LIST OF TABLES

I. INTRODUCTION

In September 1966 the Solar Division of International Harvester was awarded a contract (DA 44-177-AMC-433(T)) by the U.S. Army Aviation Materiel Laboratories (USAAVLABS) at Fort Eustis, Virginia, to conduct a program for the design and analysis of an advanced device for the diversion of high energy gas generator, turbine discharge gases. The objective of the program was to analyze the performance, mechanics, fabrication, installation, and reliability of an advanced diverter concept to permit evaluation of its acceptability for full-scale fabrication and testing.

This report presents the final results of the above program and outlines the accomplishments of the work done in the four phases into which the program was separated.

The program activities were separated into four phases:

- Phase I - Preparation of Conceptual Designs

- Phase II - Design Analysis and Selection

- Phase III - Mechanical Design

- Phase IV - Technology Demonstration Requirements

During Phase I, initial design activities of a general exploratory nature

- Revealed critical design factors.

- Established conceptual design schemes.

- Determined the best overall configuration.

During this period, numerous concepts of diverting devices were conceived based on the three basic schemes depicted in Figure 1.

The initial design studies produced two diverter valve schemes (Figures 2 and 3). Each design has separate and distinctive features. A symmetrical configuration of a butterfly valve diverter (Figure 2) embodies the following significant advantages:

- Low pressure drop

- Efficient valve sealing

- Low cost

- Reduced complexity

The significant advantage of the rotating elbow diverter (Figure 3) is its extremely low pressure drop.

Figure 1. Diverting Devices; Three Basic Schemes.

MATL: L-605

TITANIUM ALLOY (6 AL 4V)

SECT M-M

SECT L-L

COOLING AIR

CHEM-MILL ? .03
FROM .10 STOCK
MATL: RENE 41

BELLOWS SEAL (
BEARING INSERT
MATL: RENE 41

COPPER ALLOY
COOLING FINS

TITANIUM CARBIDE
BEARING INSERT

SEALING FACES

SECT M-M

COOLING

SADDLE (.010 STK.)
MATL: RENE 41
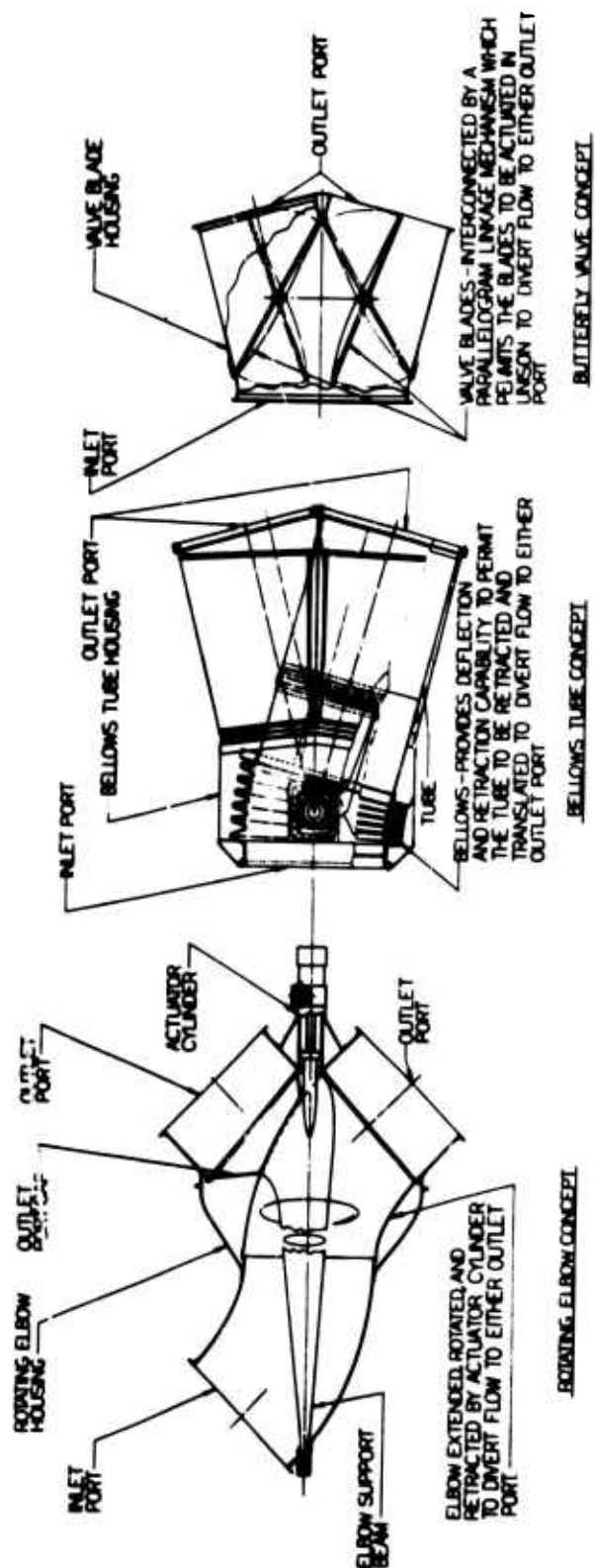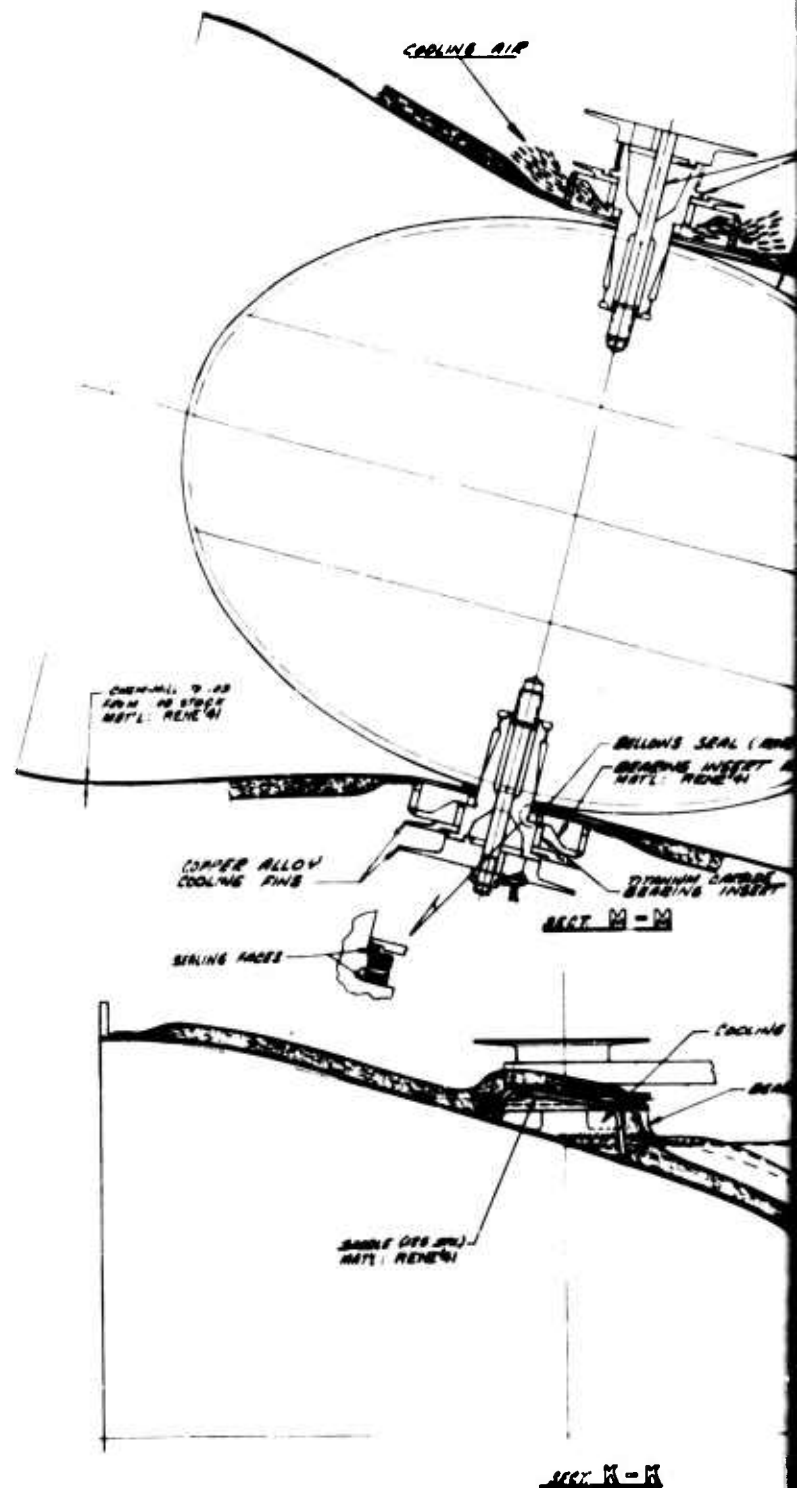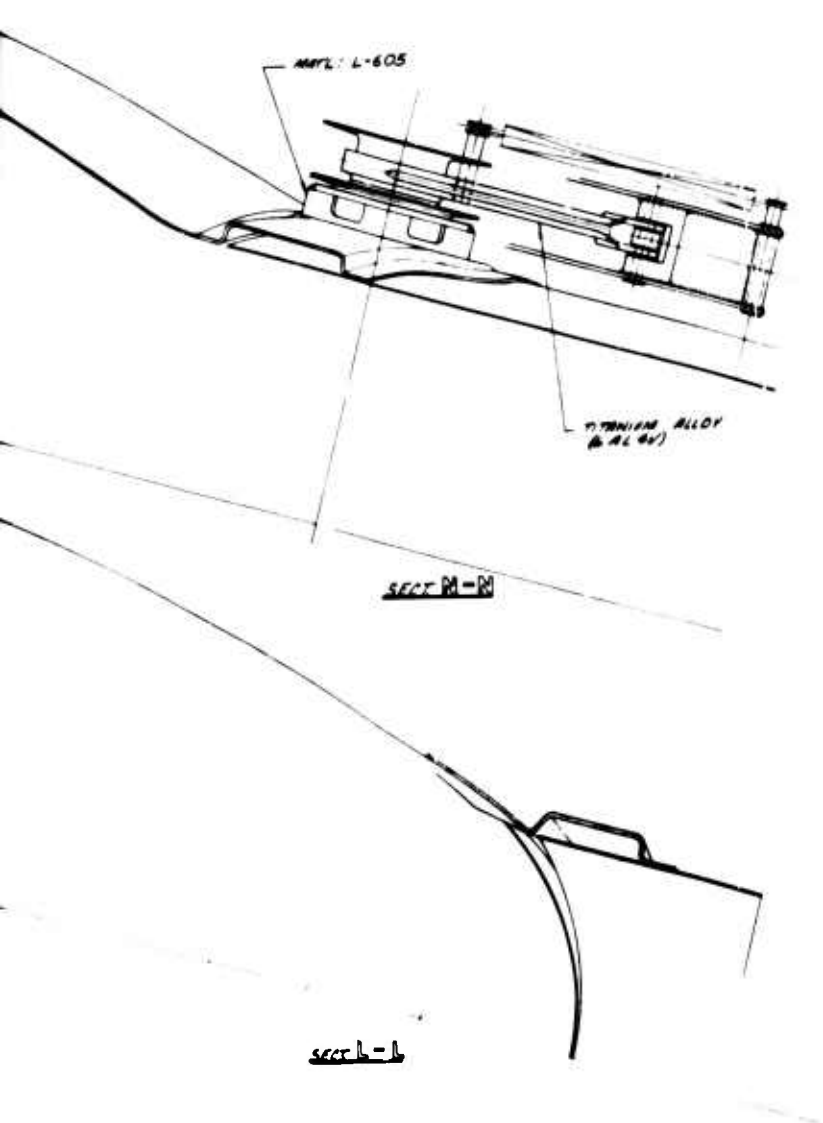
SECT K-K

Figure 2. Diverter Valve; Symmetrical Double Butterfly.

3

A

COOLING AIR

MONEL 713 C (LOW HARD)

BUTTERFLY BLADE
FOR DET. SEE
DWG 'B' 51363

BELLOWS SEAL (RENE '41)
BEARING INSERT N78
MAT'L RENE '41

.03 STOCK
MAT'L RENE' 41

ER ALLOY
NG PINS

TITANIUM CARBIDE
BEARING INSERT

HOLES

SECT M - M

COOLING AIR HOLES

BEARING SUPPORT HUB

SADDLE (TD NI)
MAT'L RENE'41
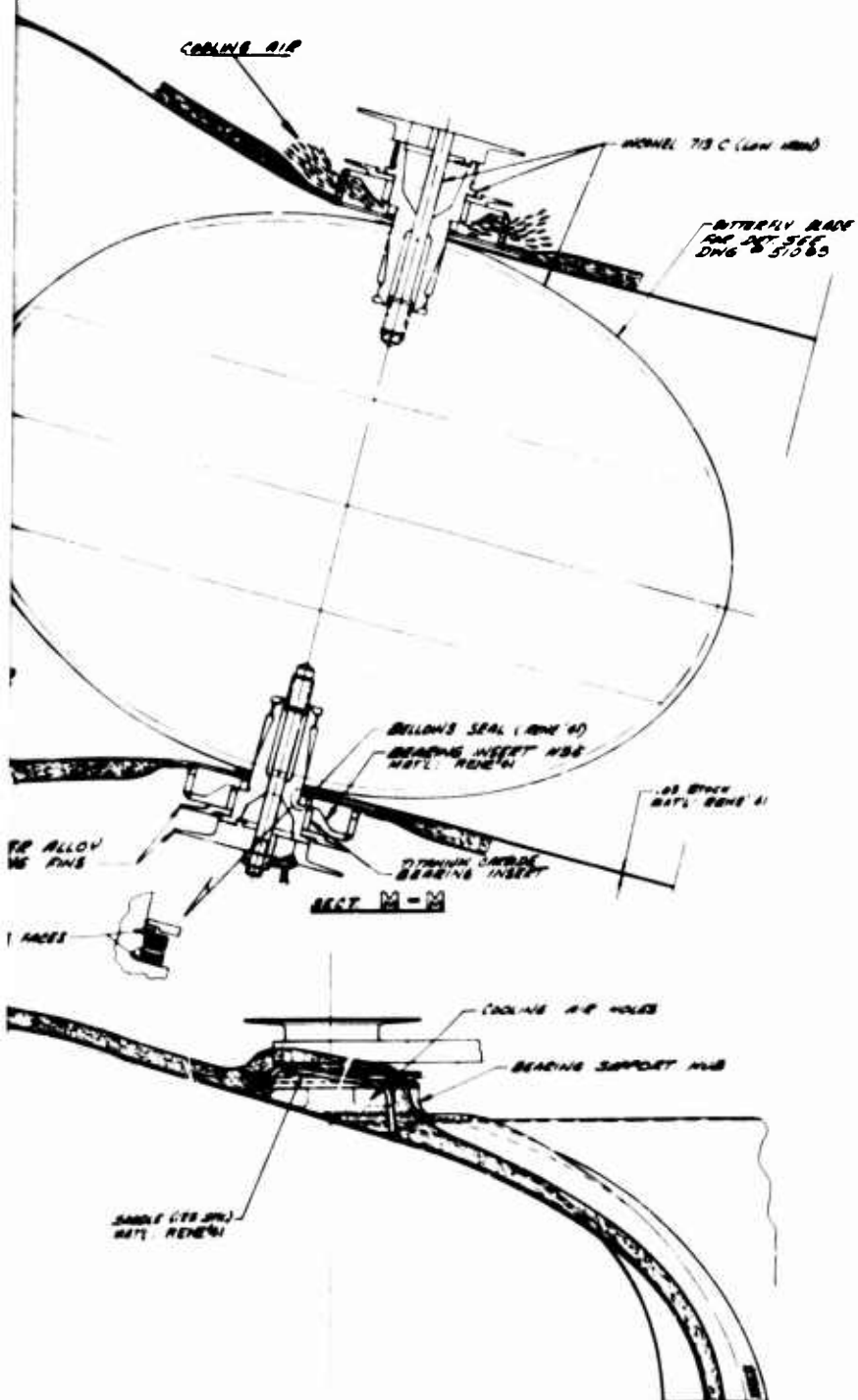
SECT K - K

SECT J - J

SECT G - G

SECT H - H

SECT F - F

B

SECT E - E

SECT B - B

SECT G - G

SECT D - D

SECT C - C

SECT F - F

SECT A - A

INSULATION
FIBRE GLASS OR
EQUIV

.002 THICK GLASS
STAINLESS STEEL

A B C D

A B C D

C

VIEW P-P

.002 THICK BRASS DIAPHRAGM
STAINLESS STEEL FOIL

A B   C   D   E   F

S1086 ACTUATOR

D
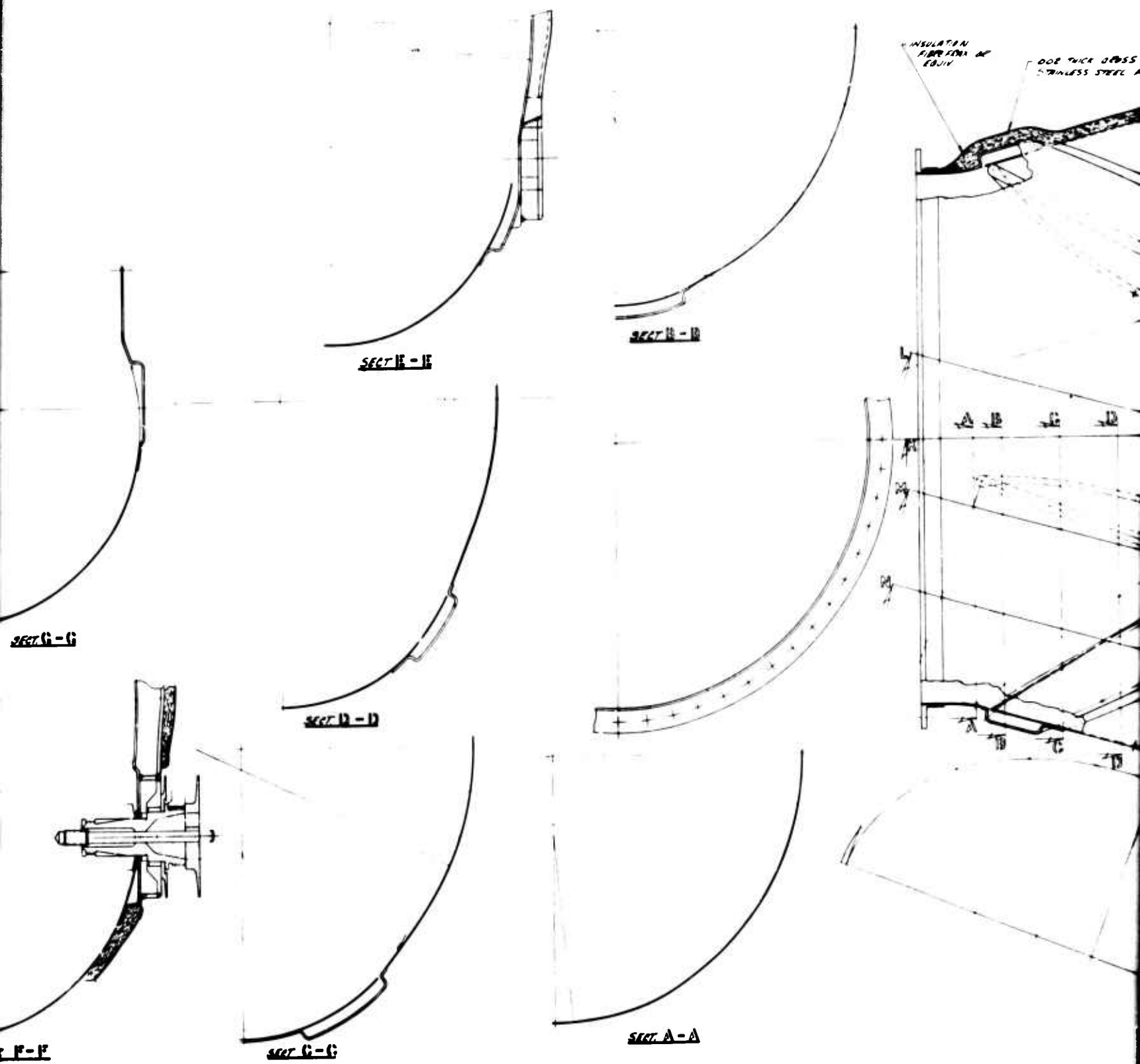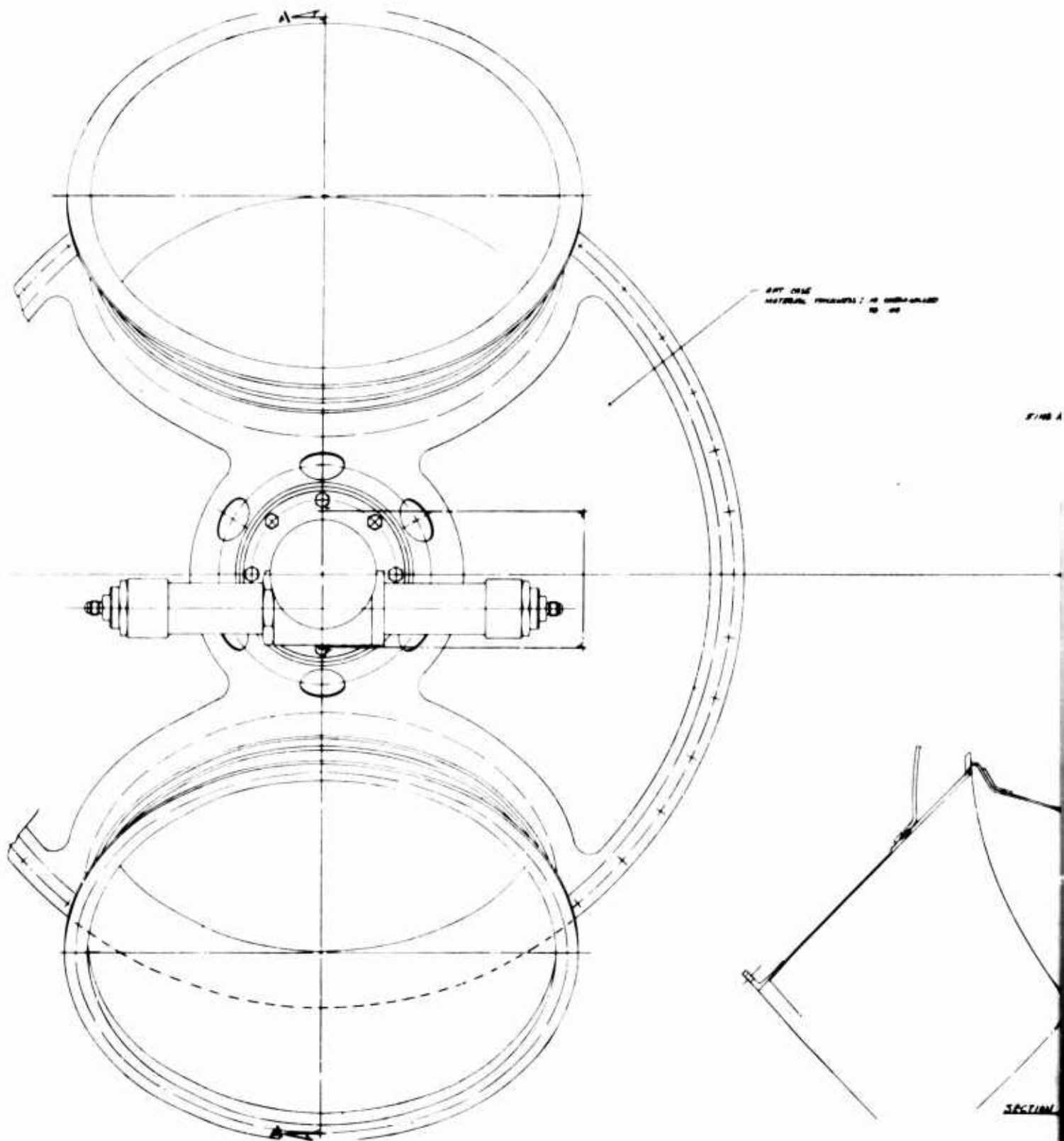
Figure 3.   Rotating Elbow Diverter Valve.

5

WT PISTON RING SEAL

ACTUATOR HOUSING

ACTUATOR SHAFT

FINAL ACTUATOR ASSEMBLY

JOURNAL & BEARING
MATERIAL TITANIUM CARBIDE

EXTENSION SHAFT

PRESSURE BULKHEAD
MATERIAL THICKNESS .07

OUTLET
MATERIAL

SECTION (3-3)

B

SECTION C-C
TYPICAL CROSS-SECTION
OF SPLITTER BEAM

SECTION B-B

SP3 BE 1N 1/4 25 BOLT
SP3 FN 1416 NUT

SPLITTER BEAM
MATERIAL .08 SHEET

C

C

D

B

INLET

FWD ELBOW
MATERIAL THICKNESS .03

DIVERTER CASE
MATERIAL THICKNESS .03

ROTATING ELBOW
MATERIAL THICKNESS .03

CLOSURE CAP

INSULATION

INLET FLANGE

OUTLET TUBE
MATERIAL THICKNESS .04 CHEM-MILLED TO
.03 IN LOCAL AREAS

NOTES:
1 ALL MATERIAL BEING 61 INCONEL

SECTION A-A

SECTION C-C
TYPICAL CROSS-SECTION
OF SPLITTER BEAM

SECTION B-B

SPLITTER BEAM
MATERIAL OD SHEET

C

C

SEAL PLATE

FLOATING PISTON RING CAGE

FWD BEARING
MATERIAL: TITANIUM CARBIDE

B

BEARING HOUSING
MATERIAL: 713 C STAINLESS STEEL

B

INLET

NOTES:
1. ALL MATERIAL RENE' 41 UNLESS NOTED

FWD ELBOW
MATERIAL THICKNESS .03

DIVERTER CASE
MATERIAL THICKNESS .03

ROTATING ELBOW
MATERIAL THICKNESS .03

CLOSURE CAP

INSULATION

INLET FLANGE

SECTION A-A

D

The evolution of the butterfly valve and the rotating elbow diverter schemes into final preliminary design and drawings to permit the initiation of Phase II Design Analysis and Selection is dicsussed in Section III.

Phase II consisted of a design analysis of the two diverter valve schemes to establish their aerodynamic, thermodynamic, and mechanical characteristics. The results and information are presented in Section IV. Based on the design analysis and an engineering conference with Solar and USAAVLABS personnel, the butterfly valve diverter (Figure 2) was selected for Phase III activities.

The rotating elbow diverter valve was not selected because:

- The actuation system was extremely complex and did not represent a functional design. Additional effort would have been required to complete and simplify its design.

- It would be a difficult and costly item to produce even if the actuation system could have been simplified.

- The through-flow loss was greater than that of the butterfly.

- The installation envelope did not appear to be compatible with the contemplated schemes for installation of exhaust gas diverting systems into VTOL vehicles.

Although the rotating elbow design had these undesirable features, the overall design concept represents an advancement in the state of the art. Considering the unique quality of design and the relatively short period in which it was conceived, it is felt that significant progress was made. Unfortunately, because of limited time, it was not possible to fully explore other mechanical arrangements to overcome the undesirable features described above.

Phase III, Mechanical Design, consisted of the activities associated with accomplishing the detail mechanical design and the supporting structural and aerodynamic analysis of the butterfly valve selected in Phase II. Phase III activities are presented in Section V.

Phase IV, Technology Demonstration Requirements, consists of a manufacturing plan describing how a prototype version of the butterfly valve will be produced. The plan defines the significant processes to be used for the fabrication and assembly of the diverter valve assembly.

7

II. DESIGN REQUIREMENTS

The diverter valve was designed to accept the exhaust gas flow of a gas turbine engine and either direct it aft 15 degrees above the horizontal axial center line of the engine or divert it 90 degrees from the aft flow outlet port. It will be designed to obtain other required design considerations including minimum weight, minimum complexity, a small space envelope, and maximum reliability. The specific requirements used in establishing the detailed design of the valve are:

- Exhaust gas flow: 70 lb/sec

- Exhaust gas temperature: 1400°F

- Total gas pressure: 60 psia

- Exhaust gas flow exit velocity: Mach 0.35 in the aft or diverted flow position

- Minimum exhaust gas pressure loss in the aft and diverted flow position

- Gas leakage through valve blade seal and hubs to be minimum possible and no greater than 1 percent of total gas flow.

- The transition from aft flow to diverted flow, or vice versa, to be less than 1 second.

- The transition from aft flow to diverted flow, or vice versa, to minimize pressure changes or surge which is detrimental to the gas turbine operation.

8

III. PHASE I - CONCEPTUAL DESIGN AND ANALYSIS

3.1 CONCEPTUAL DESIGN STUDIES

3.1.1 Butterfly Valve Diverter

Two variations of this type of diverter were investigated. One consisted of a curved elbow with a straight section of duct extending from the outer periphery of the elbow (Figure 4). The second approach (Figure 2) consisted of a Y-shaped body with two straight symmetrical branches. The significant advantages of the Y-design are reduced complexity and cost because:

- The valve blades are identical.

- The Y-body is comprised of identical halves, thus minimizing tooling.

- The straight branches are simple cylinders.

- The cylindrical valve blade seals should conform more readily to the valve blade than the double-curve seal used in the elbow design.

The primary valve structure is comprised of a main Y-shaped body made from identical halves welded together. Integrally formed into the Y-body is a U-shaped section to:

- Provide a cavity into which the valve seal is displaced when contacted by the valve.

- Reinforce the Y-body to maintain its shape while pressurized.

Straight tubular sections, inserted into each branch of the Y, protrude into the U-shaped section and perform the function of valve blade seals.

Bolting flanges have been provided at the inlet and outlet ends of the valve.

The valve blade, shown in Figure 2, has a symmetrical elliptical shape reinforced with ribs which are parallel to the gas flow. The symmetrical feature allows the blade to be used in either branch of the Y.

The valve blade pivot and bearing support housing are shown in Figure 2. To reduce the bearing temperature, air holes in the hub permit the flow of engine compartment ventilating air into the support housing. Copper alloy cooling fins dissipate the heat which is conducted through the valve shaft to the bearing area. A bellows seal minimizes leakage of hot gases from the valve interior into the bearing support housing.

The valve blades act in unison through a parallelogram, four-linkage bar arrangement. A bell crank is attached to each blade shaft. These cranks form the short sides of the parallelogram. The valve body and a connecting bar (Figure 2) form the long sides of the parallelogram. The linkage and blades are actuated by

9

changing the angle between one bell crank and the adjacent long parallelogram bar to open or close as desired. The actuator cylinder (Figure 5), designed to operate at a hydraulic pressure of 3000 psi, achieved the angle change. One end of the actuator is attached to the end of one bell crank, and the opposite end is attached to a point located in the approximate midpoint of the second bell crank. The attachment point on the bell crank was selected so that the opening torque supplied to either closed blade is 5500 inch-pounds. An overcenter spring arrangement on the linkage provides approximately 300 inch-pounds of torque to the closed blade, holding the blade against the seal when there is no hydraulic pressure on the actuator. An aerodynamic opening torque on the open blade of approximately 3200 inch-pounds during full flow is converted by the linkage into a closing torque on the blade. The total closing torque of 3500 inch-pounds (3200 plus 300) thus maintains the closed blade against the seal.

3.1.2 Bellows Tube Diverter

The lack of precedent for this type of diverter required the initial design activities to be of a general exploratory nature to:

- Reveal critical design factors.

- Establish alternate conceptual design approaches.

- Determine the best overall configuration.

This activity resulted in various bellows tube diverter approaches and several alternate approaches.

Figures 6 through 13 are schemes which evolved from the bellows tube diverter design studies. A brief description of each scheme is:

- Figure 6 - The basic bellows tube concept originally proposed with an actuating system using a retracting yoke to coordinate the upper and lower sliding pivots.

- Figure 7 - This scheme uses two sprockets mounted to the outer case with a chain drive. A pin is attached at one end to a bearing in the chain, and at the other end is attached rigidly to the diverter duct or retractable seal. The seal is retracted, the diverter duct translated, and the seal reseated by a single reversible rotary-powered drive.

- Figure 8 - This scheme uses a cam and roller arrangement to retract the duct or seal during the rotation cycle. The cam is mounted to the outer case and the roller is attached to the duct, which follows the cam slope or contour during the duct rotation cycle.

- Figure 9 - This scheme uses a retractable face seal arrangement and a fixed rotation center for the diverter tube. The face seal is retracted by a linkage arrangement originating at the fixed rotation center of the duct.

10
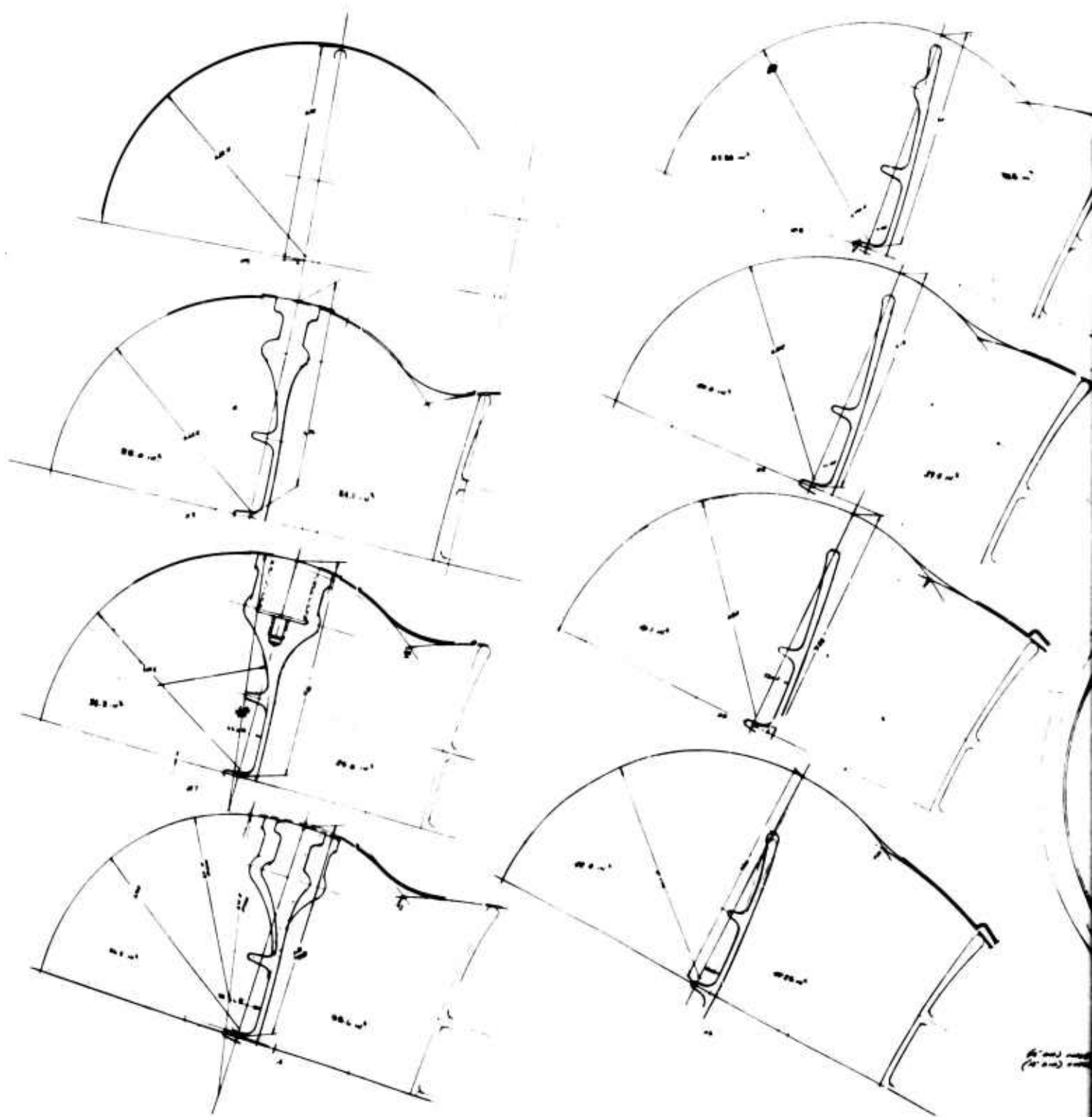
Figure 4.   Diverter Valve Nonsymmetrical Double
Butterfly.

B

Figure 5. Actuator Assembly.

- Figure 10 - This scheme uses an outer case mounted pressure capsule seal at each exit port and a fixed rotation center for the diverter tube. Compressor bleed air is used to extend the seal against the diverter seal face at the completion of the transition cycle.

- Figure 11 - This scheme uses the basic bellows tube principle; however, the bellows located at the center of rotation are replaced by an arrangement of externally pressurized bellows. This scheme eliminates the stability problem (squirm) inherent in an internally pressurized bellows. A retractable face seal arrangement similar to the one used in Figure 9 is used on this scheme.

- Figure 12 - This scheme uses a radiused diverter tube with short bellows at either end to absorb the expansion differential between the case and tube and to provide compliance at the seal ends. Diversion is obtained by rotating the tube about the inlet center line.

- Figure 13 - This scheme is similar to the one proposed in Figure 12 except that it uses a rotating Y instead of an elbow.

Figure 6. Swinging Duct Diverter - Lever Actuated.
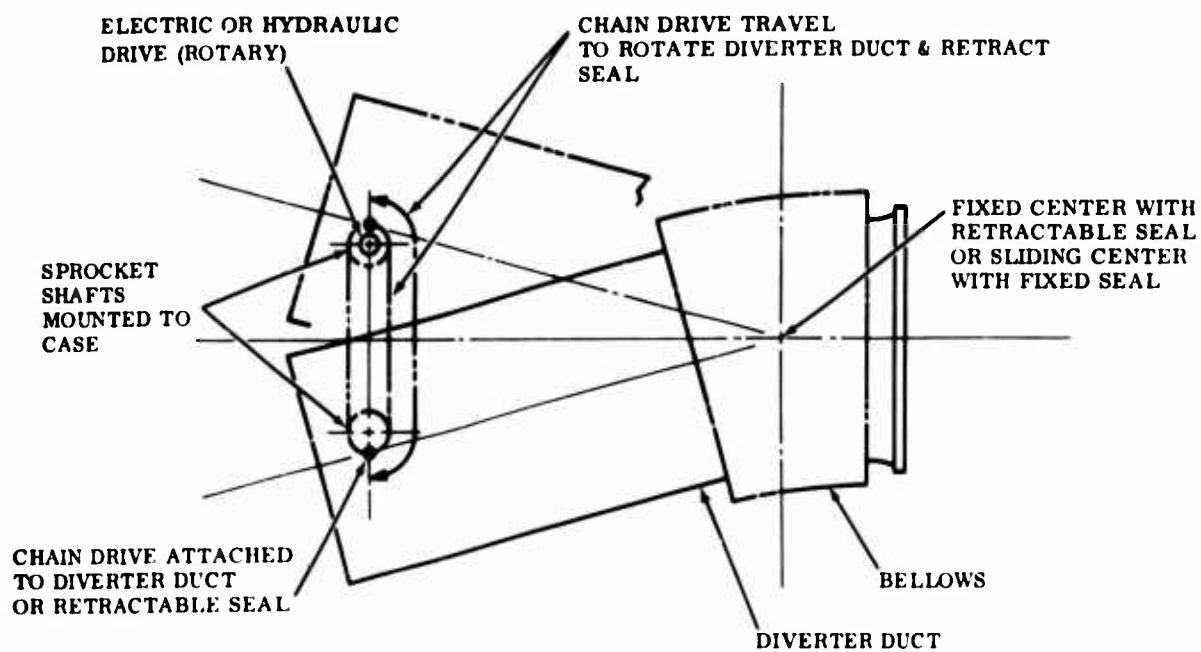
Figure 7. Swinging Duct Diverter - Chain Actuated.

14

ROLLER & CAM
TO RETRACT DIVERTER DUCT OR SEAL
DURING ROTATION CYCLE

OPERATING FORCE

SLIDING CENTER
OR FIXED CENTER
WITH RETRACTING
SEAL
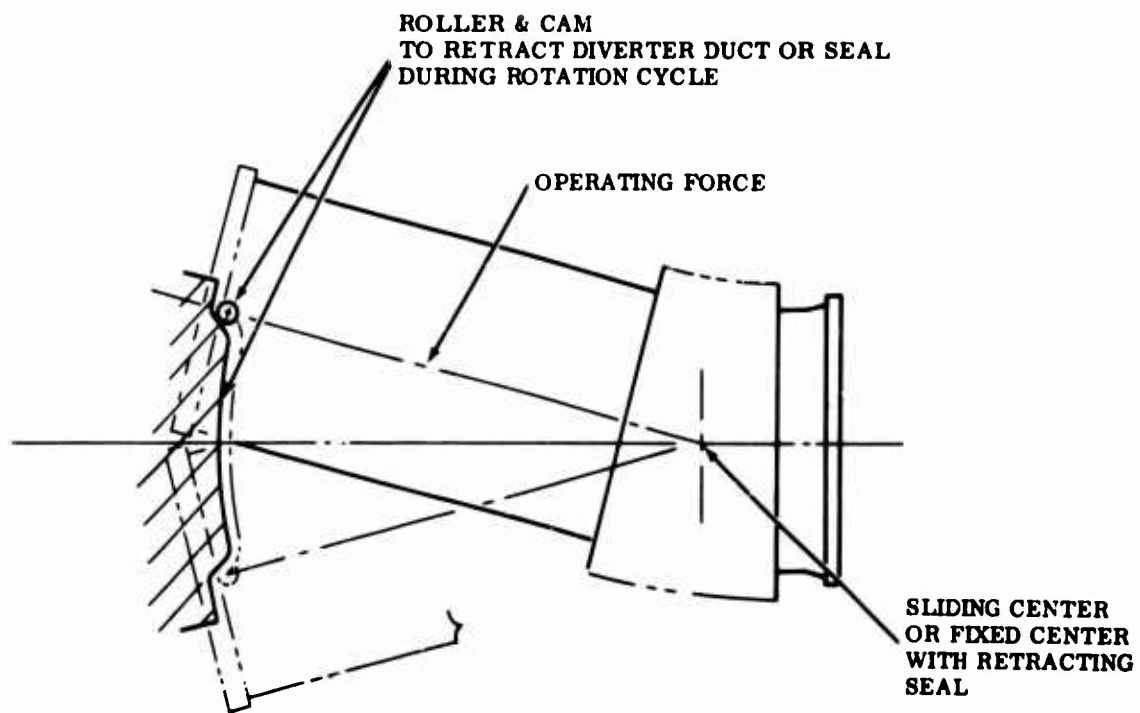
Figure 8. Swinging Duct Diverter - Cam Actuated.

RETRACT FACE SEAL
& BELLOWS

ROTATE ARM
& CYLINDER

RETRACT ARM
& CYLINDER

ROTATION
DIVERTER DUCT
(FIXED)
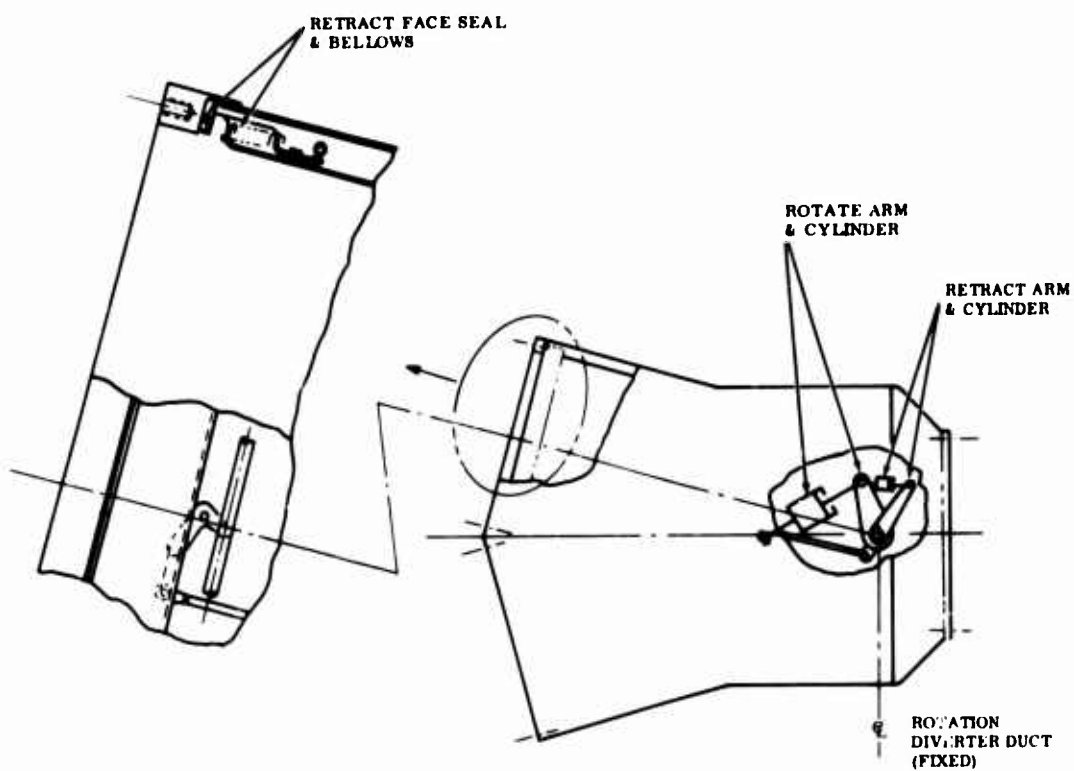
Figure 9. Retracting Bellows Seal for Diverters.

15
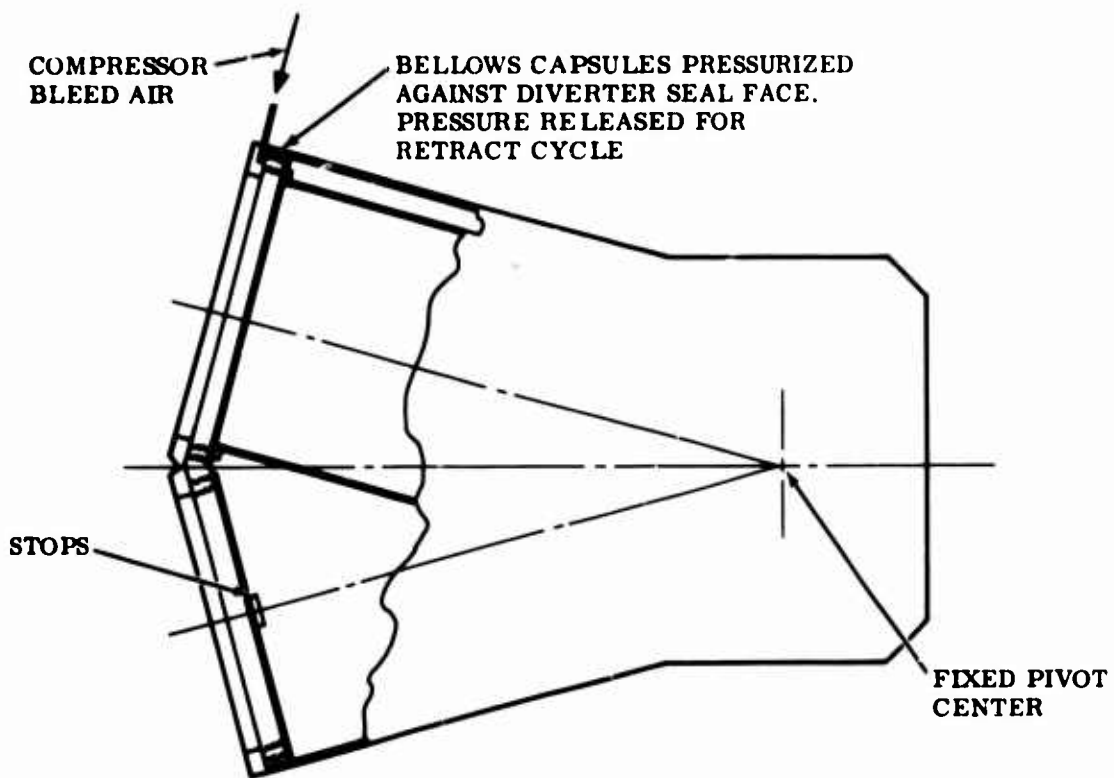
Figure 10. Expanding Bellows Seal for Diverters.
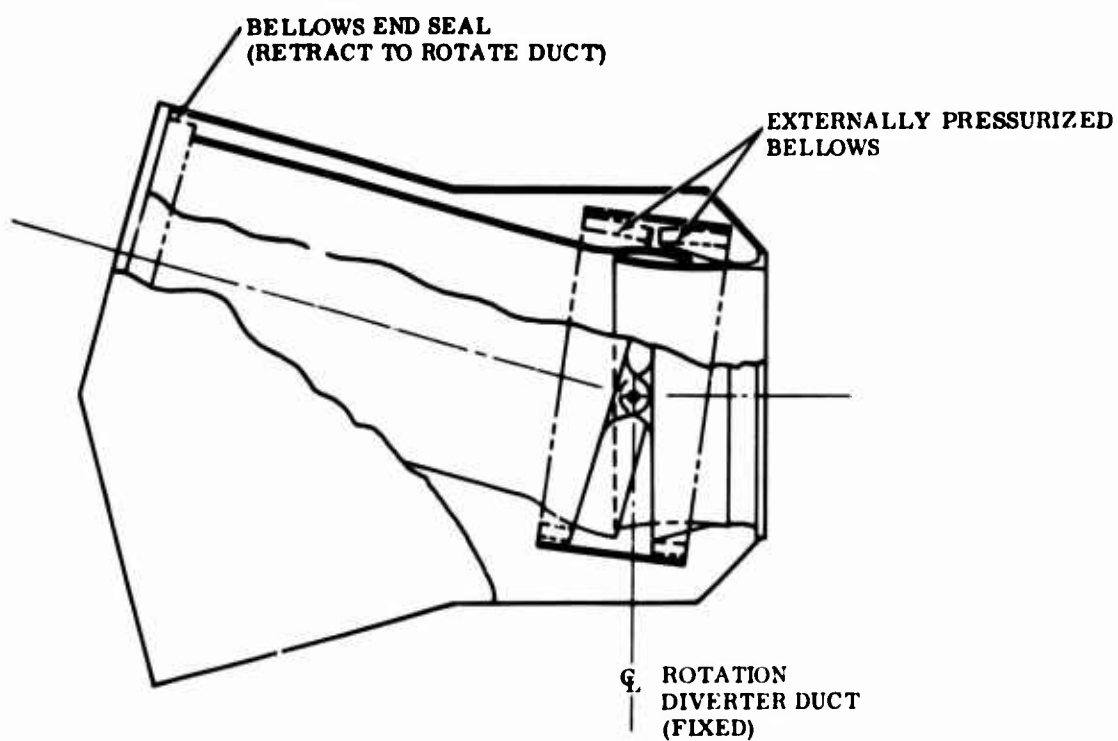
Figure 11. Swinging Duct Diverter - Externally Pressurized Bellows.

16
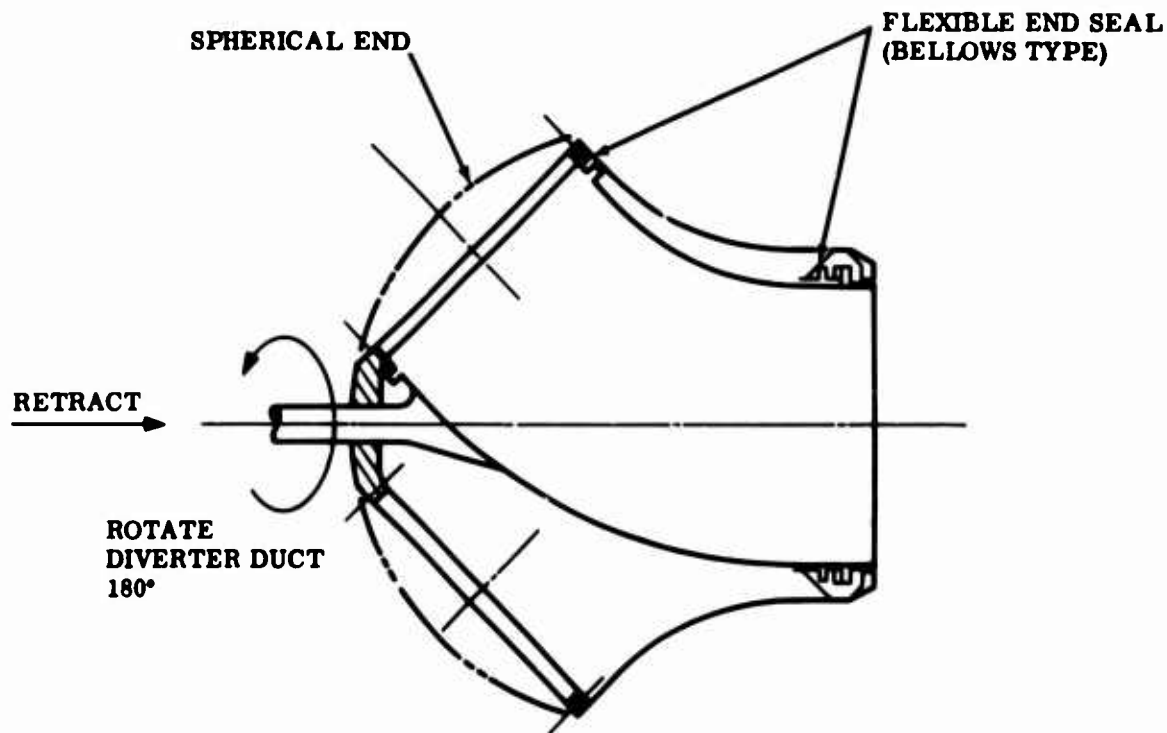
Figure 12. Rotating Elbow Diverter.

3.1.3 Rotating Elbow Diverter

The rotating duct concept evolved from the swinging duct approach and appeared to offer the following basic advantages:

- Low-pressure drop characteristics.

- Reduced loads and a minimum of concentration points.

- General overall simplicity.

- Greater flexibility for specific applications. (Angle of turn can be varied by altering overall length.)

Because of these advantages, additional studies were made to determine whether or not this approach had sufficient merit to replace the original bellows tube diverter approach.

The excellent pressure drop characteristics of this concept and the increased pay-load capability it provides appear to be so advantageous that activities were concentrated on evolving a practical configuration of this approach.

17

Figure 14 shows a preliminary design which evolved from the original concept
(Figure 12). A rotating elbow provides a 35-degree turning angle and reduces from
a 16-inch inlet diameter to a 13-inch outlet diameter to minimize the pressure drop
and outer case envelope. A support cone attached adjacent to the inlet end of the
elbow and to a bearing housing located at the outer case provides support and rota-
tional capability to the elbow. The bearing support is located outside of the high-
temperature zone and in an unpressurized and ventilated area to permit the use of
a conventional low-temperature bearing. The bearing location was selected on the
basis of the loads generated by internal pressure in accordance with the load dia-
gram shown in Figure 15.

Primary high-pressure seals are located at the inlet and outlet ends of the elbow.
The elbow is enclosed in an internal case to contain the gas which leaks past the
outlet end primary seal and during the transition period while the elbow is rotating
from one outlet port to the other. Secondary low-pressure seals are located at the
forward portion of the internal case to prevent external leakage during the transi-
tion period. The forward secondary seal is not mandatory, but eliminates over-
board leakage from the primary seal and serves as a backup in event of complete
failure of the primary seal. The outlet primary seal is retracted by a gimbal-
actuated sleeve. The gimbal is actuated by introduction of compressor pressure
bleed air into a bellows capsule. It is recognized that this particular sealing
arrangement is complex and obviously undesirable. Therefore, other sealing
arrangements are being studied and, in all probability, a simpler sealing scheme
will be evolved.

The outer case provides bolting flanges at the inlet and outlet ends of the diverter,
at the two outlet ports, and at the bearing housing support for the bearing outer
race. Holes in the outer case wall permit the flow of engine compartment ventilat-
ing air to cool the bearing.

Flow diversion is accomplished by a 130-degree rotation of the elbow about the
outer case center line and is achieved by applying power through direct gearing,
chain or cable applied, to the inner race of the bearing. The configuration
described permits the use of a rotary actuator (e.g., hydraulic or electric motor).

The diverter design (Figure 14) requires a multiplicity of seals (four) and uses a
complex seal-retracting mechanism located at the outlet end of the rotating elbow.
Since these features detracted from the basic simple principle of the rotating elbow
concept, activities were directed toward greater overall simplicity of the rotating
elbow design.

A preliminary design (Figure 3) has evolved from the design shown in Figure 14.
A forward elbow provides a complete through-flow and 90-degree diversion system.
Although this arrangement appears bulky, the elbow envelope and weight should be
attributed to a normal system installation and as such provides a system advantage,
since one bolting flange is eliminated.

The rotating elbow is supported by a central splitter beam extending through the
forward elbow. A floating piston ring cage and seal plate prevent external leakage
where the beam protrudes through the elbow. The beam end is supported by a for-
ward bearing and housing. The aft end of the beam extends outside the case between

18
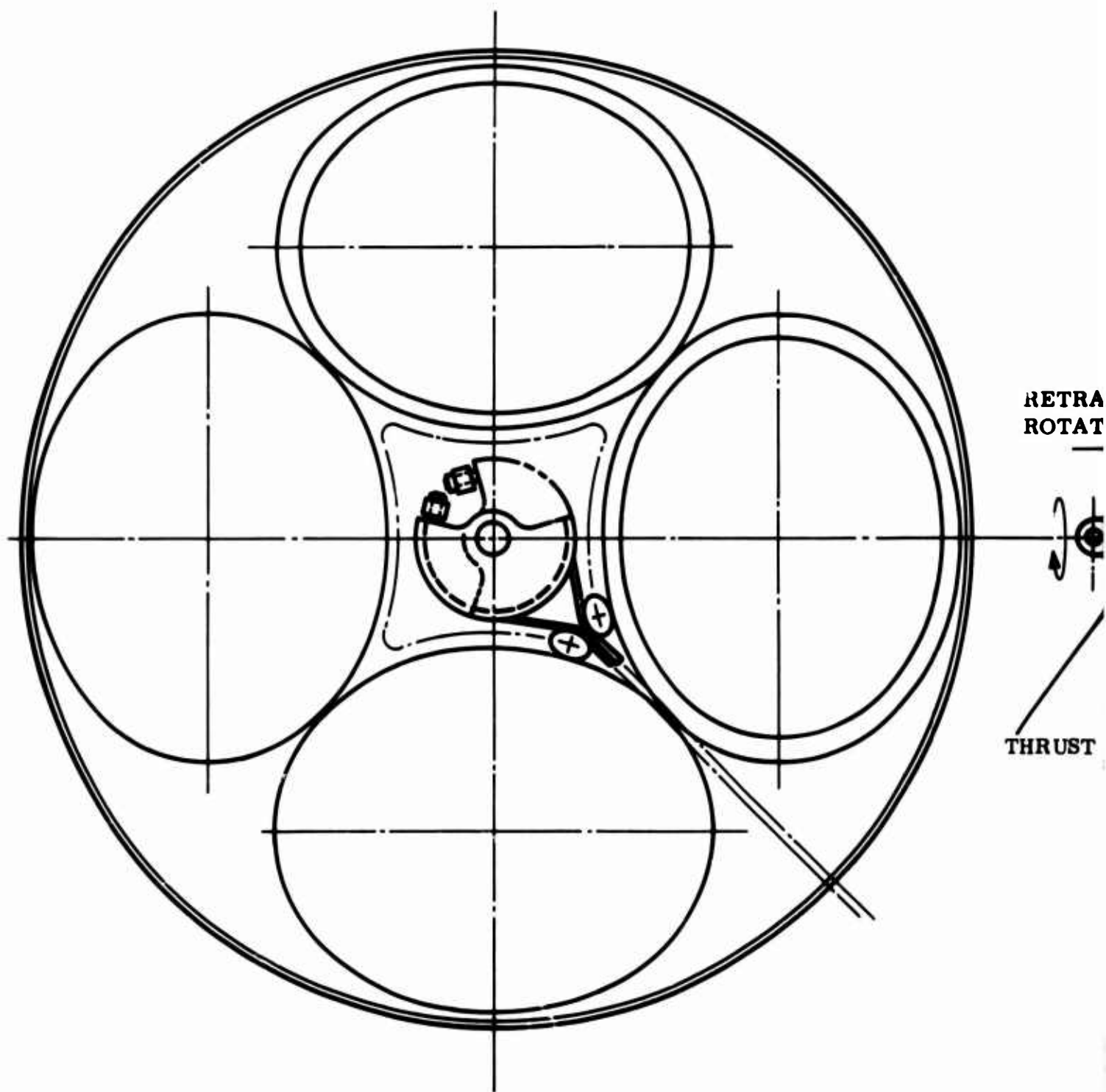
Figure 13.   Rotating Y-Duct Diverter.

BELLOWS SEALS

"Y" SECTION

RETRACT AND
ROTATE 90°

THRUST BEARING

C_L ROTATION

B

25° (2) PLACES

A

A SYM

SECTION B-B

130° (REF)
ROTATION OF ELBOW

OUTLET BOLTING FLANGE

BELLOWS ACTUATING CAPSULE

OUTLET BOLTING FLANGE

OUTLET PORT

A
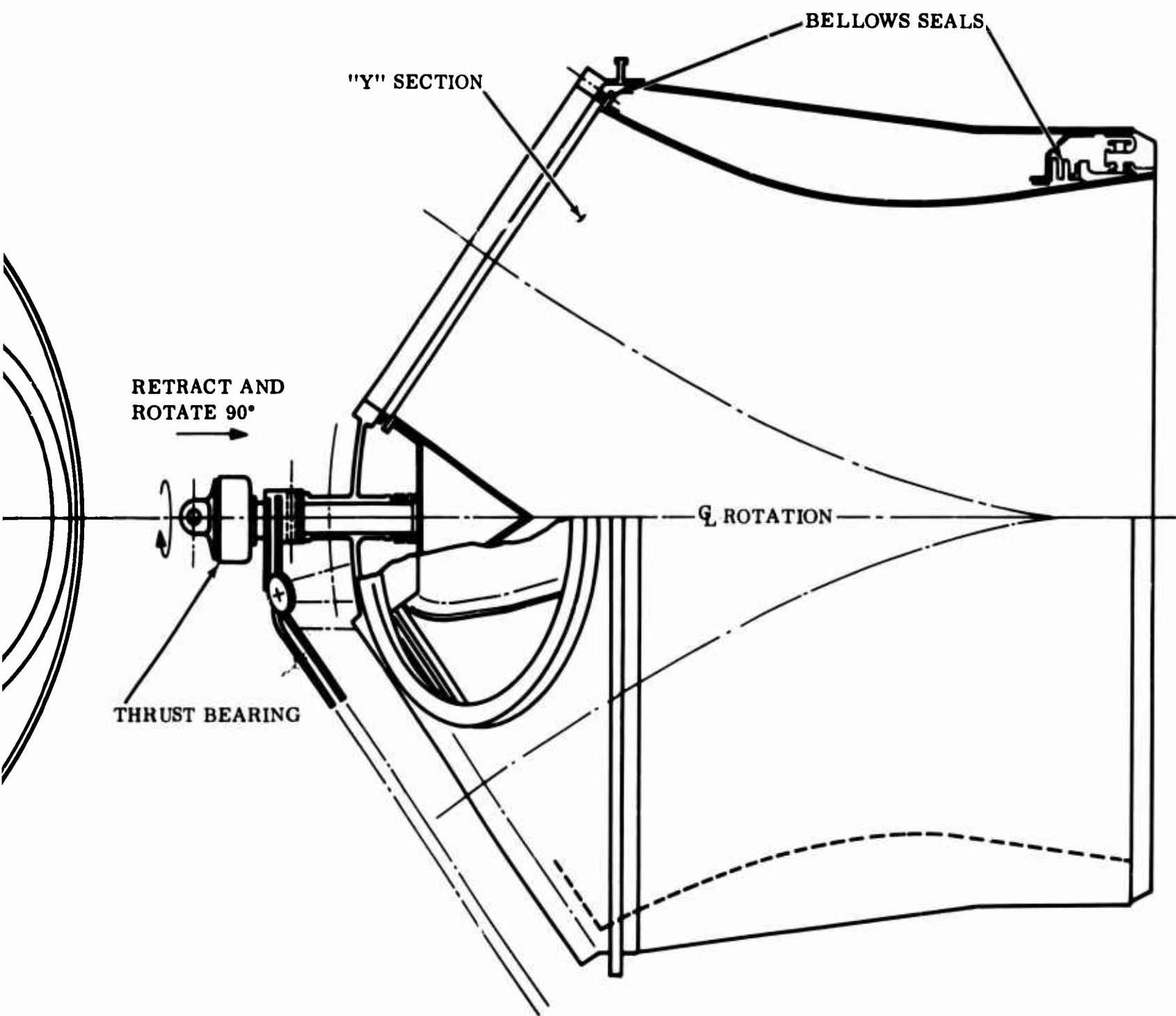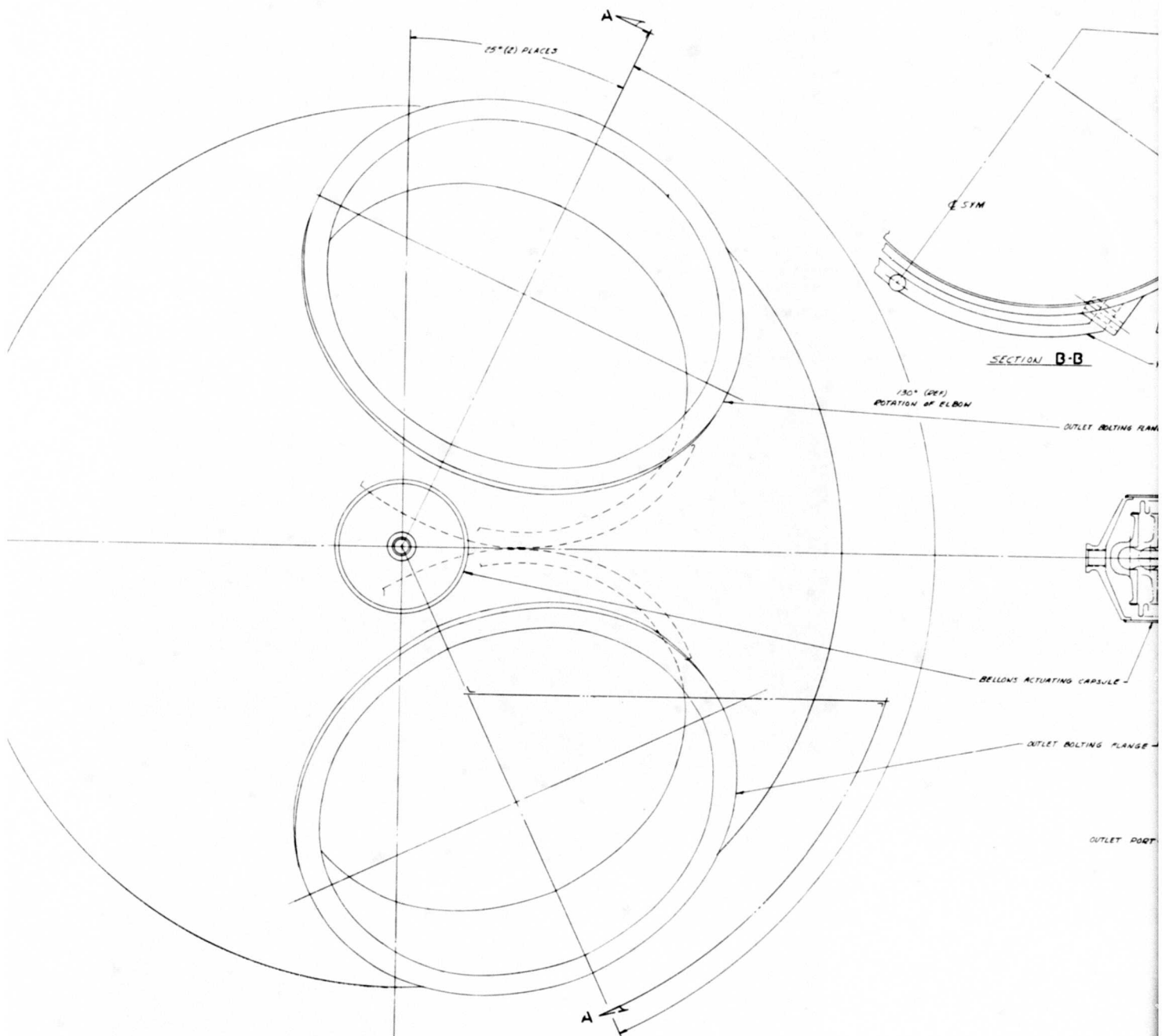
Figure 14. Rotating Elbow Diverter Valve.

21

A

OUTLET PRIMARY HIGH PRESSURE SEAL

OUTLET PRIMARY SEAL SHOWN
IN RETRACTED POSITION

SLEEVE, GIMBAL ACTUATED

GIMBAL PIVOT

BEARING HOUSING

OUTER CASE

SUPPORT

OUTLET PORT

$\mathcal{C}$ SYM

SECTION B-B

ACTUATING GIMBAL

YOKE

130° (REF)
ROTATION OF ELBOW

OUTLET BOLTING FLANGE

RETRACTED POSITION

BELLOWS ACTUATING CAPSULE

OUTLET BOLTING FLANGE

OUTLET PORT

SECTION A-A

B

OUTLET PRIMARY HIGH PRESSURE SEAL

OUTLET PRIMARY SEAL SHOWN
IN RETRACTED POSITION

SLEEVE, GIMBAL ACTUATED

GIMBAL PIVOT

BEARING HOUSING

OUTER CASE (WITH VENTILATING HOLES)

SUPPORT CONE (WITH VENTILATING HOLES)

INTERNAL CASE

ROTATING ELBOW

INSULATION

SECONDARY LOW PRESSURE SEALS

FWD SEAL

INLET BOLTING FLANGE

INLET PRIMARY HIGH PRESSURE SEAL

INLET

OUTLET PORT

RETRACTED POSITION

B

FWD

SECTION A·A

C

BLANK PAGE

Figure 15. Elbow Load Diagram.

the outlet ports. A bellows face seal at the pressure bulkhead prevents external leakage. An aft bearing located beyond the bellows seal supports the beam.

A closure cap is attached to the outside of the rotating elbow, while a port seal at the end of the cap provides a seal with the faying surface of the outlet tube flange. Capping the outlet port by the closure cap pressurizes the diverter case and allows the capped port to react the plug loads. A sealing force is obtained by the case pressure acting against the back side of the port seal.

Elbow diversion from one outlet port to the other is achieved when the splitter beam and elbow are moved in a forward direction, which disengages the port seal and transfers the plug load to the beam. After rotating 180 degrees, the elbow assembly moves in an aft direction to reengage the seal and unload the beam.

Since either edge must face the gas flow at the inlet end, the splitter beam has a symmetrical cross section (Figure 3). Presenting high length to the thickness sections in the plane of the gas flow, the slight increase in pressure drop results primarily from friction. A constant 16-inch diameter is used to the point where maximum splitter beam blockage occurs in the rotating elbow. As the blockage decreases downstream of this point, the tube diameter decreases to 15.5 inches to provide a slight diversion on the back side of the beam.

To impart the required motion cycle to the splitter beam and elbow, inclusion of a hydraulic actuator is required at the aft end of the diverter at the position indicated.

3.2 AERODYNAMIC ANALYSIS

Four different diverter valve configurations were analyzed, and their aerodynamic performance was predicted and compared. Figures 16 and 17 are the butterfly valve diverters shown in Figures 2 and 4. Figure 18 conforms to the basic bellows tube diverter originally proposed. Figure 19 is the rotating elbow approach shown in Figure 12.

The main factors considered to establish the aerodynamic quality of each configuration were:

- Total pressure loss

- Velocity gradient

- The possibility of flow separation

Conditions of flow entering any one of the four configurations were based on a mass flow of 70 pounds/second, a total pressure of 60 psia, and a temperature of 1500°F. The dynamic heads and Reynolds numbers corresponding to Mach numbers of 0.3, 0.4, and 0.5, respectively, were calculated applying compressible flow relations.

Figures 16, 17, 18, and 19 were analyzed as conforming to Figures 2, 4, 6, and 12.

Table I shows the preliminary sizing and flow conditions used in preparing the flow analysis, and Table II shows the comparison of the total pressure losses of the four configurations analyzed.

TABLE I. PRELIMINARY SIZING AND FLOW CONDITIONS				
Symbol	Units			
Mach Number	–	0.3	0.4	0.5
Area	in.^{2}	202.31	157.95	132.92
Diameter	in.	16.05	14.18	13.01
Static Pressure	psi	56.54	54.02	50.98
Static Temperature	F	1471.3	1449.6	1422.4
Static Density	lb/ft^3	0.07909	0.07642	0.07317
Velocity	ft/sec	629.9	835.1	1036.4
Dynamic Heat	psi	3.39	5.75	8.48
Reynolds Number	–	2.75×10^6	3.14×10^6	3.45×10^6
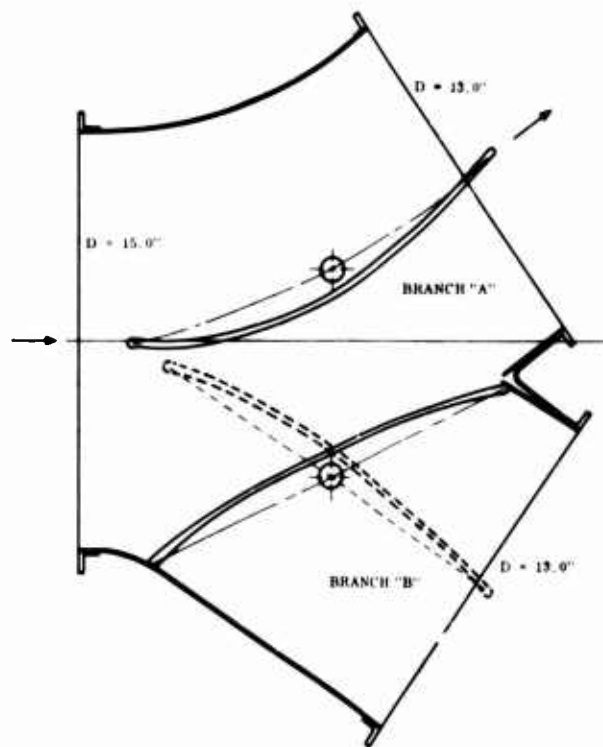
Figure 16. Butterfly Valve Diverter, Configuration A.
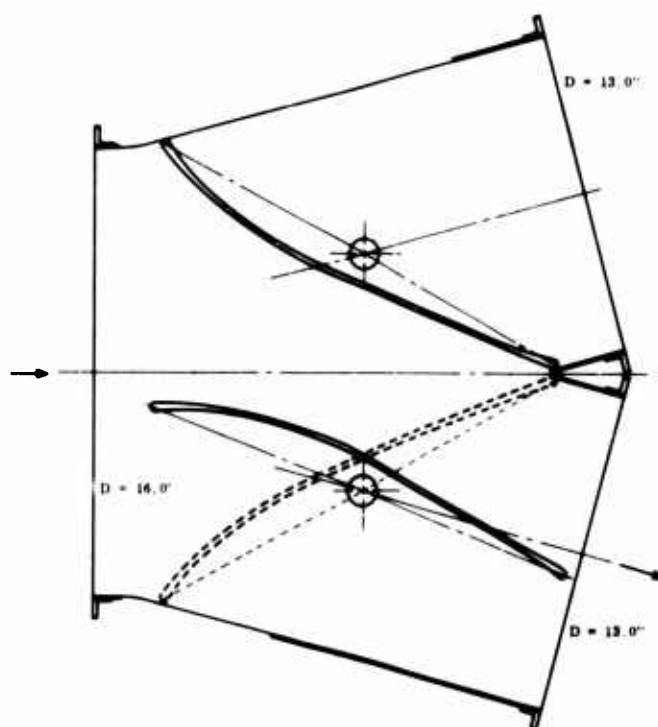
Figure 17. Butterfly Valve Diverter, Configuration B.

25
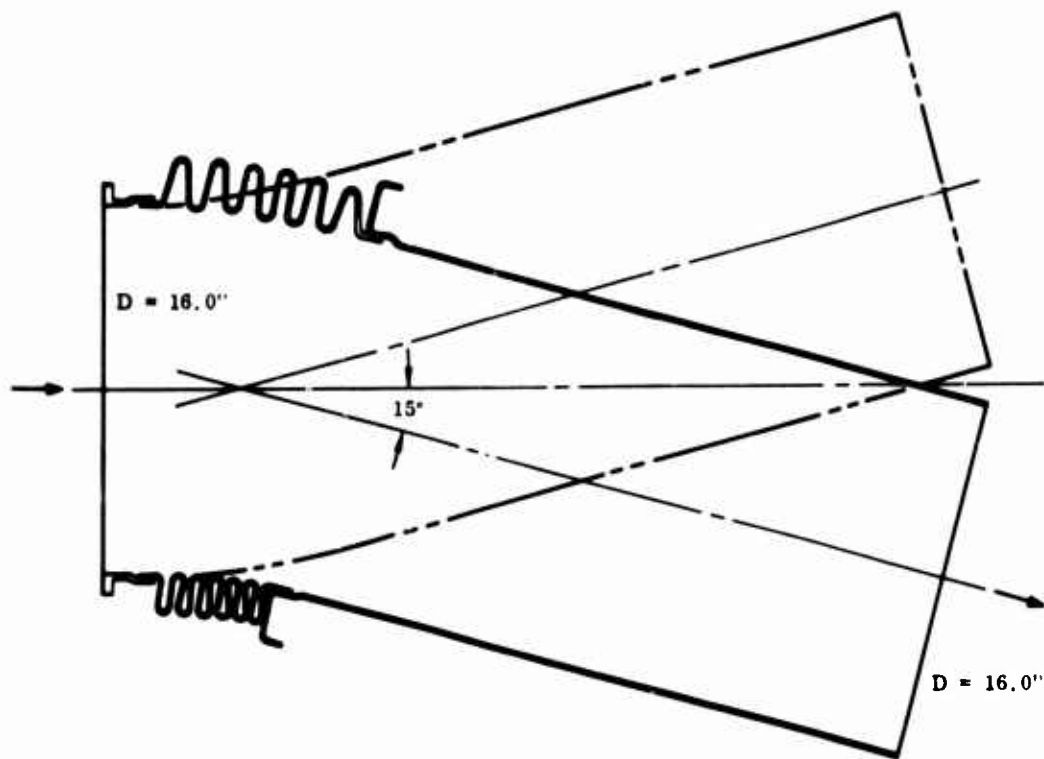
Figure 18.   Rotating Elbow, Configuration C.
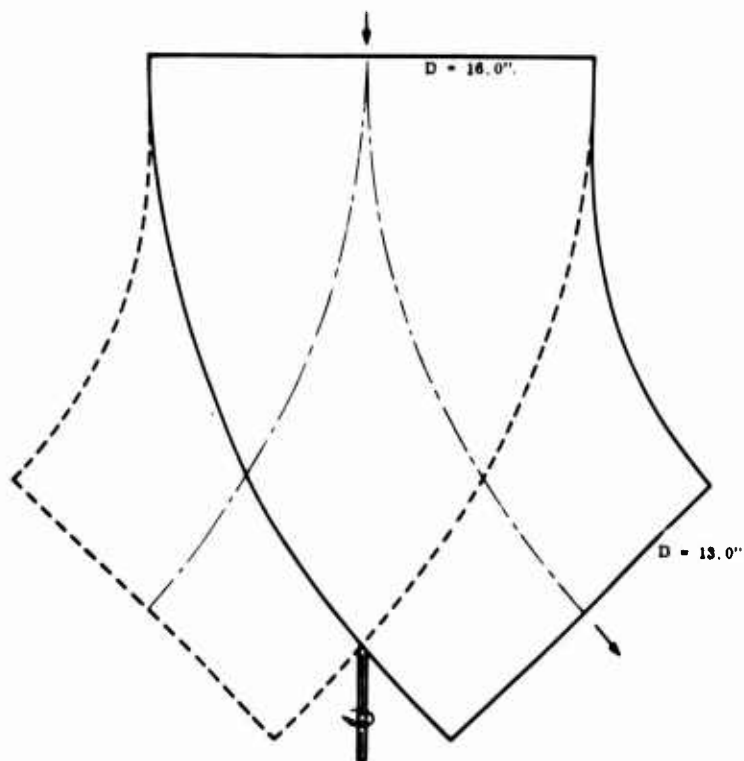
Figure 19.   Rotating Elbow, Configuration D.

TABLE II. TOTAL PRESSURE LOSSES				
Configuration	Type	Dimensions	Total Pressure Loss (psi)	$\Delta P/P_1$ (%) [1]
No. A (Figure 4)	Asymmetric duct with butterfly valve (values on top correspond to branch A)	Accelerated channels, from 15-inch diameter to 13-inch diameter	1.41 1.61	2.35 2.68
No. B (Figure 6)	Swinging duct with bellows	Constant 16-inch diameter	0.55	0.92
No. C (Figure 2)	Symmetric duct with butterfly valve	Accelerated channels, from 16-inch diameter to 13-inch diameter	1.22	2.03
No. D (Figure 12)	Rotating elbow	Converging bend, from 16-inch diameter to 13-inch diameter	0.27	0.45

The lowest pressure loss corresponds to Figure 19, with 0.27 psi. Figure 18 produced about twice as much pressure loss as Figure 19, with 0.55 psi. However, a true comparison would indicate an even greater difference between the pressure losses of both figures, since Figure 19 corresponds to a 45-degree elbow while Figure 18 considers a turning of only 15 degrees. Figures 16 and 17 have similar losses, which are much higher than those for Figures 18 and 19. The symmetrical diverter (Figure 17) has a slightly lower pressure loss, 1.22 psi, than the asymmetrical diverter (Figure 16), which has a loss of 1.41 psi in one branch and 1.61 psi in the other.

To produce low pressure losses, the analyzed Figures 16, 17, and 19 have a converging section from inlet to outlet. The accelerated flow (in these cases from a Mach number of about 0.3 to 0.5) greatly reduces the turning losses. The constant section assumed for Figure 18 corresponds to a Mach number of 0.3.

The main reasons for the higher pressure losses in Figures 16 and 17 are:

- The shape basically corresponds to a miter bend with a splitter vane in the second half of the stream path.

- The vane closing one branch presents a discontinuity to the cylindrical shape of the rest of the duct, and the resulting corners are a source of vortex losses.

- The other vane, although creating a minimum of interference with the flow, has a boss and structural support that disturbs the flow, producing contraction, expansion, and mixing losses.

The losses of Figure 18 result from skin friction, miter bend, and bellows, while the losses of Figure 19 result from skin friction and turning losses common to a bend of the circular section.

In the final analysis, the optimum design of the diverter valve will depend on the existing upstream conditions and the required downstream conditions. The final valve should be designed as part of an optimized system rather than as a separate entity; therefore, the designs analyzed here may be scaled or changed in the light of system design information.

An analysis has been completed on the diverter valves (Figures 2 and 14) to evaluate the pressure losses when there is a 90-degree relative position between through and diverter gas flow. Several component arrangements (Figures 20 and 21) have been considered. However, to optimize the diverter design, the overall engine system requirements should be established, including the selection of the diverter outlet (through or diverted) which should have the minimum pressure loss. It has been assumed that the initial inlet diverter diameter will be 16.00 inches, which corresponds to a Mach number of 0.3 when handling 70 lb/sec gas flow at $1500^\circ F$ and 60 psia. On this basis, to reduce the diverter turning losses, an acceleration to a Mach number of 0.5 could be advantageous. However, this solution assumes that there are no additional turnings downstream of the diverter valve outlet which could counterbalance this reduction in the diverter turning losses.

Predicted flow losses of four arrangements are shown in Figures 22 through 25. The bends considered in these component arrangements have an r/d of 1.5. If mechanical considerations and the space envelope would permit the use of higher valves of r/d, the pressure losses would be smaller than those indicated.

An analysis has been completed on the diverter valve (Figure 3) to evaluate the additional pressure losses produced by the splitter beam and by the maximum aerodynamic load acting on the beam.

Considering that the configuration shown in Figure 3 is similar to the Type D component arrangement shown in Figure 25, the additional pressure losses due to the beam would amount to about 0.10 psi, which would then increase the total losses in the through flow to 0.87 psi and in the diverter flow to 0.57 psi.

3.2.1 Stress Analysis

The major structural components of the two diverter valve designs (Figures 2 and 3) were subjected to a preliminary stress analysis to ensure a rational weight comparison. Creep strength was the major criterion for evaluation. It was concluded that any structural changes resulting from a rigorous analysis will be local in nature without significant effect on total weight.

The valve shells have been evaluated only on the basis of membrane pressure loads. The cases where the shell components and shell component intersections are not axisymmetric are cases not readily amenable to theoretical analysis. They are, however, considered critical areas from the standpoint of gross shell creep distortion due to localized stresses. Efforts have been made to establish analytical methods, but full confidence in structural integrity can be obtained only by development testing of prototype models. Proven methods are available for the cases of

axisymmetric shell discontinuities. These discontinuties, however, are not
generally considered critical areas, since the creep distortion resulting from high
localized stresses is also local in nature.
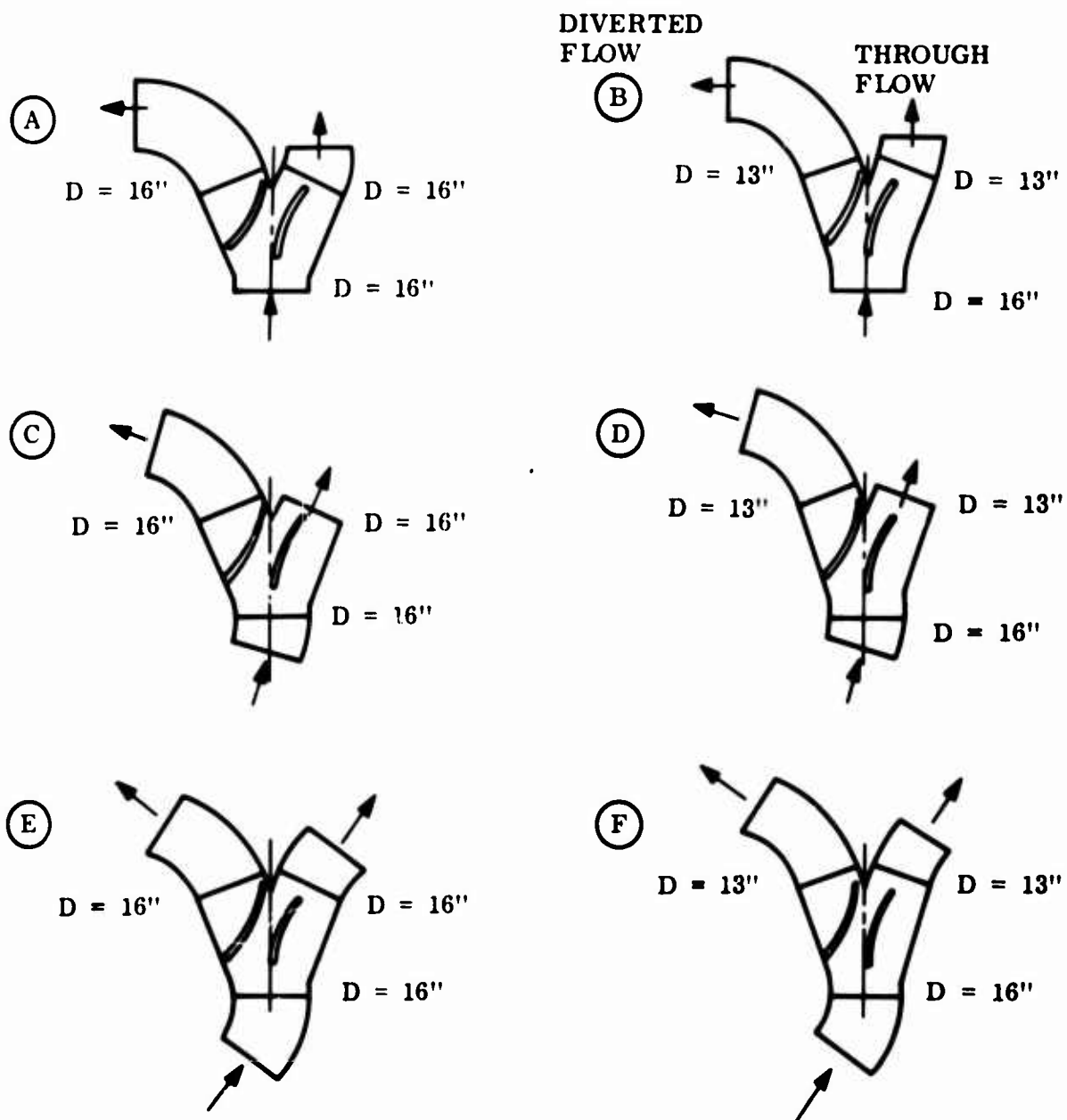
Figure 20.   Component Arrangements for the Diverter.
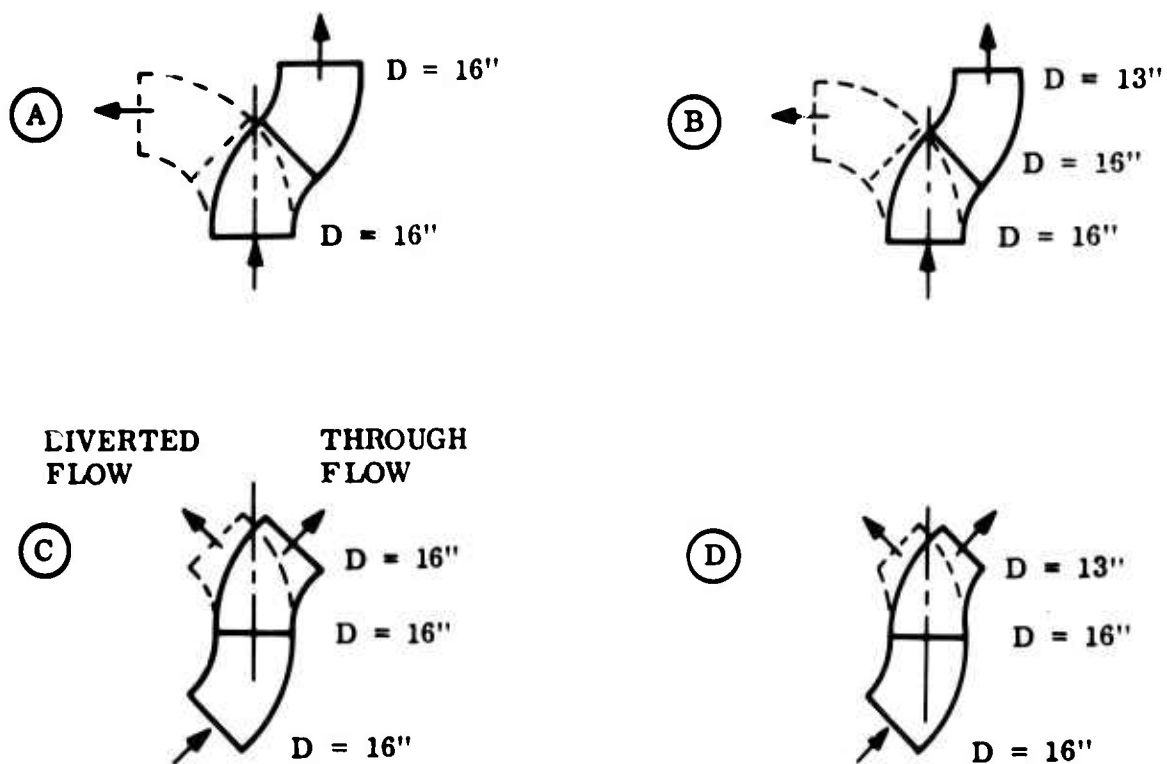
Figure 21. Component Arrangements for the Diverter.
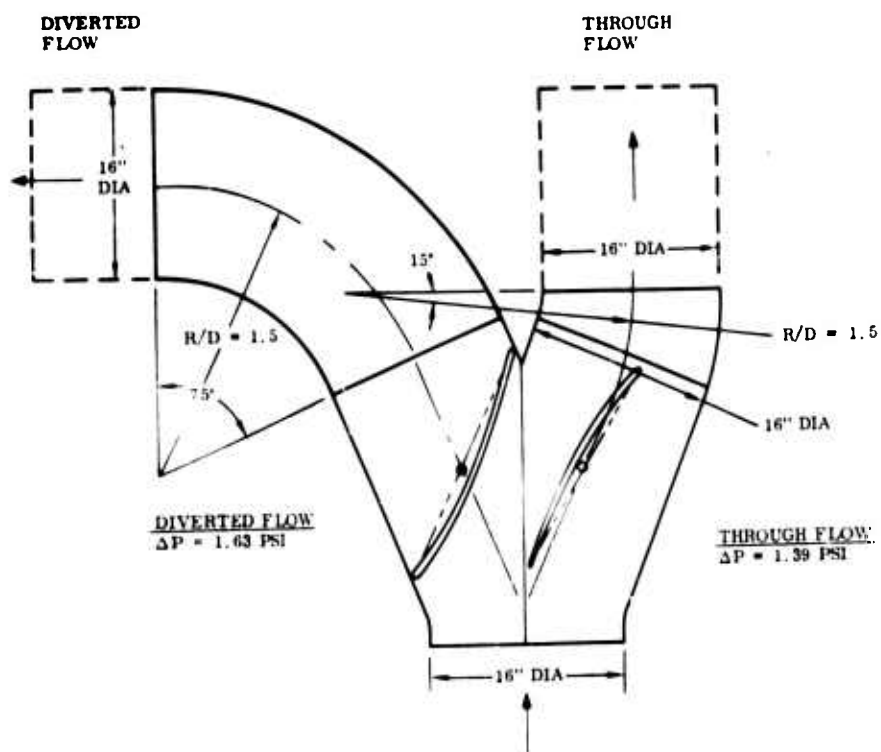
Figure 22. Type A Component Arrangement.

30
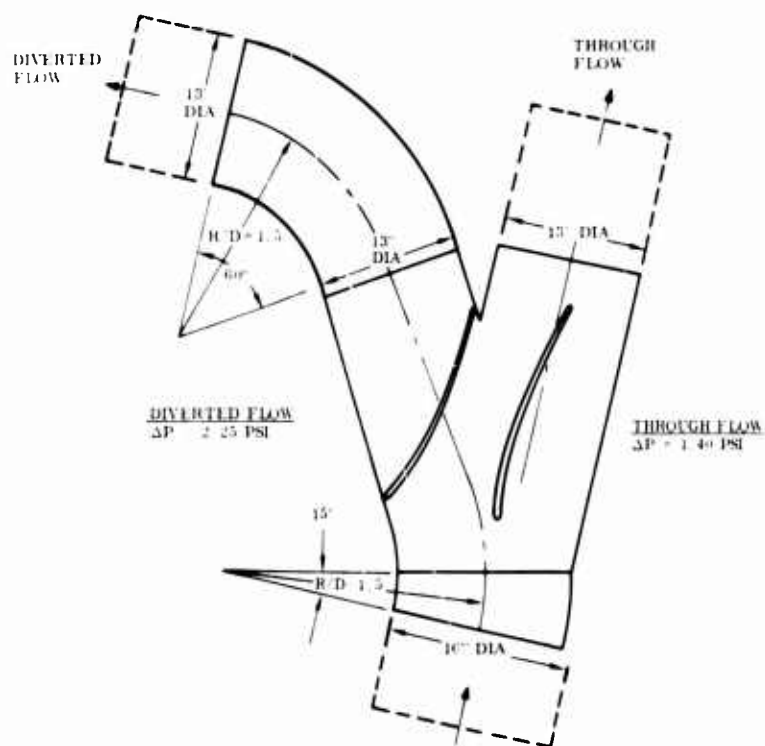
Figure 23. Type D Component Arrangement.
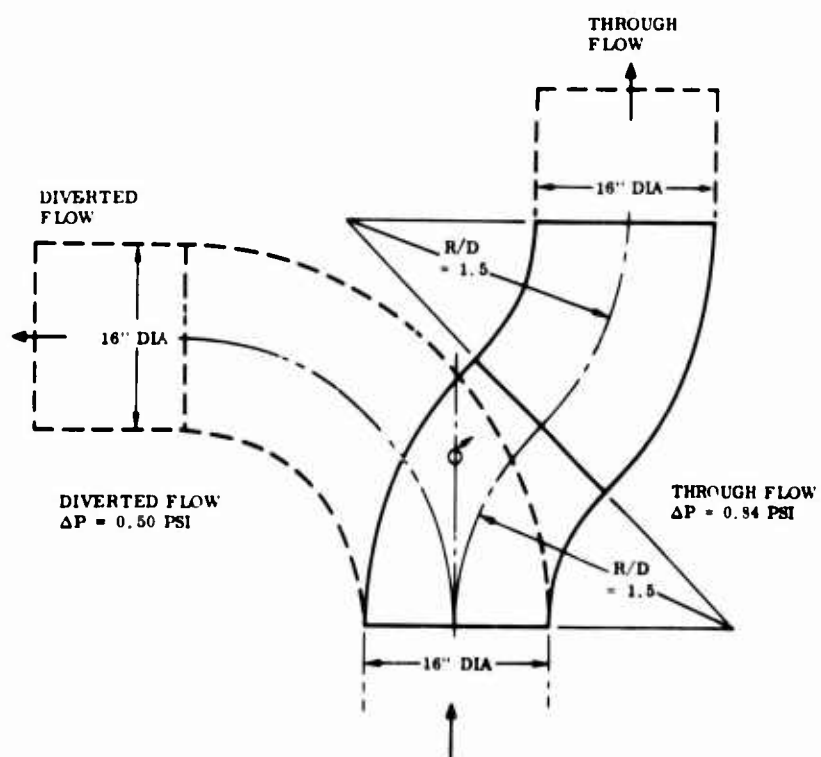
Figure 24. Type A Component Arrangement.

31
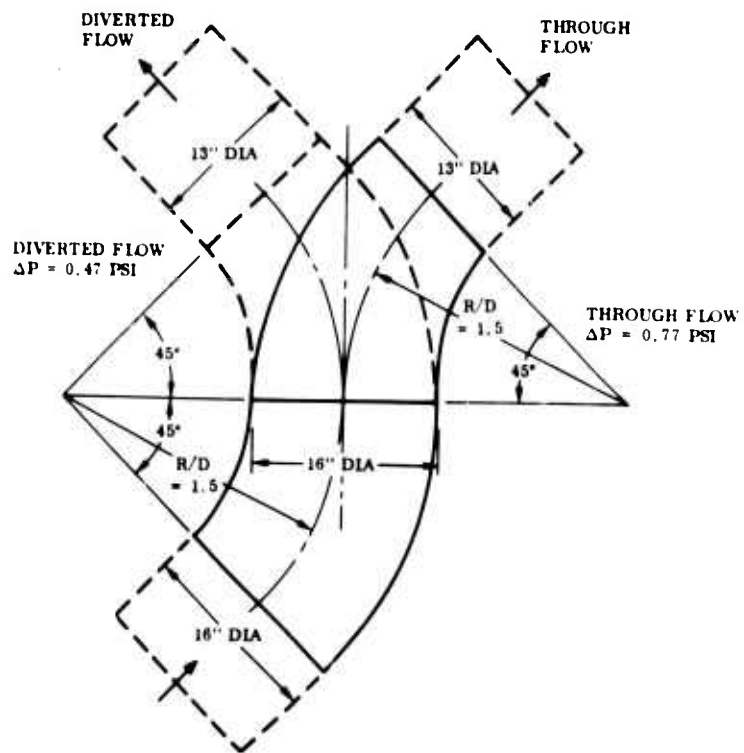
Figure 25. Type D Component Arrangement.

IV. PHASE II - DESIGN ANALYSIS AND SELECTION

Two design concepts for the diversion of high energy gas generator turbine discharge gases were prepared during Phase I. One of these is a basic interlock butterfly valve which uses existing state-of-the-art operating principles. It has, however, incorporated design improvements which have resulted in the following significant advantages:

- Lower pressure drop

- Improved valve sealing efficiency

- Reduced complexity

- Identical components

- Reduced manufacturing cost

This design concept is shown in Figure 2.

The second design concept represents a unique method of gas flow diversion and an advancement in the state of the art. Although more complex than the butterfly valve, it appears to offer advantages which may offset its complexity (Figure 3).

Because of differences in the two design approaches, each will be discussed separately.

4.1 BELLOWS TUBE/ROTATING ELBOW DESIGN

During initial design activities, numerous bellows tube and rotating elbow concepts were conceived. Both designs involved a similar retract-rotate-expand motion cycle during which large loads must be handled at high temperatures. Therefore, the majority of the effort was applied toward devising and inspecting numerous variations of the two schemes to reduce the diverter and its mechanism to a point where it would compare with the inherent simplicity of the butterfly approach.

Since the motion sequence is a problem common to both schemes, the following advantages provided the basis for selecting the rotating elbow diverter for further development.

- Pressure Drop

    A converging 45-degree turn can be obtained for a pressure loss of half that for the 15-degree turn estimated for the bellows tube diverter.

33

- Smaller Envelope

   The compactness of the diverter section cuts the length in half and
   reduces the overall height of a 90-degree and a through-flow system
   (Figure 26). The body diameter is 26 inches against 22 inches, but
   this loss is offset in part by the space consumed by the side-mounted
   actuator required for the bellows diverter.

- Reduces Verification Testing

   Little or no data are available to predict the effects of creep, pres-
   sure instability, or convolution reshaping for bellows. Unless the
   bellows design was unnecessarily conservative (at the expense of
   weight and increased actuation loads), high-temperature bellows
   verification testing would be required.

- Sealing

   Ignoring shaft seals, which are common to both systems, only a port
   seal, the absolute minimum necessary for any type of diversion, is
   required for the rotating elbow diverter.

4.1.1 Rotating Elbow Design Considerations

The study of the bellows tube diverter and its evolution into and through various
configurations of the rotating elbow diverter consumed a major portion of the time
allocated to Phase I activities. Therefore, it is necessary to define and discuss
the basic configuration (Figure 3) without the benefit of more detailed examination
of several other variations of the same concept. The two variations shown in
Figures 27 and 28 are presented for the reduction or elimination of the complex
motion cycle required for transition and sealing.

This consideration must be kept in mind when evaluating the concept with existing
state-of-the-art diverters. The basic advantage of the rotating elbow diverter lies
in the low pressure loss characteristics which approach the minimum obtainable
for turning through the desired angles.

The rotating elbow is heavier and more complex than a conventional butterfly valve
diverter and its associated ducting. The greater weight and added complexity are
offset by the vertical lift efficiency of the rotating tube diverter system. Obviously,
a quantitative comparison can be made on a system basis only where the vehicle
weight, payload, and range are established. For this, the diverter should be
optimized into the system based on the nature of the upstream and downstream
ducting (e.g., short straight tailpipes allow the use of a converging elbow in the
diverter to further increase the overall efficiency).

If reasonable manufacturing control is maintained, the self-energizing type of face
seal suggests effective sealing capabilities.

34

15.5 DIA

BELLOWS DIVERTER

16 DIA

31

54
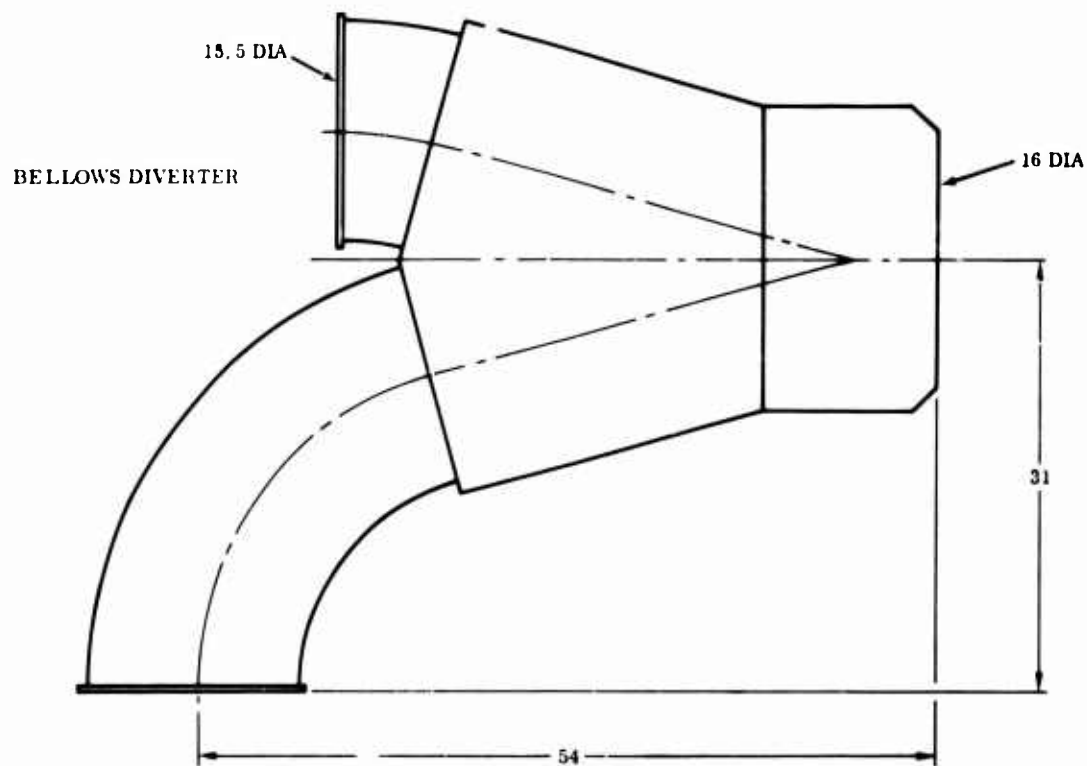
Figure 26. Typical Envelope; 90-Degree and Through-Flow System.

ACTUATION SEQUENCE
OPEN VALVE - ROTATE - CLOSE VALVE

RETRACT VALVE
- NORMALLY OPEN TO CASE
  PRESS. (EXTENDED)
- VENTED TO ATMOSPHERIC
  & CLOSED TO CASE (RETRACTED)

SEAL PLATE
PRESSURIZED ONTO SEAL BY
CASE PRESSURE IN BELLOWS
PLENUM. RETRACTED BY VENTING
PLENUM. CASE PRESS ACTS ON ANNULAR
AREA BETWEEN SEAL & MEAN DIA OF
BELLOWS TO COLLAPSE BELLOWS

BELLOWS
PRESSURIZED EXTERNALLY ONLY
DURING TRANSITION. MAY BE OF
LIGHT GAGE MAT'L DUE TO LACK
OF ΔP DURING LONG-TIME SOAK.

Figure 27. Gas Retracted Seal.

35

ELBOW ASSY LIFTED
TO CASE CENTER LINE
TO CLEAR SEAT
PRIOR TO ROTATION.
MOTION MAY BE ACHIEVED
BY LINKAGE OR ECCENTRIC
COUPLED TO LINEAR
ACTUATOR ──────

ACTUATION SEQUENCE

LIFT - ROTATE - DROP
OR
TRANSLATE & ROTATE
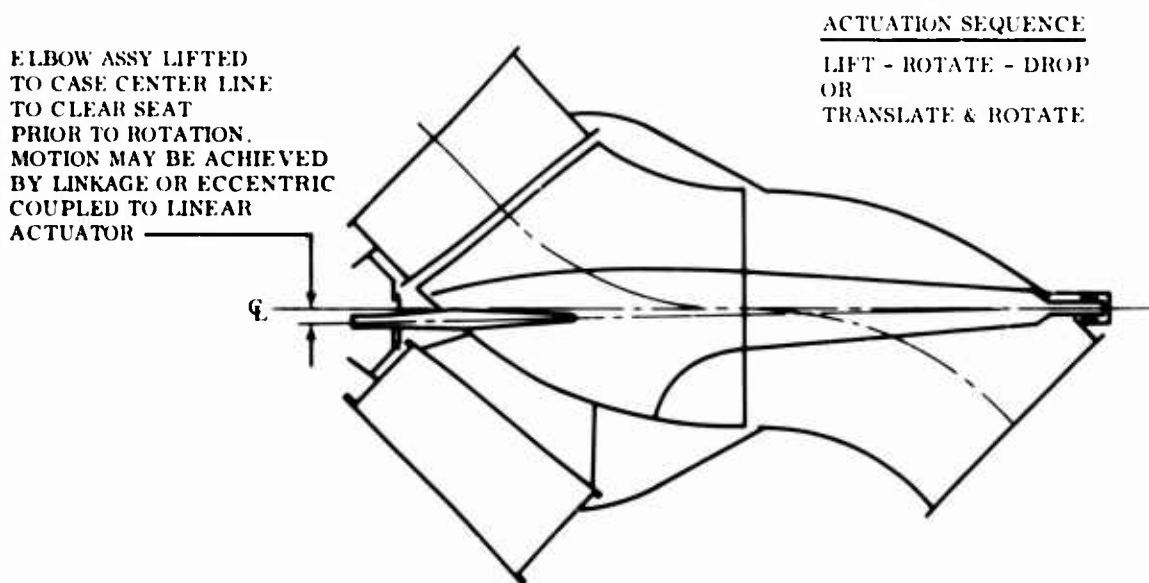
Figure 28.   Linkage or Eccentric Actuation.

The diverter envelope appears somewhat large because of the necessity of incorporating the forward elbow to allow the use of small diameter bearings external to the heat zone. However, in a 90-degree and through-flow system it compares reasonably well with a butterfly valve system (Figure 26).   The latter system provides a thinner envelope, but this advantage is partly offset by the clearance required for the side-mounted actuator and bearings. Without a particular installation in mind, it is difficult to assess whether the vertical offset in the horizontal center line would be objectionable. Although this feature is inherent in the design, some variation can be obtained by reducing the bend angle of the rotating elbow and increasing the angles of the fixed tubes to bias the lift-to-thrust efficiency ratio.

In its present form, the most undesirable feature lies in the relative complexity of the actuation system and its effect on reliability, weight, and cost.

Additional effort should be aimed at reducing these components to a simpler mechanical sequence or providing of a pure rotary motion through a different approach to the sealing method as suggested previously.

Two adaptions of the rotating elbow principle which may be of interest for specific applications are shown in Figures 29 and 30.

36
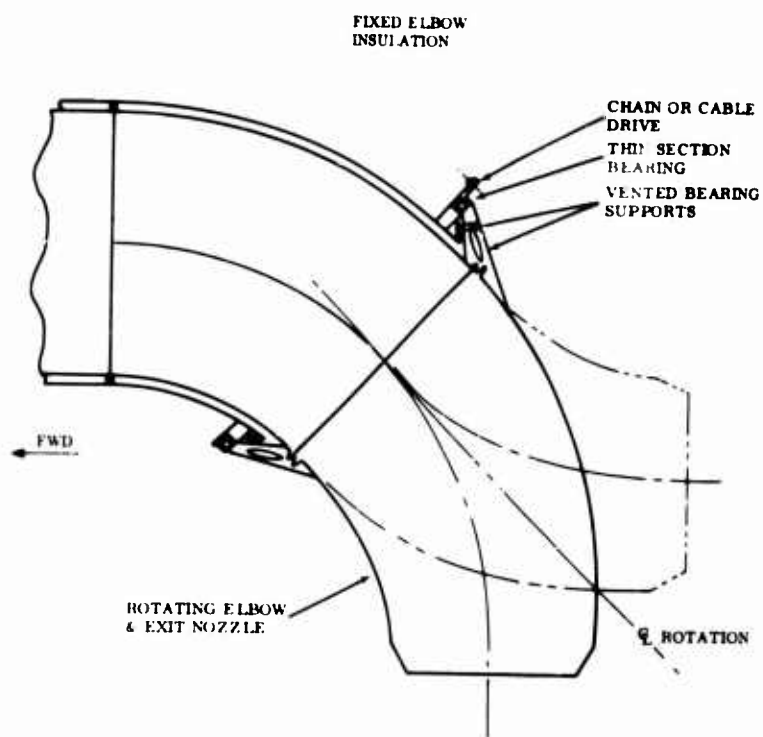
Figure 29. Rotating Elbow Diverter, Located at End of Tailpipe.
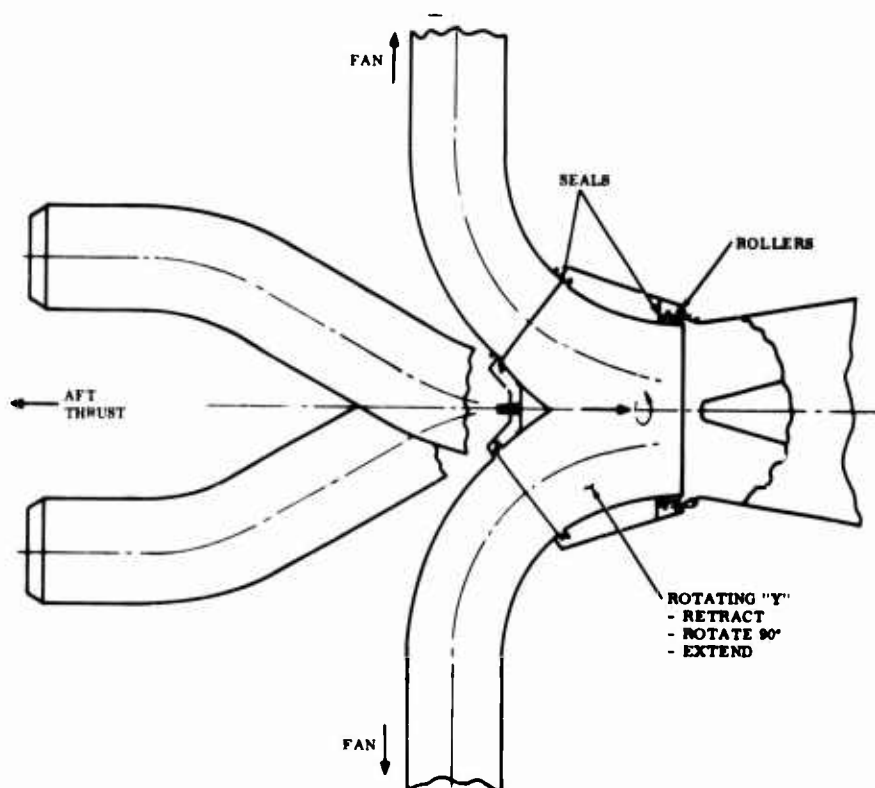
Figure 30. Split Flow Diverter.

37

Figure 29 shows the simplest configuration possible. The diverter elbow is mounted on the end of the tailpipe and is not actually a valve. Being mounted externally, the need for a case is eliminated and the diverter section is reduced to a simple elbow, one rotary seal, and a large diameter bearing located outside the high-temperature zone. Diversion is accomplished by simple rotation of the elbow. Since no downstream ducting must be considered, advantage can be taken of the turning efficiency of a converging elbow.

To avoid side thrust during transition, this concept is best adapted to a two-engine system with two contrarotating diverters.

Figure 30 shows a concept applicable to twin- or single-engine systems where downstream splitting of the flow would otherwise be required (e.g., lift fan vehicles).

By using a rotating Y in the diverter, the flow is split internally, thereby providing a decrease in system envelope and weight coupled with an increase in system efficiency.

The retract-rotate-expand motion cycle required for diversion is the same as for the internal rotating elbow diverter. However, since theoretically no lateral gas loads are involved in the Y-piece, the inlet end can be stabilized with rollers or the entire section can be cantilevered from the outlet end of the case.

4.1.2 Design Description

The initial preliminary design of the rotating elbow concept is shown in Figure 14. The multiplicity of seals, the complex seal retracting mechanism, and the location of the bearing in a ventilated environment detracted from the basic simplicity of the rotating elbow concept. Additional studies eliminated the objectionable features described above, and the diverter assembly design shown in Figure 3 was prepared.

This assembly has a 16-inch diameter inlet, 1.5 r/d ratio bends, and outlet diameters of 15.5 inches. The change in diameter results from converging the section slightly downstream of the point where maximum blockage is caused by the splitter beam. On installations allowing higher exit velocities, greater convergence would be employed to obtain a decrease in pressure drop, case diameter, and weight.

As shown on the drawing, it uses a forward elbow which normally would be used in a vehicle installation of a straight-through and 90-degree diversion system.

The forward elbow is attached to the engine exhaust or transition cone by the inlet flange and joins the diverter case on the outlet end.

The diverter case consists of two basically conical sections joined at the center by bolting flanges to provide for installation of the inner rotating members. The pressurized zone is blocked off at the aft end by a conical pressure bulkhead which also supports the aft seal and the actuator housing.

The rotating elbow, splitter beam, and closure cap form an internal assembly which retracts and rotates about the diverter case center line. The forward end of the beam is attached directly to a shaft which passes through a piston ring seal

38

to a forward bearing mounted externally to the high-temperature zone. Bearing loads are transmitted through a bearing housing into the inlet flange.

The two small section piston rings are housed in a cage which floats radially to absorb misalignment due to manufacturing and differential thermal expansion. Sealing around the OD of the cage is accomplished by a thin seal plate which is pressurized against the side of the cage at all times.

To provide minimum heat conduction, the bearing housing contacts the inlet flange only at the bolting pads and is cut away in the center to provide a longer heat path and to allow circulation. Locating pins between the housing and flange maintain correct positioning during assembly.

The aft extension shaft is bolted between reinforcing plates welded to the inner surfaces of the splitter beam, and the forward end is allowed to float axially to account for thermal expansion. The aft end of the shaft incorporates a piston ring seal and is splined to the actuator shaft which is supported radially by a journal bearing. Although primarily a compression joint, the spline is pinned to transmit tension during ground testing when the diverter is unpressurized.

The actuator is supported on one end by an extension of the aft end of the case to the actuator mounting flange and by a slip fit in the pressure bulkhead. Cutouts in the support, housing, and shaft of the actuator allow cooling air circulation throughout the area.

The splitter beam consists of half stampings that are welded along the edges and stabilized by welded spacer pins shown at Section C-C in Figure 3. The aft end of the beam is flanged out (Section D-D) to provide a spot-welded attachment to the rotating elbow.

The closure cap is welded to the back side of the elbow to form a conical cap which seats on the sealing flange of the unused outlet tube.

The sealing flange and closure cap are ground to provide a cylindrical sealing surface. The cylinder axis is parallel to the seat and is on an axial plane passing through both outlet ports.

In the normal or seated position, the closure port is capped off and the entire diverter case is pressurized. With this arrangement, the minimum number of seals possible (one) is used and problems of differential expansion in localized areas are avoided, since all internal surfaces are exposed to approximately the same temperature.

An additional advantage of this arrangement is that the combined plug and dynamic load is normally reacted by the outlet port tube rather than being carried in bending by the splitter beam for the long-time temperature exposure.

When seated, the closure cap lip is loaded against the outlet port seal face by the combined plug and dynamic load (11,300 lb), assuring conformity between the two faces. Therefore leakage is a function of surface finish or local discontinuities, which can be controlled at manufacture. With both surfaces ground to a matching

39

radius, the actual leakage would appear to be a small percentage of the 1 percent maximum allowed, since this is equivalent to a 0.018-inch continuous gap around the sealing periphery.

As transition is initiated, the actuator moves the splitter beam forward to lift the closure cap off its seat and create clearance for rotation. At this point, since the narrow annular outlet remains choked, the pressure in the case remains essentially the same as that in the gas stream. Therefore the splitter beam is in its fully loaded position.

When extended, the actuator rotates the internal assembly 180 degrees and then retracts to cap off the opposite port and unload the beam.

At the 90-degree position, the outlet end of the rotating tube has sufficient clearance from the case to provide an annular flow area exceeding that required for choking (98 in.^{2}) to prevent the possibility of engine surge caused by a pressure buildup. Therefore pressure inside the elbow remains essentially constant, but the case pressure drops as both outlet ports are open. Splitter beam loading in this position consists of the gas turning load plus the plug load resulting from the differential pressure across the rotating elbow.

Since 10,000 diversion cycles represent less than 3 hours' total time, the beam structure can be designed on the basis of strength levels approaching the short-time properties of the material.

4.1.3 Diverter Actuation

Figures 31 and 32 show a hydraulically operated rack and pinion actuator which provides the retract-rotate-expand motion cycle required to power the rotating elbow assembly. Since the schemes shown on Figures 27 and 28 suggest simplification of the actuating mechanism, no attempt has been made to finalize this particular concept pending their investigation.

The actuator consists of an axial piston to provide extension and retraction and a transverse double-ended piston with a centrally located rack to provide rotation.

Approximately 180-degree indexing of the actuator shaft is attained by slotting the piston skirt to match the cylinder head. Its primary purpose is to prevent inadvertent retraction during rotation resulting from a drop in hydraulic pressure. If gas pressure is maintained in the diverter, the closure cap cannot drift off the seat in the event hydraulic power is lost in the selected position.

Accurate positioning of the rotating duct center line may be obtained after assembly by adjusting each cylinder head against which the piston is bottomed.

To maintain concentricity between piston, piston rod, and actuator shaft bearing, both the actuator and actuator housing are of single-piece construction. The forward end of each is drilled to permit cooling air circulation around and inside the hollow actuator shaft. Therefore considerable surface area is exposed which will maintain reasonable actuator and hot-end bearing temperatures.

40

PINION

SEQUENCE VALVE
LOCATION

CROSSOVER PISTON & RACK

180° INDEX
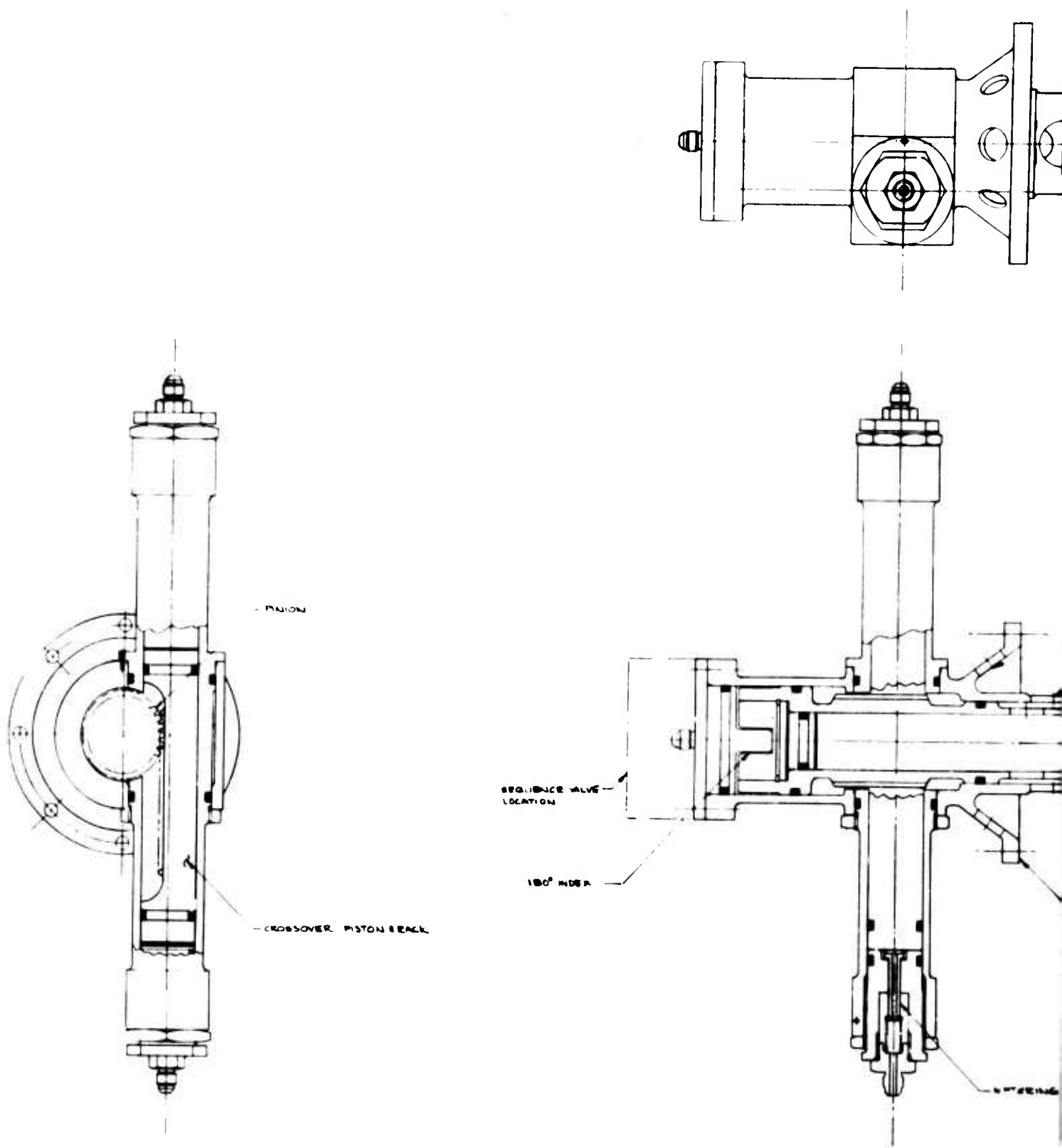
Figure 31. Actuator Assembly.

41

COOLING AIR VENTS

SPLINE

SEQUENCE VALVE
CTION

HIGH TEMPERATURE
JOURNAL BEARING

180° INDEX

ACTUATOR SHAFT

ACTUATOR HOUSING

METERING VALVE

nbly.

B

Figure 32. Valve Schematic.
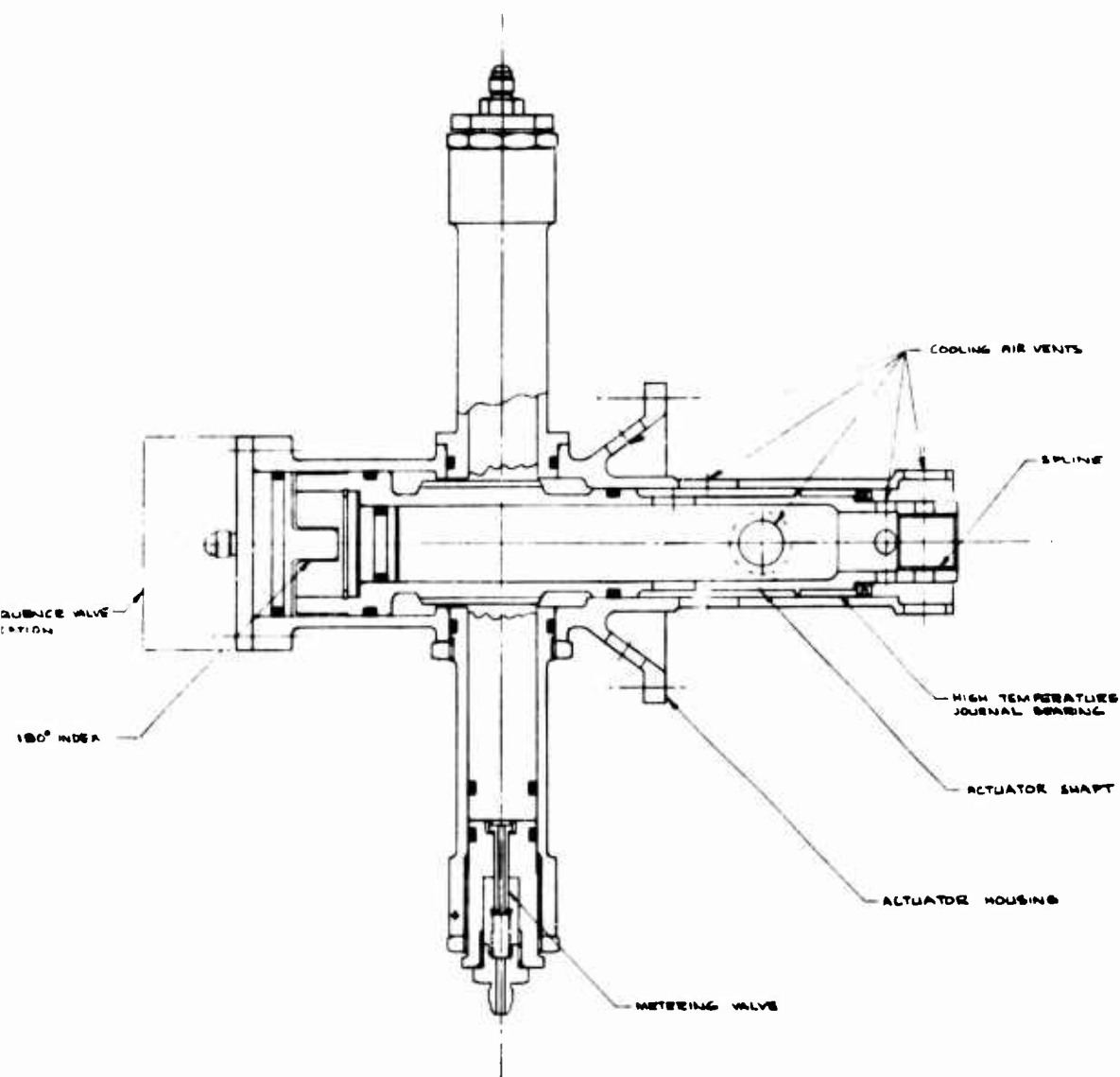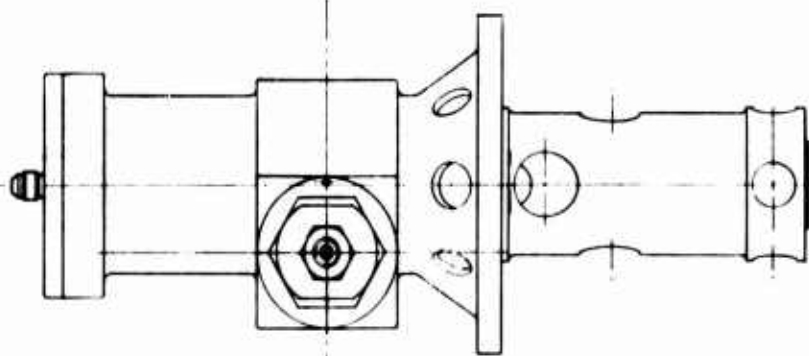
Damping at the end of the rotational stroke is accomplished by the metering valve which is integral with the cylinder heads of the rotational actuator. When the piston contacts the valve, the exit flow is restricted. Internal pressurization of the sleeve on the reverse cycle allows full flow into the cylinder because the seat diameter is larger than the valve body.

The valve diagram to control and sequence the actuator is shown in Figure 32. In packaged form, the changeover valve and lockout valves would be incorporated into the actuator cylinder head and would be positioned mechanically by the actuating piston skirt. This configuration would limit the external piping to a minimum.

Position A shows the start of a diversion cycle with pressure applied to the actuator piston but locked out from the crossover piston until the end of the stroke is approached, as shown by Position B.

At the end of the crossover stroke (Position C), rotation of the actuator piston reverses the changeover valve to provide retraction, but pressure is retained on the crossover piston. The system holds in this position pending reselection by the pilot.

Position D has been added to show initiation of the sequence when the pilot's selector valve is reversed. The system is energized in the same manner as Position A, but provides rotation in the opposite direction.

4.1.4 Installation and Maintenance Requirements

Installation

Figure 33 shows a typical vehicle installation in which the rotating elbow diverter has been fixed to the engine outlet transition. Support by two vertical links and one horizontal link perpendicular to the planes passing through the fixed support of the engine minimizes the effect of thermal expansion.

Vertical and horizontal tailpipes are shown attached directly to the outlet ports and, depending on their length, may be provided with similar supports.

Using the actuator (Figure 31), a hydraulic supply of 2.1 gpm at 3000 psi would be required for a 1-second cycle.

Maintenance

Once past the developmental stage, line maintenance should be limited to functional and leakage checking of both the actuator and diverter system.

Replacement of the actuator and valve seals together with the high-temperature bearings and piston ring seals on the actuator would be expected at the 1000-hour overhaul period.

Special tools are limited to the wrenches required for installation of the forward seal and both bearing retention rings.

44
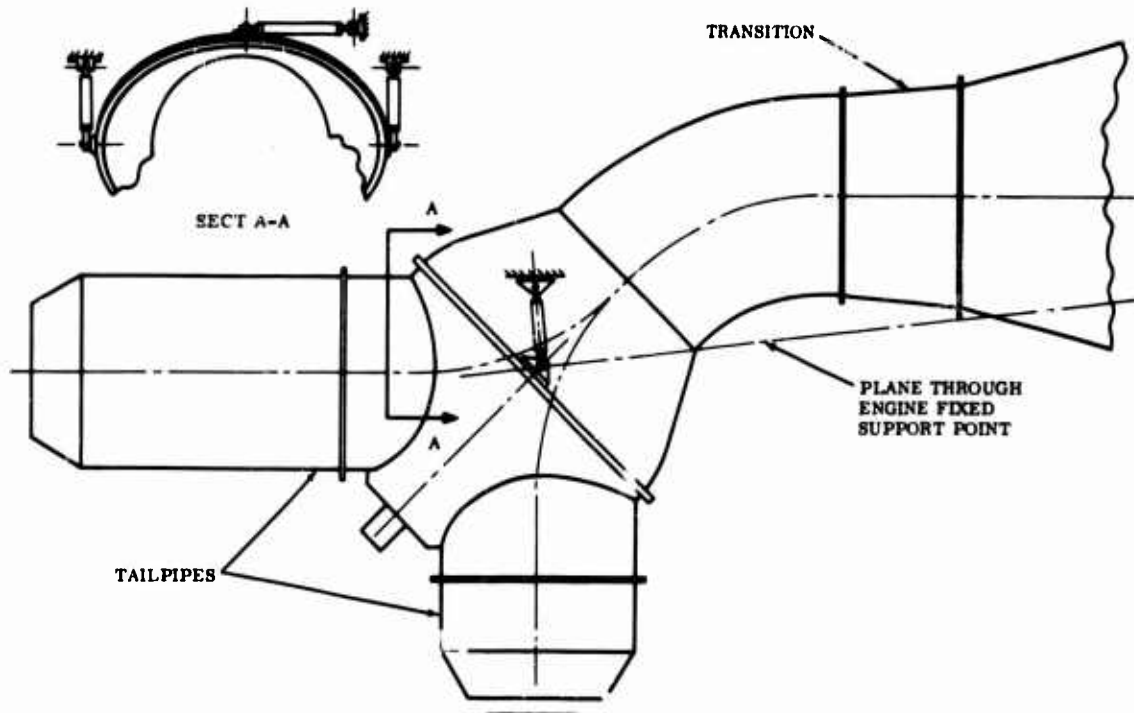
Figure 33. Typical Method of Support.

4.1.5 Weight

The estimated weight of the diverter (Figure 3) is 121.7 pounds. A breakdown of the weight is:

	(lb)
• Aft case	44.26
• Forward case	26.80
• Rotating components	32.60
• Actuator	13.00
• Valves	5.00

4.2 BUTTERFLY DIVERTER DESIGN

Two configurations of this type of diverter were evolved during Phase I design activities. The first design conceived is shown in Figure 4, and basically is similar in configuration and component arrangement to the diverter valve designed

45

for the Hummingbird vehicle. However, numerous design improvements are incorporated to overcome the deficiencies of the Hummingbird design. The second design is shown in Figure 2; because of its reduced complexity, it has significant advantages over the first design.

The inherent design simplicity of the valve (Figure 2) embodies the following significant advantages:

- Simple actuation mechanism

- Proven design principle

- Manufacturing simplicity

- No critical areas requiring major development

- Reduced weight

- Minimum envelope

- Efficient sealing

4.2.1 Design Description

The configuration and design of the butterfly valve shown in Figure 2 were firmly established at the midpoint of the Phase I design activity.

Seal Design

Sealing of the valve is required in the following areas:

- Blade shafts

- Bolting flanges

- Closed blade

Sealing of the shaft is accomplished by a bellows seal (Figure 2). The surface against which the bellows will seal is expected to be a carbide-cobalt matrix to provide low friction and to prevent galling resulting from rotary motion between the sealing surface and the bellows end. The internal pressure coupled with the spring load of the bellows provides the force to maintain the bellows ends against the sealing surfaces.

For sealing the bolting flanges, it is anticipated that a thin gage (0.010-inch-thick) Rene' 41 gasket lightly crimped around the inner edge would be sufficient to achieve an extremely low leakage joint.

With respect to closed valve leakage, it is estimated that it will be less than the 1 percent maximum allowed, since this is equivalent to a 0.010-inch continuous gap around the valve periphery. Because of the sealing principle involved and the

seal development program described below, it is expected that a gap of 0.002 to 0.005 inch can be achieved.

For sealing purposes, the blade/seal relationship (Figure 2) is similar to an elliptical plate rotating inside a thin-wall cylinder. The elliptical blade's major axis is long enough to prevent its binding the cylinder due to coefficient of friction; in addition, the sealing plane does not come within 45 degrees of a plane normal to the duct axis. The cylindrical seal is provided by inserting the downstream duct approximately 2.0 inches into the U-shaped section of the Y-body, where it extends approximately 0.20 inch beyond the mating sealing line of the valve blade edge.

The sealing action occurs when the forward end of the seal is stretched in hoop tension over the edge of the elliptical blade. The elliptical blade is forced into interference with the cylindrical sealing element with a torque of approximately 3000 inches/pound. The seal is stretched in hoop tension. The nominal hoop stress in this portion of the seal is below the allowable 0.2-percent creep stress.

The flexibility of the 2-inch extension of the sealing cylinder affords a fair degree of conformability to the blade. This conformability permits some deviation from a perfect-shape relationship between the blade and seal while still attaining an almost perfect seal. Any local high spot on the seal that experiences higher stresses tends to creep to a shape of better conformability. A slightly oversized bearing around the blade shaft permits a small amount of floating capability of the blade to allow centering of the blade.

Reduction of sealing effectiveness can occur as a result of the following conditions:

- Cylindrical seal not close enough to its nominal shape or location

- Sealing edge of blade not close enough to its nominal shape

- Blade not centered sufficiently relative to the cylindrical seal

- Nominal shapes of the blade and seal not sufficiently well established to accommodate their relative distortions resulting from thermal gradients and internal pressure

To resolve these conditions, the manufacturing and development test plan described below would establish the optimum shape of the blade sealing edge relative to the flexible sealing element. It is anticipated that this type of development program would be required only one time. Sufficiently accurate reproducibility would ensure good sealing on subsequent valves.

The development program would consist of the following steps:

1. A cylindrical seal would be installed as close as possible to its nominal shape, size, and location in a complete valve body.

2. The sealing edge of the blade would be ground as close as possible to its nominal shape and size relative to its shaft center line. This procedure would present a cylindrical intersection when viewed parallel to the axis of the cylindrical seal.

47

3. The assembled valve with the blade in the closed position would be pressurized at room temperature to operating pressure or slightly higher. Feeler gage measurements would indicate the relative effect due to pressure if leakage occurred.

4. Using the gap measurements of Step 3, any change in the nominal shape of the blade sealing edge judged desirable could be achieved either by grinding or building up and regrinding the blade edge.

5. Steps 3 and 4 would be repeated as required to obtain approximate zero leakage.

The shape of the blade established by the preceding steps would serve as a pattern for all subsequent blades.

The development test should include tests of both blades to ensure that both the cylindrical seals and the two blades are sufficiently symmetrical to operate with just one blade shape. It would be desirable during the development test to determine, at least approximately, how much variation in relative shapes could be tolerated without causing significant leakage. This determination would permit the tolerances to be only as tight as necessary and therefore would contribute toward the lowest cost for the production unit.

4.2.2 Diverter Actuation

The parallelogram linkage and mechanical arrangement used to achieve valve blade actuation have been discussed previously. A description of the desired stages of the diversion cycle and performance of the actuating mechanism will now be provided.

When the closed blade begins to open, an opening torque capability of 5500 inches/pound overcomes an estimated 3500-inch/pound closing torque resulting from the aerodynamic forces and the overcenter spring. When the blades approach the midpoint of the movement cycle, the sum total of the aerodynamic torque and overcenter spring torque total passes through a zero point. As the opening blade passes the middle of the cycle and continues on toward its open position, the aerodynamic torque, overcenter spring torque, and actuator torque are all additive, tending to rapidly open the opening blade and rapidly close the closing blade. Since the rapidly closing blade would damage the seal, the actuator must be snubbed to a control speed.

Additional features which the actuator and actuating mechanism must provide are:

- The valve blade must be held against the seal with sufficient force to meet the sealing requirements with or without continuous hydraulic pressure in the actuator.

- The blade must be free to float against the seal to maintain a continuous seal during variations in the relative sizes of the blade and seal resulting from varying thermal conditions and pressures.

48

- After snubbing is complete, the total closing torque on the closed blade resulting from aerodynamic force on the open blade, the over-center spring, and the actuator pressure should be low enough that the hoop stress in the seal is below the allowable creep stress of the seal material.

- A small continuous flow must be maintained through the actuator to keep it below the allowable working temperature.

The required characteristics described above are provided by the linkage and actuator. A description of the actuator (Figure 5) operation and the actuating mechanism is as follows:

- Compactness and simplification (Figure 5, Sec. A-A) are achieved by installing the orifices and check valves in three holes in one end of the piston shaft.

- Snubbing is accomplished in a conventional manner by gradually closing off a trapped volume of fluid with a conical shaft passing through the unbroken bronze ring (Sec. D-D). Snubbing is completed before the piston reaches the end of its stroke. During the last portion of piston travel, the trapped cavity of fluid is completely sealed except for controlled leakage by the seal ring passing along a constant diameter of the shaft length. The controlled leakage through the Lee Visco jet bypasses the seal ring.

- The piston never seats directly against the cylinder head. The actuation cycle is stopped by the blade's coming to rest against the seal. The blade floats against the seal to accommodate the changes in relative size due to temperature and pressure.

- An overcenter spring on the linkage, providing about 300 inches/ pound of closing torque to whichever blade is closed, holds the blade against the seal when there is no hydraulic pressure.

- An aerodynamic opening torque on the opening blade estimated to be 3200 inches/pound maximum during full flow is converted by the linkage into a closing torque on the closed blade. The total closing torque of 3500 inches/pound (3200 plus 300) holds the closed blade against the seal. The seal limits the angular travel of the closed blade.

- The net piston area (and therefore the net piston load) is greater at the beginning of the cylinder extending stroke than it is at the beginning of the cylinder shortening stroke by the area of a piston shaft.

- Based on the previously estimated total closing torque of 3500 inches/pound, an opening torque greater than this value is required to cause the closed blade to begin to open. Using a hydraulic pressure source of 3000 psi, the actuator can provide an opening torque of 5500 inches/pound to the closed blade to overcome the 3500 inches/pound closing torque.

49

- The attached point of the actuator to the bellcrank has been selected so that the opening torque supplied to either closed blade at the beginning of its opening cycle is 5500 inches/pound, even though the cylinder loads are different due to different net piston area.

- At the end of the stroke, the piston force is proportional to the differential pressure across the piston head and to the effective area of the piston. The differential pressure is kept relatively low by using large and small orifice jets. The large orifice permits flow across the piston head and has some pressure drop. However, the principal pressure drop occurs through the small orifice. Therefore, by sizing the large and small orifices, almost any desired differential pressure across the head can be achieved. The large orifice is still small enough so that during most of the actuating stroke, the leakage through this orifice is no greater than five percent of the total flow required to operate the cylinder in the required time. The large orifice acts during the entire stroke, the small orifice only after snubbing has begun.

- The selection of the orifice size must take into consideration that at one end of the piston travel, the effective force is just the difference between piston and shaft area times the differential pressure. At the other end of piston travel, the force is the same differential area times a low-differential pressure plus the shaft area times a high-differential pressure.

- Speed of actuation can be controlled with an orifice of the desired size at either the inlet or the outlet.

- To attain higher reliability and to reduce hydraulic pump output, it would be advisable to provide an adequate accumulator near the diverter so that any diversion cycle, if initiated, would be completed even if there were a failure elsewhere in the hydraulic system.

- To reduce the energy consumption of the hydraulic pump, it would be advisable to reduce or remove the hydraulic pressure on the actuator after an actuating stroke has been completed. However, the actuator has been designed to accommodate continuous full hydraulic pressure.

- The energy and power requirements of the actuator vary with the actuation time. Slower actuation times may require more energy because of the small controlled leakage through the piston.

- By proper selection, orifice diversion in either direction can be accomplished in an elapsed time ranging from 0.25 second to several seconds.

- For an actuation time of one second, the energy consumption should not exceed about 8400 inches/pound (i.e., 3000 psi x 1.02 sq in. piston area x 2.50 in. stroke x 1.1 conservative controlled leakage factor). This energy consumption would represent a power input of

50

1.27 horsepower. Since this power requirement exists for such a short time, it suggests desirability of the accumulator previously discussed.

4.2.3 Aerodynamic Design

Appendix I contains the aerodynamic analysis of the butterfly. The basic value configuration and its inlet and outlet diameters were selected

- To keep the angle of divergence as small as possible to minimize flow disturbance and losses.

- To prevent the blade from deviating very far from the probable flow streamlines through the diverter.

- To create a strong convergence through the turn to suppress flow separation and the associated losses.

4.2.4 Suggested Diverter Installation

Figure 34 shows a suggested method of adapting the basic butterfly valve diverter to a typical vehicle installation. A 15-degree, 18-inch-diameter, 36-inch-radius elbow would be used upstream of the diverter. At one outlet to complete the 90-degree diversion, a 60-degree cascade would be used. To achieve minimum weight and envelope, the basic diverter (Figure 2) has been modified to incorporate the cascade turn. The estimated weight increase over the diverter to accomplish this installation is 21.5 pounds. Thus, the total weight of the diverter plus the proposed adaption to achieve a 90-degree turn is 105.9 pounds.

4.2.5 Development Testing

Development testing falls into two categories:

- Development to obtain adequate performance

- Development to yield improved diverter performance

In the first category of testing, there would be only one area of tests required, and this area would involve development of the optimum shape of the blade relative to the seal to minimize leakage.

Testing in the second category would consist of the following:

- A model flow test to indicate areas where significant flow separation and its resultant losses were occurring.

- A flow test to determine the aerodynamic torque on the blade. The losses and aerodynamic torque are probably dependent on the blade angle of incidence.

- Pressure testing to determine the change in shape of the valve body while subjected to operating pressure.

51
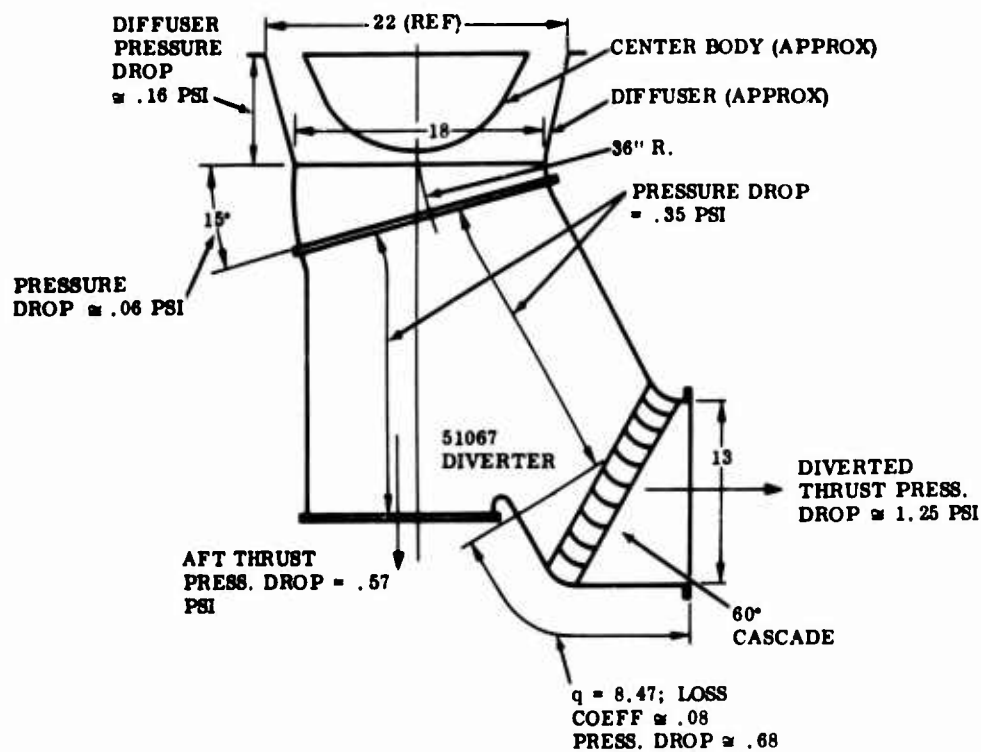
Figure 34. Basic Butterfly Diverter Valve, Adaptation for Maximum Aft Thrust.

4.2.6 Weight

The estimated weight of the diverter (Figure 2) is 84.4 pounds. A breakdown of the weight is:

	(lb)
• Valve body (includes cylindrical sections)	18.4
• Valve blades	40.0
• Actuating mechanism (includes actuator cylinder)	5.0
• Flanges	7.4
• Shafts, bearings, and reinforcement	11.6
• Insulation	3.0

4.3 STRUCTURAL ANALYSIS

A preliminary structural analysis of the butterfly (Figure 2) and rotating elbow (Figure 3) diverter valve designs was limited to the basic structural components for the purpose of providing a realistic comparison of weight.

The following material properties were assumed for the preliminary analysis:

	Rene' 41	Alloy 713C	6AR-4V
0.2% Yield Strength at 1400°F	130,000	110,000	
Stress for 0.2% Total Creep Deformation in 5000 Hours at 1400°F	25,000	30,000	
0.2% Yield Strength at 300°F			120,000

Low-cycle fatigue test data for Rene' 41 and 713C alloys at 1400°F have not been obtained to date; however, analysis of thermal and mechanical cycling fatigue will not be made until the choice of a diverter concept is final.

The only loading condition considered for the preliminary analysis was direct pressure load; namely, the membrane stresses in the shell elements and the blade bending stresses for the butterfly valve design. Because of the lack of symmetry of the shell elements and shell element intersection areas, an accurate theoretical discontinuity analysis cannot be readily performed. For the final valve concept, an experimental validation of strength in the discontinuity areas will be proposed.

Flight maneuver loads, in accordance with the requirements of MIL-E-5007C, have been reviewed in a qualitative manner. It is not felt that these loads will necessitate any major change in the structure of the proposed concepts. In like manner, the aerodynamic and unbalanced static pressure forces were investigated and do not appear to be of major significance. A complete analysis of the above loads can be made only when flow system and installation support details are available.

Each valve design contains basic pressure loaded shell elements which are not symmetrical and, therefore, not amenable to rigorous theoretical analysis. Because of these elements, it is proposed that structural design verification tests be performed on prototype elements. For the butterfly design, the blade, seal, and valve body would require tests; for the rotating elbow design, the valve body, elbow, and splitter beam would be submitted to simulated load tests. Since long-time creep distortion resistance is considered the primary structural requirement, and since actual tests at temperature are not practical, an accurate knowledge of stress field is required to predict creep behavior. To obtain these data, brittle lacquer tests to describe the stress field followed by strain-gage measurements are proposed.

4.4 AERODYNAMIC ANALYSIS

The aerodynamic analysis of the diverter valve designs (Figures 2 and 3) is presented in Appendix I. Table III contains pressure loss details for the butterfly diverter valve (Figure 2). Table IV contains pressure loss details for rotating elbow system (Figure 3).

TABLE III. DIVERTER VALVE SYMMETRICAL DOUBLE BUTTERFLY SYSTEM PRESSURE LOSS DETAIL	
Through-Flow Position	
15-degree bend at inlet:	
Turning losses:	$\Delta P_1 = 0.051$ psi
Skin-friction losses:	$\Delta P_1 = 0.011$ psi
Miter bend losses:	$\Delta P_2 = 0.195$ psi
Skin-friction losses: (including drag of butterfly valve):	$\Delta P_3 = 0.179$ psi
Total losses:	$E\Delta P = 0.436$ psi
Inlet dynamic pressure:	$q_1 = 2.14$ psi
Pressure loss coefficient:	$E\Delta P/q_1 = 0.20$
Diverted-Flow Position	
15-degree bend at inlet:	
Turning losses:	$\Delta P_1 = 0.051$ psi
Skin-friction losses:	$\Delta P_1 = 0.011$ psi
Miter bend losses:	$\Delta P_2 = 0.195$ psi
Skin-friction losses: (including drag of butterfly valve):	$\Delta P_3 = 0.179$ psi
60-degree bend at outlet:	
Turning losses:	$\Delta P_4 = 0.713$ psi
Skin-friction losses:	$\Delta P_4 = 0.235$ psi
Total losses:	$E\Delta P = 1.384$ psi
Inlet dynamic pressure:	$q_1 = 2.14$ psi
Pressure loss coefficient:	$E\Delta P/q_1 = 0.65$

TABLE IV.   DIVERTER VALVE ROTATING ELBOW SYSTEM

Through-Flow Position

Turning losses:	$\Delta P_1 = 0.664$ psi
Skin-friction losses:	$\Delta P_2 = 0.107$ psi
Strut drag losses:	$\Delta P_3 = 0.103$ psi
Total losses:	$E\Delta P = 0.874$ psi
Inlet dynamic pressure:	$q_1 = 3.46$ psi
Pressure loss coefficient:	$E\Delta P/q_1 = 0.25$

Diverted-Flow Position

Turning losses:	$\Delta P_1 = 0.353$ psi
Skin-friction losses:	$\Delta P_2 = 0.107$ psi
Strut drag losses:	$\Delta P_3 = 0.103$ psi
Total losses:	$E\Delta P = 0.563$ psi
Inlet dynamic pressure:	$q_1 = 3.46$ psi
Pressure loss coefficient:	$E\Delta P/q_1 = 0.16$

V. PHASE III - MECHANICAL DESIGN

The diverter valve assembly is shown in Figure 35. The diverter consists basically of a symmetrical Y-shaped duct with two butterfly blades that selectively divert the gas flow through either branch of the Y.

One branch of the Y is closed by one of the butterfly blades. The other butterfly blade is open and oriented so as to cause the least pressure drop through the other branch of the Y. The position of the blades can be reversed by an actuator to divert the flow through the other branch of the Y.

The flow through either branch of the Y is diverted 15 degrees from the plane of symmetry.

A 60-degree cascade turn is attached to one branch of the Y just downstream of the butterfly blade to complete a 75-degree turn from the inlet flange of the diverter.

If a full 90-degree turn of the diverted flow is desired and if no turning in the through-flow mode also is desired, a 15-degree elbow would be desirable upstream of the diverter inlet.

A 3000-psi hydraulic actuator and linkage is mounted on two shafts, one shaft extending from each of the two butterfly blades. The time (0.85 second) for the actuator to reverse the blade positions is controlled by orifices.

The design flow conditions are 70 pps of turbine exhaust gas at 60 psia and 1400°F.

The diverter was sized to produce an exit velocity slightly below 0.35 Mach for either through or diverted flow into a 12-psi atmosphere.

For the preceding conditions, there is a calculated pressure drop of 0.25 psi in the diverter during the through-flow mode and a calculated pressure drop of 0.79 psi when the flow is diverted through 75 degrees.

Leakage past both the closed butterfly blade and the shafts is expected to be so low that it is negligible. Sealing in each case is accomplished by a flexible sheet metal element conforming to a smooth stiff metal part.

All components of the diverter are made of corrosion-resistant materials. The high-temperature portions of the diverter are made of heat-resistant materials.

The diverter has been designed for a 1000-hour life under the design conditions. The butterfly blades and the actuation mechanism have been designed for 10,000 reversals of position.

Bolt flanges are used at the inlet and exits of the diverter to minimize weight. The inlet flange ID is 20.70 inches. The ID's of the exit flanges are both 14.95 inches. To minimize leakage through the bolted joints, it is expected that crimped thin sheet metal gaskets will be used.

Figure 35. Valve Assembly, Diverter.

This is a technical engineering drawing with multiple detail and section views. The following text labels are visible:

51219-2

MS 924526

M81042L-6

-9 (REF)

51219-3 (REF)

1.533 (REF)

.898 (REF)

5.205

SECT B-B

DETAIL -2

DETAIL -3

5121B

-B-

-C-

-D-

DETAIL -1

SECT A-A

51214-2

M99360-2

51213-1

MS209

13

-A-
.0002
515
.300
020
013

SCALE: 10 X SIZE

51216-1
51216-2
51214-1
51213-2 △
5218
51215-1
(8)(9) ⚄
51219-3
MS 9245-26
51219-4
(1)
51217-2
51217-1
(2)

△

MS 9245-26

51219-5

SCALE: 2 X SIZE
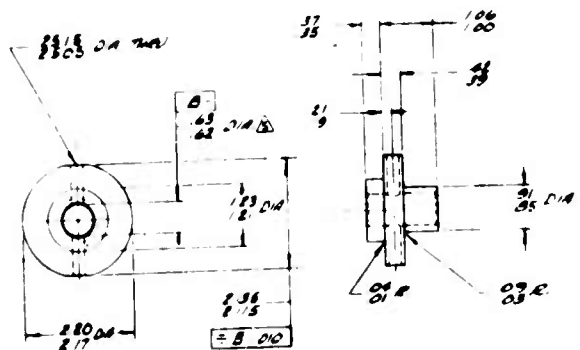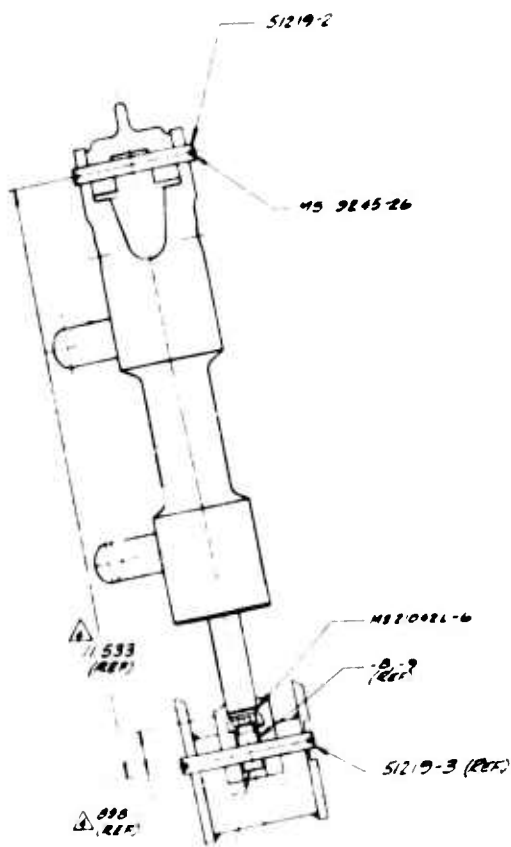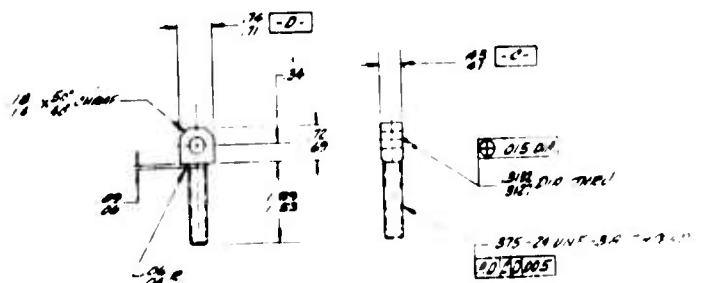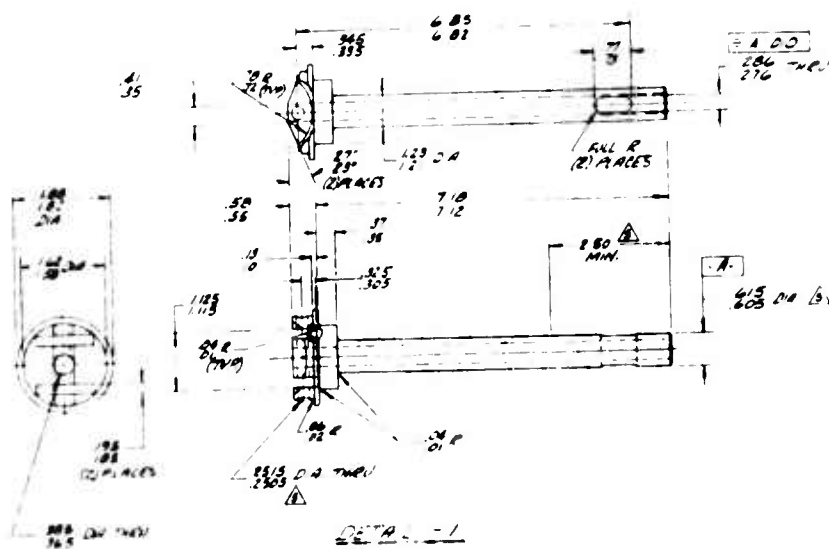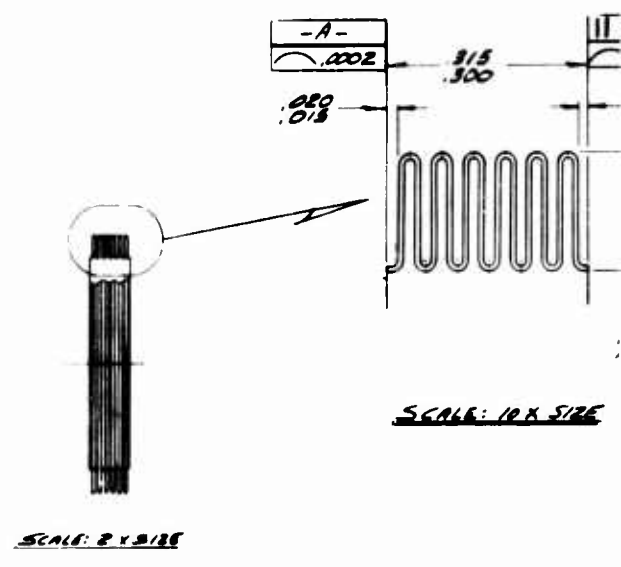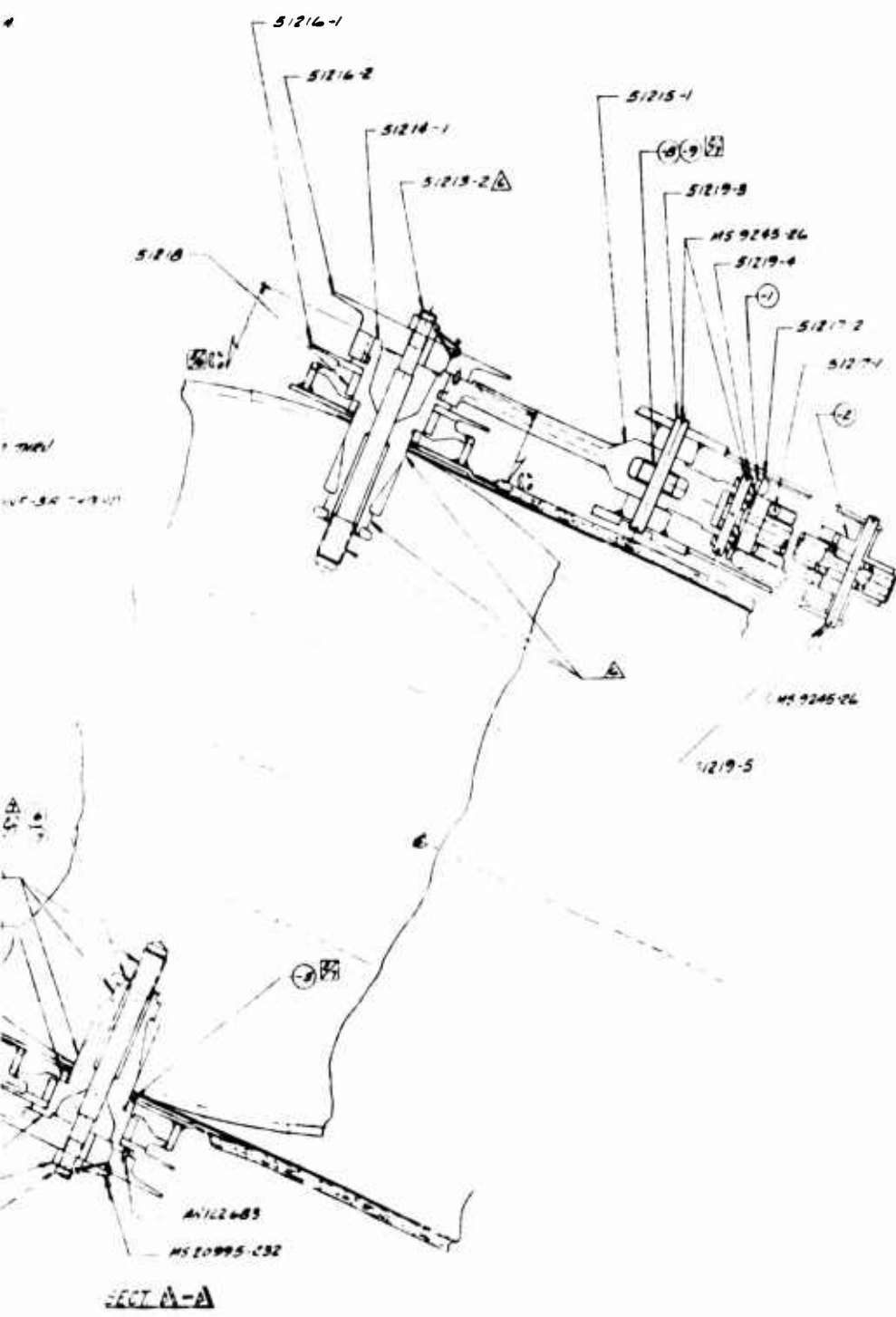
DETAIL - 4 ⚄

NUMBER OF CONVOLUTIONS --- 6
PITCH ---------- .048
MAT'L THICKNESS -------- .00
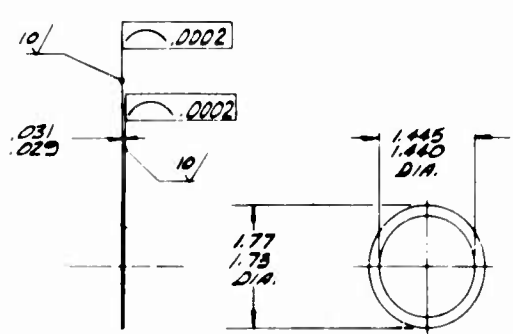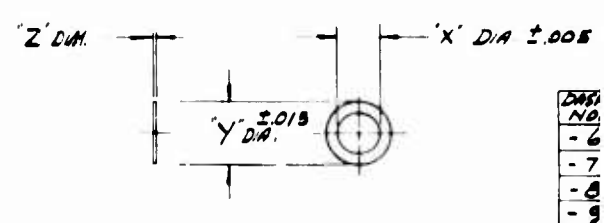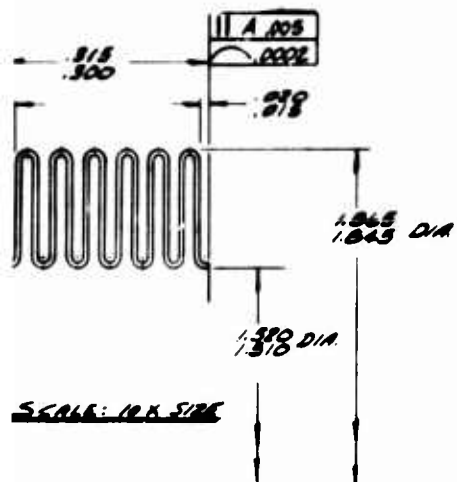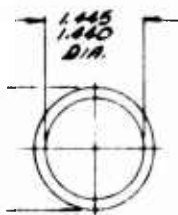
10   .0002
          .0002
.031
.029   10

1.445
1.440
DIA.

1.77
1.73
DIA.

DETAIL - 5 ⚄

"Z" DIA.   "X" DIA ±.005
"Y" DIA ±.013

DASH NO.
-6
-7
-8
-9

DETAIL -6, -7, -8 & -9

THRU

AN122683
MS 20995-C32

SECT A-A

C

.815
.300

A .005

.0002

.278

1.865
1.823 DIA.

1.388 DIA.
1.318

SCALE: 10 X SIZE

'OLUTIONS ... 6

.048

.008

1.445
1.440
DIA.

'X' DIA ±.005

DASH NO.	'X DIA.	Y DIA.	Z DIM.
-6	.578	.92	.002
-7	.578	.92	.005
-8	.328	.69	.002
-9	.328	.69	.005

6-9

'V' NOTCH POSITION RELATIVE TO ℄ P/N 51210
TO BE AS INDICATED BELOW. ℄ OF EACH
BELL CRANK TO BE COINCIDENT WITH 'V' NOTCH

℄ P/N 51231-1

4°2' (REF)

'V' NOTCH IN
P/N 51214-1

℄ P/N 51210 (REF)

4°2' (REF)

℄ P/N 51215-1
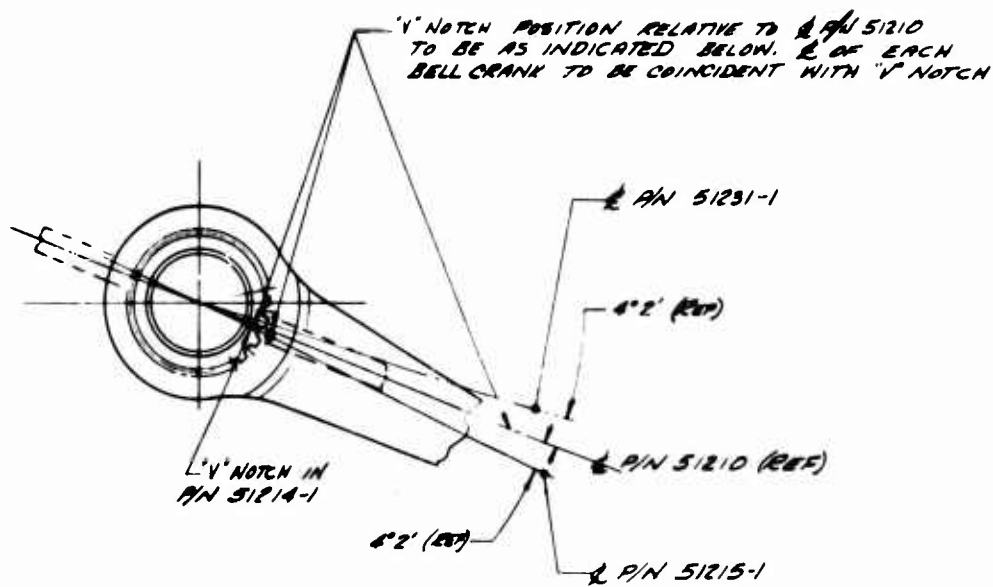
SECT. C - C

D

Metal-covered insulation envelops all of the diverter except the flanges and the areas close to the shaft bearings where cooling is beneficial.

The total calculated weight of all components shown on the diverter assembly (Figure 35) is 118.76 pounds.

5.1 VALVE HOUSING

The valve body or housing is shown in Figure 36. Basically, the housing is a Y-shaped duct. Each branch of the Y becomes a 14.95-inch ID cylinder. A 60-degree cascade turn is attached to the downstream end of one branch of the Y.

Each branch of the Y ends with a 14.95-inch ID bolting flange. The inlet bolting flange has a 20.70-inch ID.

A major portion of the housing is supplied by one-half stamping (Figure 36). Since this part of the diverter is symmetrical, two identical parts are butt welded to form the near and far sides of the Y.

This half stamping is made of 0.009-inch-thick Rene' 41 sheet. In some areas where strength, stiffness, and thermal distribution permit, the thickness of the half stamping is reduced by chemical milling to minimize weight.

The 14.95-inch ID cylindrical portions (Figure 36) of the Y branches are made of 0.03-inch-thick Rene' 41. The cylinders are resistance welded to the downstream edges of the 0.09-inch-thick half stampings.

The upstream edge of each cylinder extends about 3 inches forward of the resistance weld to the half stamping. This 3-inch extension is a relatively flexible member that can conform to the shape of the closed blade to make a seal.

A raised bead near the downstream edge of each half stamping provides a cavity in which the seal can flex. This bead also acts as a circumferential stiffener around each Y-branch.

Holes are provided through both the seal and the 0.090-inch half stamping to accommodate the shaft of the butterfly blades.

The bearing housing (Figure 36) is isolated from the hot structure by an open truss standoff. This standoff permits ventilation to keep the bearing well below the allowable temperature.

If no restraints were provided, the Y-shaped diverter would be grossly distorted by pressure tending to bulge the flat sides of the Y.

Restraint is provided by the shafts acting in tension to prevent the bearing housings (Figure 36) from bulging apart.

The valve housing between the bearing housings is prevented from bulging by a welded box beam (Figure 36).

59

The Y-branch in the area of the cascade turn consists of two half stampings (Figure 36).

The hollow airfoil cascade vanes protrude through holes in the half stampings and are fillet welded to the stampings. By extending the vanes through the stampings, any possibility of the vanes' coming loose in the event of weld cracking is minimized.

The ends of the vanes have sheet metal plugs (Figure 36) welded across them to maintain the hoop tension capability of the duct wall.

Insulation covers all of the valve housing except for the flanges and around the bearing housing. The insulation is expected to minimize sharp thermal gradients that might cause thermal fatigue cracks.

5.2 BLADE SHAFT AND BEARINGS

All of the loads on each blade are transmitted from the blade (Figure 37) into the shaft (Figure 38) and out through the bearing (Figure 39). Since the blade shear load is cantilevered approximately 0.75 inch from the blade to the bearing, a bending moment is developed in the shaft.

In the shaft (Figure 38) which also transmits the actuator torque loads, the shear, bending moment, and torque stresses are additive where the shaft enters the blade. The spline for transmitting torque between shaft and blade is located near the bottom of the cavity. This location removes the stress concentrations from the shaft and blade where the stresses are highest at the entrance to the cavity. Otherwise the shaft would be larger and heavier and the blade hub would be thicker walled and heavier.

Both the shafts and the stud (Figure 40) are made of Inconel 713C (low iron, low carbon), the same material as the blade, because the hot ends of these parts carry high stresses.

The hub, shaft, and bearing designs (Figure 35) have been arranged to keep the bearing cooled below approximately 1100°F. Past experience has demonstrated that the titanium carbide bearing will operate satisfactorily below this temperature.

The bearing housing is isolated from the hot valve housing by a wire support strut (Figure 36) that permits ventilation. Contact between the blade and shaft has been minimized to reduce heat pickup. The outer end of the shaft is further cooled by two cooling fins (Figure 41).

The studs (Figure 41) act in tension to keep the bearing and valve housing from moving away from their nominal position relative to the blade when the valve housing is pressurized. This restraint helps maintain the shape of the valve housing and the seal.

60

Figure 36. Housing Assembly Valve (Sheet 1 of 2).

61

SIMILAR TO -2
EXCEPT AS SHOWN

B20

16.268
16.235
DIA.

14.960
14.960
DIA.

15.75 DIA.R
-D-

.063 TYP 500
--10 & 41

.28 DIA. THRU (60) PLACES
EQUALLY SPACED

6°

⊕ D .02 DIA

M

N

2.181

3.55 R.

16.193

.063 TYP
(3) PLACES

30
APPROX.
TANGENT

10
(REF)

FIT AROUND DETAILS
-8 & -9 APPROXIMATELY
AS SHOWN AT SECT.G.G
ON SHEET #4

TACK WELD TO FLANGE
8 TO -19 AS
NECESSARY

565   2.667   4.951

1.910

2.974

14.960 DIA.
14.960 DIA.

15°

22.015 DIA.
21.985 DIA.

20.710
20.680
DIA.

21.500
DIA. R.
-B-

.210 DIA. THRU (72) PLACES
.211 EQUALLY SPACED

5°

⊕ B .R DIA

VIEW A-A

9.42

12.10 R

10.58

.41
.35

SECT. D-D

(12) PLACES
SPACED

.19

18.26 R.

℄ SYM.

℄ SYM.

SECT. B-B

9.92

℄ SYM.

11.05 R.

41/.35

℄ SYM.

SECT. C-C

8.84

℄ SYM.

14.78 R.

10.58

41/.35

℄ SYM.

SECT. E-E

8.26

℄ SYM.

22.08 R.

41/.35

9.62

8.67

℄ SYM.

15.340
(REF)

SECT. F-F

C

Figure 36. Housing Assembly Valve (Sheet 2 of 2).

MINIMUM RADIUS ON
UPSTREAM SIDE OF
DETAIL B BLEND
SMOOTH INTO ADJACENT
AREAS

15.940
(REF)

SECT U-U

SECT B-B

CONSTANT

SECT V-V

SECT S-S

2950

VANE CROSS SECTION CONSTANT
SCALE 5 × SIZE

SECTION N-N
CENTER OF SPHERE

11. CUT, FIT, RESISTANCE TACK
CLAMP SOLAMI 'C' TO PROD
SNUG COVERING.

12. SOLAMI 'C' FOIL MAY BE
SOLAR, DIVISION OF INT'L.
2200 PACIFIC HWY SAN D

13. MAT'L TO BE APPROX .25 INCH
(2) PLIES MAY BE PURCHASE
H. I. THOMPSON FIBER GL
600 WEST 135th ST.
GARDENA, CALIF.

14. UNLESS OTHERWISE SHOWN,
RADII TO BE 1.5 TO 2 × M

15. HEAT TREATMENT SOLUTION TREA
FOR 30 MIN PLUS 1650°F

QTY REQ'D	QTY REQ'D	PART NUMBER	DESCRIPTION	MATERIAL	SPECIFICATION	UNIT WT	
		-16	BAND	MIL-S-6721	TYPE I (CRES)	.30	
		-15	SOL ANN'G FOIL	MIL-S-6721	TYPE I (CRES)	.92	
		-14	INSULATION	A-100		1.57	
		-13	VANE CAPS	AMS 5545	.025 CRES SHEET		
		-12	VANE	AMS 5545	.025 CRES SHEET		
1		-11	FLANGE	AMS 5759 B	BAR STOCK		
2		-10	FLANGE	AMS 5759 B	BAR STOCK	1.90	
4		-9	HOUSING, BRG.	AMS 5759 B	BAR STOCK	.88	
4		-8	WIRE SUPPORT	AMS 5796	.156 DIA. WIRE	.07	
4		-7	CAP PLATE	AMS 5537A	.156 CRES SHEET	.12	
4		-6	SADDLE BRKE	AMS 5537A	.125 CRES SHEET	.15	
1		-5	STAMPING, ELBW	AMS 5545	.09 CRES SHEET	.9	
1		-4	STAMPING, ELBW			1.9	
1		-3	TUBE EXHAUST			.143	
1		-2	TUBE EXHAUST		.09 CRES SHEET	9.00	
2		-1	STAMPING, HALF	AMS 5545	.09 CRES SHEET	3.66	

LIST OF MATERIAL (PARTS LIST)

ASSY NO.

NOTES: UNLESS OTHERWISE SPECIFIED

1. DIMENSIONS LOCATING THE TRUE POSITION ARE BASIC

2. DO NOT SCALE DRAWING. WORK TO DIMENSIONS GIVEN

3. DRAWING INTERPRETATION PER MIL-D-1000 & SOLAR SPEC 9-32 & 9-4, SECTION 5.0 6.0 & 7.0

4. ALL POINTS OF DIAMETER [A] WITHIN AREA SHOWN TO BE WITHIN .003 OF TRUE POSITION.

5. ALL POINTS OF DIAMETER [A] WITHIN AREA SHOWN MUST BE WITHIN .01 OF TRUE POSITION.

6. ALL POINTS OF DIAMETER [A] WITHIN AREA SHOWN, MUST BE WITHIN .03 OF TRUE POSITION.

7. EXCEPT AS SHOWN, DIMENSIONS APPLY AT POINTS PERPENDICULAR TO INLET EDGE OF -2 & -3

8. THICKNESS TO BE OBTAINED BY CHEM-MILLING OR EQUIVALENT PROCESS

9. IDENTIFY PER SOLAR SPEC. 9-6 CLASS "M".

10. CONTOUR OF VANE TO BE WITHIN .01 OF BASIC SHAPE

(left column fragments)

...TANCE TACK WELD & BAND
...'C' TO PRODUCE NEAT,
...ING.

...L MAY BE PURCHASED FROM
...ON OF INT'L HARVESTER CO
...WAY SAN DIEGO 12, CALIF.

...PPROX .25 INCHES TOTAL THICKNESS
...BE PURCHASED FROM.
...SON FIBER GLASS CO.
...135TH ST.
...CALIF.

...WISE SHOWN ALL INSIDE BEND
...1.5 TO 2 X MAT'L THICKNESS

...SOLUTION TREAT -O ASS'Y AT 2150°F
PLUS 1650°F FOR (4) HOURS

Figure 37. Blade (Sheet 1 of 2).

FLAME SPRAY THIS AREA USING STELLITE 6 (B)
MIN DEPTH AFTER FINISHING TO BE .010
FLAME SPRAY COATING TO BLEND SMOOTHLY
WITH CAST SURFACE OUTSIDE OF THE 15°
(MIN) AREA

℄ CYLINDER WITH
BLADE IN
CLOSED POSITION
(REF)

AN CONSTANT
SURFACE OF BLADE WHICH IS
TANGENT TO THE 16.95 DIA
CYLINDER IS TO BE WITHIN
.002 OF BASIC LOCATION

2 2.95
(4) PLACES

M 6° (TYP)
EXPOSED CASTING SURFACE
TO BE WITHIN .02
OF BASIC LOCATION

2 2.85
(4) PLACES

THIS POINT IS
TANGENT TO THE
16.95 DIA CYLINDER
(REF)

THIS POINT IS ON THE ELLIPSE
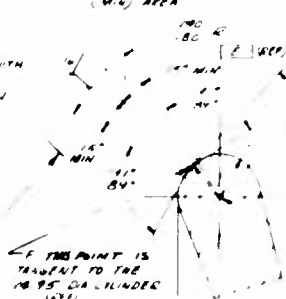
DETAIL T   SCALE 4X
CONSTANT AROUND EDGE OF BLADE
FROM POINT B TO POINT B
EXCEPT FOR BLEND WITH ADJACENT
SURFACES NEAR POINTS B & B

THIS POINT IS ON THE ELLIPSE

THIS POINT IS TANGENT TO THE 16.95 DIA CYLINDER (REF)

6° (TYP
EXPOSED CASTING SURFACE
TO BE WITHIN .02
OF BASIC LOCATION

FLAME SPRAY THIS AREA USING STELLITE 6 (B)
MIN DEPTH AFTER FINISHING TO BE .010, FLAME
SPRAY COATING TO BLEND SMOOTHLY WITH CAST
SURFACE OUTSIDE OF THE 15° (MIN) AREA

16.95 DIA.
CYLINDER
(REF)

AN CONSTANT SURFACE OF BLADE WHICH IS
TANGENT TO THE 16.95 DIA CYLINDER IS TO
BE WITHIN .002 OF BASIC LOCATION

DETAIL   SCALE 4X
CONSTANT AROUND EDGE OF BLADE
FROM POINT A TO POINT A EXCEPT
FOR BLEND WITH ADJACENT SURFACES NEAR
POINTS A & A

BASIC SURFACE BETWEEN 16.95 DIA & 1.91 DIA
IS THE 16.95 DIA CYLINDER.
FLAME SPRAY THIS AREA USING STELLITE 6 (B),
MIN DEPTH AFTER FINISHING TO BE .010, FINISHED
FLAME SPRAY SURFACE TO BE WITHIN .002 OF
BASIC LOCATION, FINISHED FLAME SPRAY SURFACE
CONSTANT TO BLEND SMOOTHLY WITH ADJACENT FINISHED
EXCEPT BLEND FLAME SPRAY SURFACE INDICATED IN DETAILS U & T
AREA SHOWN

16.95 DIA
CYLINDER
(REF)

SECTION W-W
(TYP BOTH HUBS)

B

BLANK PAGE

SECTION A-A

SECTION B-B

SECTIONS J-J, K-K, L-L, M-M, N-N, P-P, R-R & S-S
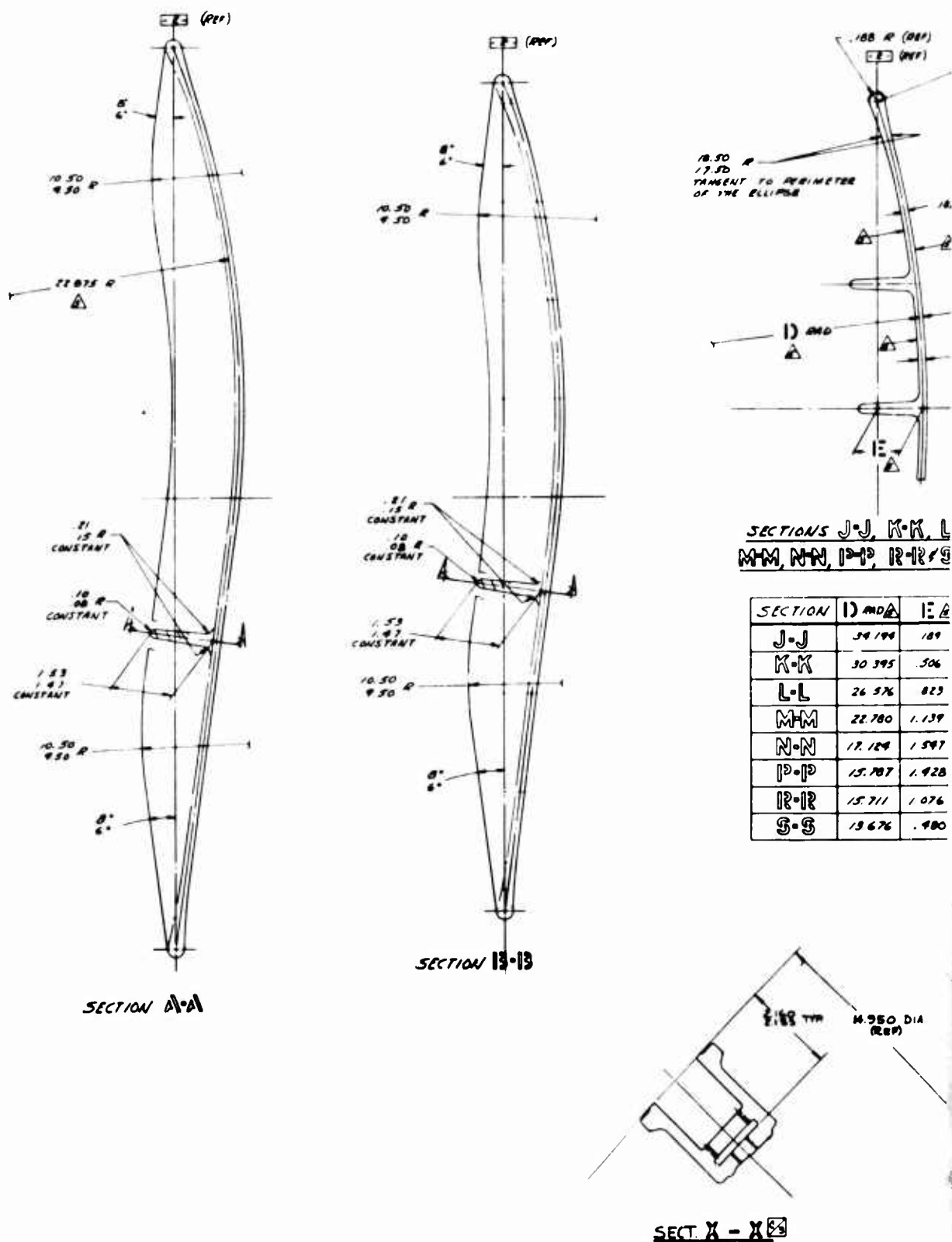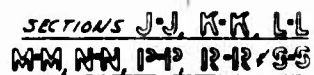
SECTION	D MOD	E
J-J	34.194	.189
K-K	30.395	.506
L-L	26.576	.823
M-M	22.780	1.139
N-N	17.124	1.597
P-P	15.707	1.428
R-R	15.711	1.076
S-S	13.676	.480

SECT. X-X

Figure 37. Blade (Sheet 2 of 2).

SECTIONS J·J, K·K, L·L
M·M, N·N, P·P, R·R, S·S

SECTION	D RAD	E
J·J	34.194	.189
K·K	30.395	.506
L·L	26.576	.623
M·M	22.780	1.139
N·N	17.124	1.597
P·P	15.707	1.428
R·R	15.711	1.076
S·S	13.676	.980

SECTIONS C·C, D·D, E·E
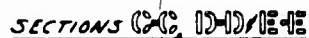
SECTION	B RAD	C RAD
C·C	.28 / .22	5.06 / 4.99
D·D	.53 / .47	3.81 / 3.69
E·E	.78 / .72	3.06 / 2.99

SECTIONS F·F, G·G, H·H
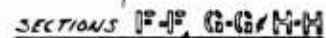
SECTION	A RAD
F·F	2.81 / 2.69
G·G	2.56 / 2.44
H·H	2.91 / 2.19

SECT. X - X

SECTION V·V

B

2).

Figure 38. Shaft, Tabulated.

Figure 39. Bushing.

69

Figure 40. Stud, Tabulated.

Figure 41. Fin, Cooling.

70
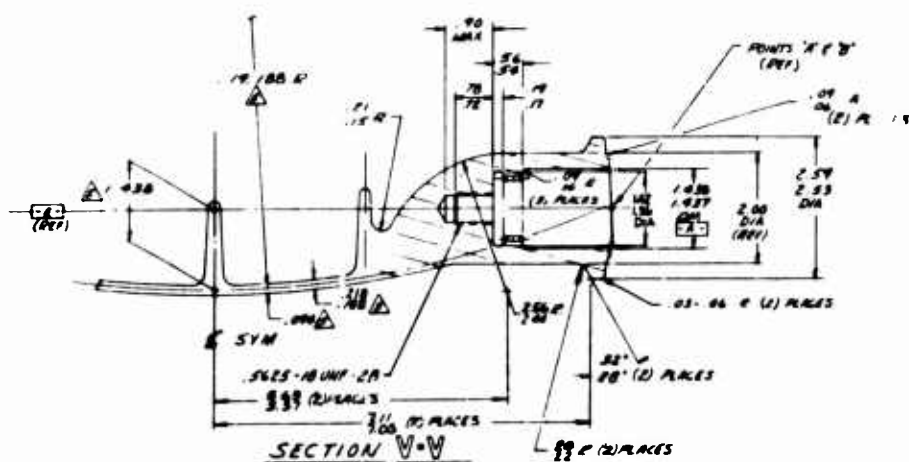
5.3 VALVE BLADE

The butterfly blade is shown in Figure 37. It is an investment casting of a low-iron, low-carbon version of the Inconel 713C alloy selected because of its higher creep strength and elongation.

The edge of the blade approximates an elliptical shape. The shell of the blade is dished to provide a double curved surface. For the same weight, the dished shape has a much greater allowable bending load than a flat blade. The shell shape does not vary greatly from streamlines of the gas flow; therefore, drag and pressure drop are kept low. Integral stiffeners parallel to the flow prevent the relatively thin shell from buckling.

The edge of the blade is flame sprayed with Stellite 6, a carbide-bearing cobalt-base material, to minimize friction, wear, and galling against the Rene' 41 nickel-base seal.

The two hubs on each blade have cavities to accommodate the shafts. An internal spline, to transmit torque to the shaft, is located near the bottom of the cavity. This internal spline keeps stress concentrations away from the more highly stressed areas of the shaft and hub at the top of the cavity.

5.4 BLADE LINKAGE MECHANISM AND ACTUATION SYSTEM

The linkage mechanism and actuator arrangement are shown in Figure 35.

The valve blades act in unison through a parallelogram four-bar linkage. Bell cranks (Figures 42 and 43) are attached to the shafts (Figure 38). These bell cranks form the short ends of the parallelogram. The valve body is one of the long sides. The linkage (Figure 44) forms the other long side.

A double-acting hydraulic cylinder (Figure 45) actuates the parallelogram linkage to reverse the positions of the open and closed blades. The cylinder actuates the linkage by forcing the angle at one corner of the parallelogram to open or close.

An overcenter spring arrangement (Figure 46) provides 1500 inch-pounds of closing torque to the closed blade. The linkage converts aerodynamic opening torque on the open blade to closing torque on the closed blades.

After flow tests show the amount of aerodynamic torque, the springs will be adjusted to provide a total of 1800 inch-pounds of closing torque to the closed blade. The spring torque can be adjusted by using either one or both of the springs or by designing other springs.

The aerodynamic torque is subject to considerable variation from the calculated value for several reasons. The dynamic pressure at the trailing edge of the blade is four times the dynamic pressure at the leading edge because of the flow convergence. No test data are available for a butterfly blade in a strongly convergent duct nor for a curved thin shell butterfly blade in a duct bend. Because of these

71
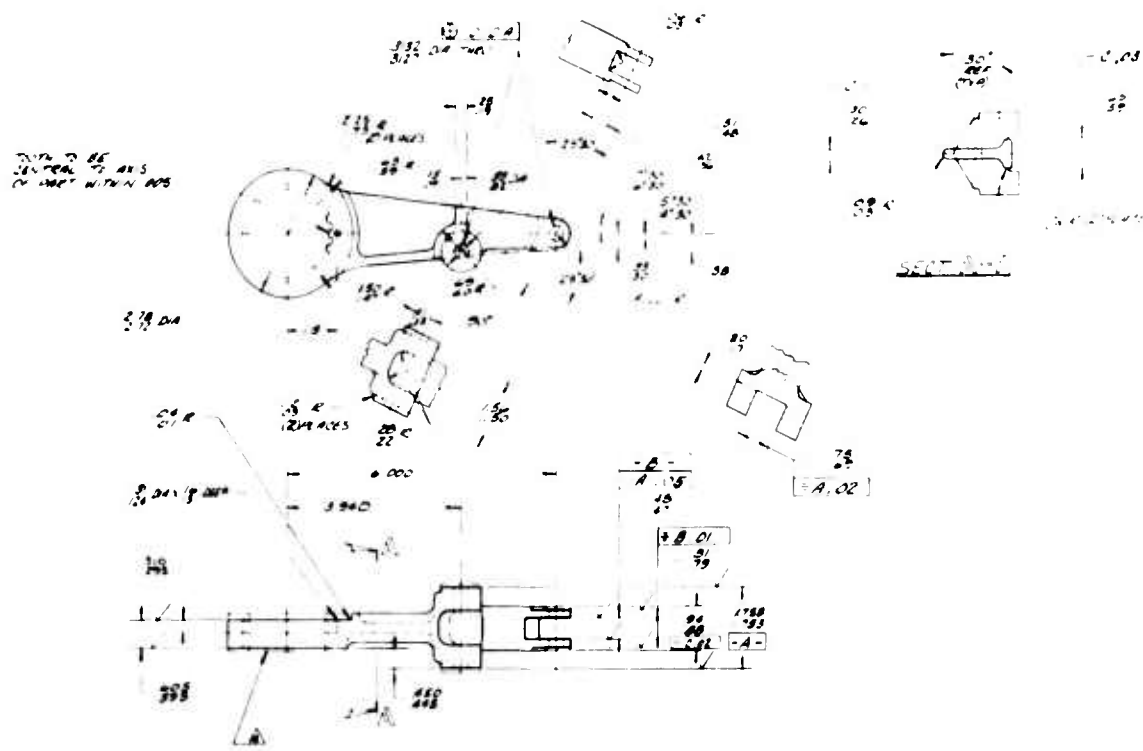
Figure 42. Bell Crank, Short.
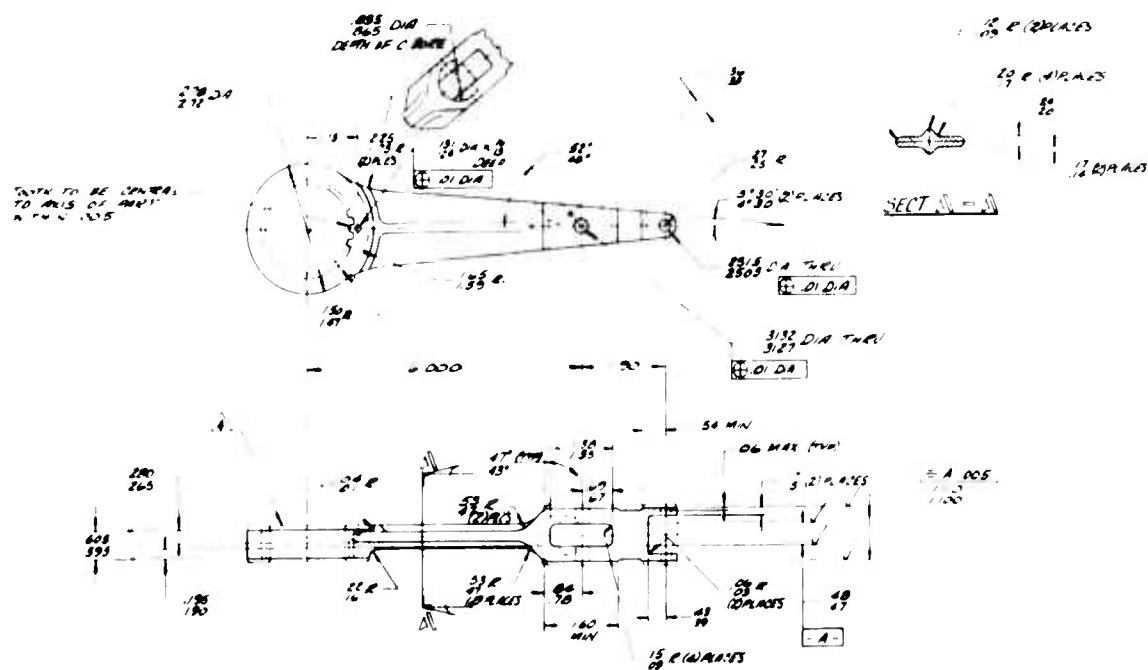
Figure 43. Bell Crank, Long.
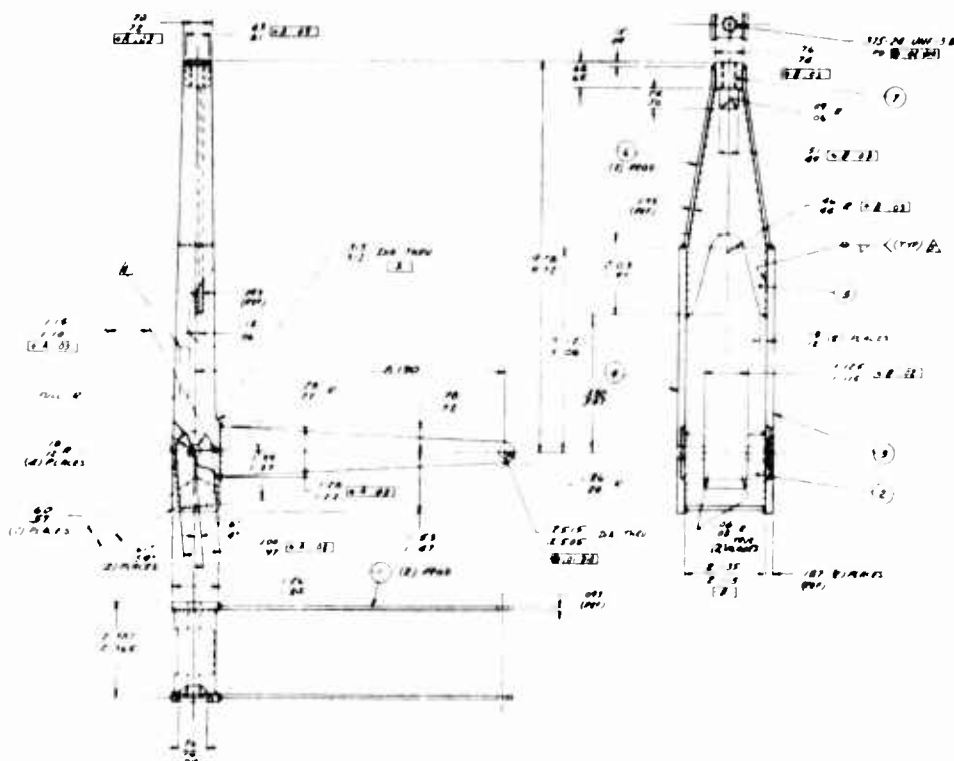
Figure 44. Linkage Assembly.

considerations, particularly the variation in dynamic pressure, the aerodynamic torque is expected to be less than the calculated value which was based on a symmetrical butterfly blade in a straight duct with no variation of dynamic pressure.

At the beginning of an actuation cycle, 1800 inch-pounds of torque holds the blade closed. The 300-psi hydraulic cylinder provides 2700 inch-pounds of opening torque to overcome the 1800 inch-pounds of closing torque on the closed blade, leaving a net 900 inch-pounds of opening torque.

The operation of the hydraulic cylinder and the blade linkage will be described in detail. The description is the same no matter which of the bosses (Figure 45) acts as the inlet port.

The 3000-psi hydraulic pressure enters through the port in the (Figure 45) boss. The 187-CKF-005 Leechek (Figure 45) check valve in the boss permits the incoming flow to bypass the 187-5-03000-0808 Lee Jet orifice (Figure 45).

The incoming flow passes through a hole in the wall of the cylinder (Figure 45) into an annular groove in the cylinder and the cylinder body. Then the 187-CKR-005 Leechek check valve (Figure 45) permits the incoming flow to bypass the 187-5-08000-0808 Lee Jet orifice and the piston rings (Figure 47).

Thus, the 3000-psi fluid is able to pressurize the annular cavity between the outside diameters of the piston rod and head. The net piston area is 0.468 square inch.

73

Since the rotational inertia of the blades is relatively small, the blades rotate very quickly. Within approximately 0.010 second, the blade has accelerated to a rotational velocity limited by an orifice in the outlet boss. On the downstream side of the piston head, the fluid flows freely through open passages until it reaches the flow control devices in the outlet boss. The 187-CKR-005 Leechek check valve closes and permits flow only through the 187-5-03000-0508 Lee Jet orifice.

As the closed blade opens, the closing, or resisting, torque from the overcenter spring and from the aerodynamic force reduces until at mid-cycle the resisting torque is zero. The net pressure drop across the orifice in the outlet boss and the rotational speed of the blades are increasing.

As the cycle passes over center, the aerodynamic, overcenter spring and actuator torques become additive and the blade speed continues to increase, limited only by the orifice in the outlet boss.

To prevent the closing blade from damaging the seal during the seating phase, most of the kinetic energy in the blade is dissipated by a snubber just prior to seating.

The snubbing action begins as the piston rings (Figure 47) enter the body (Figure 45). The piston rings seal the cavity between the piston head and the body except for flow through the 187-5-08000-0808 Lee Jet (Figure 45), through the 13 VC5CM Lee Visco Jet (Figure 45), and a possible slight leakage of the rings.

The 187-CKR-005 Leechek check valve in the body is closed during snubbing. The orifice in the outlet boss also contributes to the snubbing.

The kinetic energy in the blades is relatively small, so most of it is dissipated within 0.020 inch of piston travel.

The blade stabilizes at an approximately constant equilibrium velocity prior to seating. The piston and blade velocities are limited to a low value after snubbing by the orifices in the body and in the outlet boss.

The time for the entire sequence is calculated to be 0.85 second. This can vary slightly due to friction and tolerances on orifices. The time can be varied by changing orifice sizes (replacing the Lee Jets).

A very small orifice (13VC5CM Lee Visco Jet, Figure 45) permits a small cooling flow of fluid if desired. Cooling is not expected to be required if the temperature remains below 250°F.

The maximum differential pressure across any of the seals during snubbing is not expected to exceed about 4000 psi. Both static and dynamic seals adjacent to the snubbing cavity are rated at 5000 psi.

The total energy supplied by the hydraulic fluid is about 3750 inch-pounds. Most of it is dissipated through the orifices. The average power requirement is about 0.75 horsepower for 0.85 second. The peak is about 2 horsepower. It is expected that an accumulator could easily provide this requirement for 1 second.

74

Figure 45. Cylinder Assembly, Hydraulic (Sheet 1 of 2).

CP18 (8) PLACES △
(REF)

(4) REQD
IN ADJACENT
S TO BE APPROX.
APART

A

A

P1 (8) REQD

CP2 (4) PLACES
INSTALL PER MS 33540

CP3 (8) REQD △

CP3 (2) REQD △

CP4

SECTION A · A
TYPICAL (2) PLACES

(Sheet 1 of 2).

B

Figure 45.   Cylinder Assembly, Hydraulic (Sheet 2 of 2).

·4 DET

DETAIL NO SCALE

·8 DET   ·7 DET

·10 ASSY

raulic (Sheet 2 of 2).

B
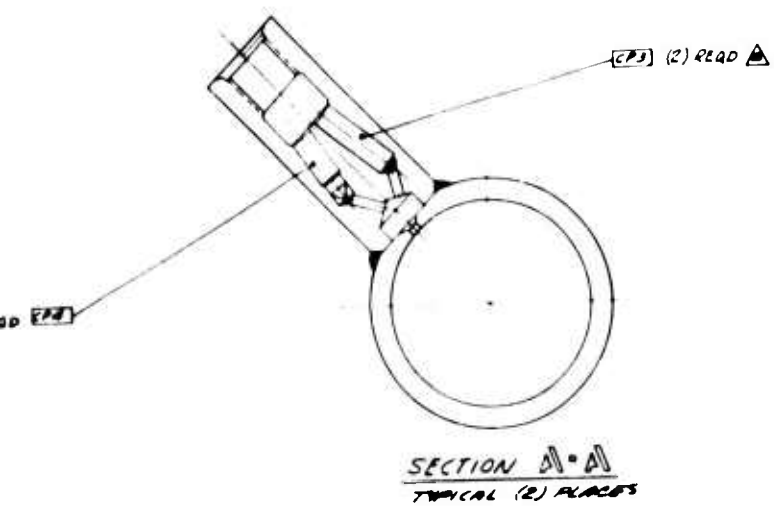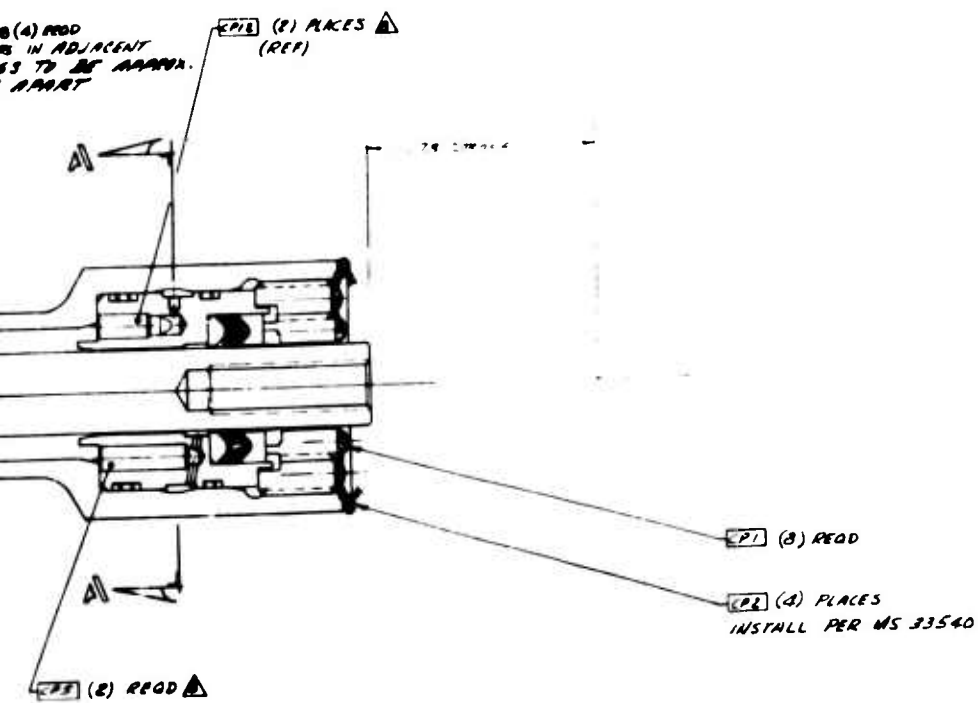
	-2 DET	-1 DET
O.D. INCHES	2.00 ± .018	1.19 ± .015
WIRE DIA - INCHES (TOL PER MATL SPEC)	.375	.250
MATERIAL	CRES 17-7 CH 900 △4	CRES 17-7 CH 900 △4
DIRECTION OF HELIX	RH	LH
ENDS	SQUARED & GROUND	SQUARED & GROUND
MIN No. OF ACTIVE COILS	13.5	17
MAX SOLID HEIGHT	5.67	4.97
AT COMPRESSED LENGTH OF	6.00	5.28
LOAD SHALL BE	109.5 - 116.5 LBS	494 - 534 LBS
APPROX No. OF TOTAL COILS	15.75	19.5

Figure 46. Spring, Tabulated.
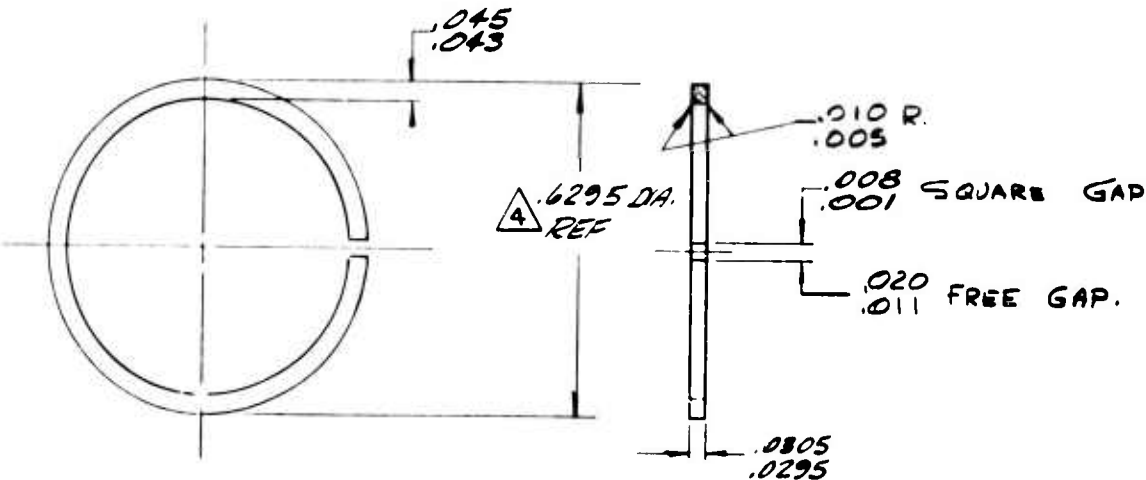
Figure 47. Ring Piston.

5.5 SEALING PRINCIPLE

Five areas require sealing against leakage. These seal areas surround the four shafts for both the open and closed blades and are around the edge of the closed blade where it meets the duct.

The success of the diverter depends largely on how effectively all leakage paths are sealed. The sealing approach, combined with good manufacturing practice and development testing, is expected to achieve a nearly zero leakage seal.

The sealing principle is similar at each location. A flexible sheet metal element conforms to a smooth stiff metal part. The rubbing materials, which consist of pairs of cobalt-base versus iron- or nickel-base materials, minimize friction, wear, and galling.

The four shaft seals use a bellows slightly compressed at installation. Internal pressure expands the bellows ends firmly against the flat mating surfaces. The finish and flatness of the bellows ends and mating surfaces are controlled so that almost no leakage exists in these areas.

The seal around the closed blade is similar to a seal formed by rotating a rigid ellipse inside a flexible thin-wall circular duct. The duct diameter is the same as the ellipse minor diameter. A portion of the thin-wall duct is stretched around the blade in a manner similar to a barrel hoop. If the blade edge and the flexible cylindrical seal are close to their nominal shape and location, a snug metal-to-metal fit will be produced. Very low leakage would be expected.

Pressure and temperature gradients are expected to cause the seal around the blade to vary somewhat from its nominal shape. Development testing probably will be required to obtain the nominal blade shape for the best fit against its seal.

The specified maximum permissible leakage of 0.5 percent permits an average gap of nearly 0.010 inch. It is expected that the actual leakage will not exceed 0.1 percent of the total flow - an average gap of 0.002 inch - if the seal development program outlined in the development test section is followed.

5.6 AERODYNAMIC DESIGN CONSIDERATIONS

A minimum pressure drop and a minimum flow distortion at the exit were two objectives considered during design of the diverter for both the through flow and the diverted flow.

The internal flow configuration of the diverter resulted from a balance of several considerations.

The design requirement was for a diverter that would not change the direction of the through flow, but that would change the direction of the diverted flow by 90 degrees.

80

The loss coefficient for a duct with a turn of a given angle would be expected to be less for a smooth, well-designed turn than for a turn that includes a curved butterfly blade. A greater loss coefficient results from the blade and from the duct wall intersections as well as other inevitable flow discontinuities, even when minimized, which contribute to flow separation and increased drag or pressure drop. Therefore, it was decided that no greater turn than necessary should occur in the area where the primary diversion function occurred (i.e., in the area of the blade). Also, flow distortion would be less with a smaller angle. Additional turning required to complete the 90-degree, or other, turn could be accomplished more efficiently with a conventional turning device.

If the through flow were to be essentially undiverted, relative to the turbine axis, another bend equal to and opposite any bend that occurred in the symmetrical diverter would have to be added to straighten the flow, making an S-bend. Therefore, the loss for the through flow for this S-bend would be increased approximately proportional to the angle of primary diversion.

To keep the angle of turn small through the diverter, it was desirable to have the entrance diameter larger than the exit diameter. This arrangement permitted a strongly convergent flow throughout the length of the blade. Convergence is helpful because it can suppress small tendencies toward flow separation which could increase the pressure drop.

The design requirement was for a velocity of $M = 0.35$ from each exit of the diverter. This requirement caused the exit flow diameter to be 14.95 inches. The entrance flow diameter that provided the best balance of all the considerations is 20.70 inches. The entrance velocity for this diameter is $M = 0.17$.

The median line of the thin-shelled butterfly blade was designed to deviate as little as possible from the probable flow streamlines. The actuator linkage was designed to permit the angle of the open blade to be adjusted slightly to obtain the lowest pressure drop. The optimum angle of opening can be determined from either a flow test model or a prototype of the diverter.

The angle of diversion in the area of the blade is 15 degrees. The through flow then requires an opposite or S-bend of 15 degrees. To keep the pressure drop to a minimum, it is desirable to have the opposite 15-degree bend at the upstream end ($M = 0.17$) rather than at the downstream end ($M = 0.35$).

This 15-degree upstream elbow is not included in the diverter assembly. It is expected that if necessary it would be incorporated in the adjacent upstream section of ducting.

By having the 15-degree elbow in the adjacent duct, the two bolt flanges between the elbow and diverter have sufficient circumferential stiffness to contribute to the pressure stability of the diverter body.

For the diverted flow, the 15-degree turn of the upstream elbow and the 15-degree turn in the blade area are additive. To complete a 90-degree turn, a downstream device to turn the flow an additional 60 degrees is required.

81

A simple elbow with a center line bend radius to diameter ratio of 2.0 (about a 30-inch radius) will turn the flow efficiently. However, the flow can be turned as efficiently in a much smaller envelope if a mitered joint with a cascade, or row of turning vanes, is used. The weight and cost of the assembly are increased by the cascade turn and are believed to be justified by the reduction in envelope.

The cascade has other advantages. Perhaps the most important is that it can accommodate a flow with a considerable swirl or distortion or with a varying angle of incidence without suffering a significant loss in efficiency. These variations of flow can easily cause flow separation and greatly increased pressure drop in a simple elbow.

The other principal advantage of the cascade is that the outgoing flow will usually have less distortion than a simple elbow because secondary flow is limited. The cascade has a flow-straightening capability.

Of course, in an installation where the envelope would permit a simple elbow instead of the cascade, the cost and weight reduction of the simple elbow probably would be justified. In such an instance, a flow test should demonstrate that the pressure drop and other flow characteristics are satisfactory.

Three types of turning vanes were considered:

- Thin circular arc

- Thin noncircular arc

- Thick airfoil vanes

The thin circular arc vanes usually have a higher pressure drop, so they were not seriously considered. The thin noncircular arc vanes can have almost as low a pressure drop as the thick vanes if the flow is uniform. Also, the cost and weight are lower. However, they cannot tolerate much variation in angle of incidence without considerable flow separation and pressure drop. The thick vanes were selected because they can tolerate considerable variation in angle of incidence without much change in pressure drop. These vanes were made hollow by fabricating from sheet metal to minimize weight.

Tests by several investigators have shown that more efficient turning occurs if the vanes near the inside of the turn are spaced progressively closer. Therefore, the vanes for the 60-degree turn are spaced in this manner.

5.7 STRUCTURAL ANALYSIS

Stress analysis calculations for the diverter valve (Figure 35) are included in Appendix II. Within the limitations of the analysis, no areas of marginal structural integrity are indicated. Due to the difficulty in establishing rigorous analytical methods, experimental determination of complex stress is recommended for a reliable confidence level of structural integrity. This would be accomplished on simple prototype parts.

The basic load and design criteria for the stress analysis are:

- Internal gas temperature - 1400^OF

- Maximum internal gas pressure - 48 psig

- Stress condition not to exceed that for 0.2-percent total creep strain in 1000 hours

- Aerodynamic loads in accordance with the requirements of Appendix III.

- 10,000 blade diverter actuation - 10,000 cycles

The basic criterion for structural integrity is the short-time 0.2-percent offset yield strength. In this particular case, although the analysis is not exactly rigorous, it is generally possible to select conservative assumptions to provide relative criteria for acceptance. Because of the complexity of shapes involved in the diverter valve blade and body components, such an approach has been necessary. However, the basic criterion for func'ional integrity, i.e., exceeding allowable leakage, is the total creep deformation in a 1000-hour operation period. A target value not to exceed 0.2-percent creep has been selected as not having significant effect on leakage. However, creep capability is much more difficult to evaluate due to the presence of a multidirectional stress field, variable bending moment stresses, and shear effects. Also, the stress redistribution resulting from local creep in a stress gradient will improve the long-time creep capability, but cannot be rationally predicted for the complicated stress condition of the diverter valve. In this case, the acceptability of stress levels is based on judgment relative to the known creep characteristics under uniaxial uniform stress conditions. The effect of excessive creep under operational conditions would certainly become noticed by evidence of leakage long before the functional capability was seriously affected.

The stress report has the following limitations:

- A thermal analysis of diverter valve metal temperature distribution has not been made; therefore, no attempt to evaluate transient or steady state thermal stress has been made.

- The method of structural support for valve installation has not been specified. Therefore, the effect of flight maneuver loads and gas turning torque has not been considered. The "plug" load has been considered by a limiting case assumption. Gravity and twisting support provisions have been provided in the welded box beam (Figure 36) between the two blade bearings. This beam could be suitably revised for the required load capability.

Due to the inability to rigorously analyze the stress conditions, an experimental determination is recommended. This determination would be simple and use only prototype configuration components. Strain field determination would be made for pressure and maneuver loads using brittle lacquer techniques followed by quantitative determination of stress by stiain gages.

5.8 AERODYNAMIC ANALYSIS

The main factors considered in estimating the aerodynamic quality of the diverter valve were:

- The total pressure losses

- The velocity gradient

- The possibility of flow breakaway

Also, as a support to the mechanical design, the aerodynamic forces acting on the system and the leakage problems have been analyzed.

The conditions of the flow entering the diverter valve were based on a mass flow of 70 pounds/second, a total absolute pressure of 60 psia, and a temperature of 1400°F. The diameter of the inlet section is 20.70 inches, while the diameter of the outlet section is 14.95 inches. The Mach number of the flow entering the system is about 0.17, while the Mach number of the flow leaving the system is about 0.35.

The total pressure loss evaluation includes the skin-friction, turning, contraction, and expansion losses. The calculations were made, in general, in accordance with the procedure of SAE Aero-Space Applied Thermodynamics Manual, Section 1. The effects of compressibility have been included. The system was split into a number of portions and each one was related to a typical case for which pressure loss coefficient data are available. The overall pressure loss is obtained as the sum of all the partial losses. The analyses of the system in the through-flow and in the diverted-flow positions are made independently. The procedure of analysis is similar since the two positions are symmetrical, with the exception that the diverted-flow position has, additionally, a 60-degree vaned bend.

In either of the two positions (through flow or diverted flow), when one butterfly valve is open and the other one closed, the valve in the open position in effect subdivides the system into two channels. The butterfly valve in the closed position makes a sharp 44-degree angle with the upstream duct direction, while the butterfly valve in the open position receives the flow at zero incidence and smoothly turns it 15 degrees. One of the two channels is defined by the surfaces of the two butterfly valves and the casing wall, while the other channel is defined by one surface of the open butterfly valve and the casing. In the diverted-flow position, the two channels lead to the entrance of the 60-degree vaned elbow.

The predicted total pressure loss in the through-flow position amounts to about 0.25 psi, which corresponds to 22 percent of the inlet dynamic head or 0.4 percent of the inlet total pressure.

The predicted total pressure loss in the diverted-flow position amounts to about 0.79 psi, which corresponds to 69 percent of the inlet dynamic head or 1.3 percent of the inlet total pressure.

The calculations have not considered the effect of a probable swirl coming out of the engine or the effect of the diffuser upstream of the system, all of which will affect the behavior of the flow through the valve.

The cross section of the two channels in each position presents corners resulting from the discontinuity of the vanes to the conical shape of the main duct. These corners are a source of vortex losses. Also, there is a discontinuity in one of the channels due to the boss, which produces contraction and expansion losses and wakes. The accelerated flow should minimize this effect.

The velocity gradient of the flow leaving the system is expected to be small especially in the through-flow position, where the flow is required to turn only 15 degrees. The diverted-flow position requires an additional 60-degree turn, which is a source of high losses and high velocity gradient when the radius of curvature of the turn is small. To minimize those problems and at the same time to use as small a space as possible, a bend of small radius of curvature with airfoil cascade has been adopted.

Although this diverter valve is expected to produce acceptable losses with small velocity gradient and no flow breakaway, the irregular internal shape of the system makes it desirable to have a scale model flow test that will evaluate the pressure losses and indicate if further refinements of valve body and blade contour are required.

5.9 MATERIAL SELECTION

Nickel-base alloys are used for nearly all of the hot parts of the diverter.

Rene' 41 sheet was chosen for the valve body. Although it is more difficult to form and weld than some of the other wrought materials, it has at least four times the allowable creep yield stress of any other candidate material. Rene' 41 obtains its higher allowable creep yield stress because it can be heat treated and retain some of its heat-treated strength characteristics at 1400°F. To use the L605 cobalt-base material instead of Rene' 41 would increase the weight approximately 40 pounds.

The blades are vacuum investment cast from a low-carbon, low-iron version of Inconel 713C. It has even better creep yield strength than Rene' 41. The low carbon and low iron give it acceptable ductility and impact strength. There are no candidate materials that are likely to reduce the cost of the blade significantly without greatly increasing the weight. This material is used in the as-cast condition.

The shafts, and the studs that hold them into blades, are of the same material as the blade because of the strength and temperature requirements.

The bearing combination is a titanium carbide bushing rubbing around the Inconel 713C shaft. This bearing combination is expected to perform in a manner similar to the titanium carbide/Rene' 41 combination which proved successful on an earlier design for a 1200°F application. The bearings are ventilated to keep the temperature below about 1100°F. It may be that a development test would show that these

85

materials are capable of performing well at a higher temperature. If this were true, a lower-weight, lower-cost bearing design could probably be used.

High-conductivity beryllium/copper alloys are used for the cooling fins which also serve as bearings. The weight can be reduced if the cooling requirements are not too severe.

The outer ends of the shafts are cool enough to allow the use of Ti-6Al-4V alloy for the bell cranks and the actuator linkage. It has good strength and lower density.

The 17-7PH900 stainless steel springs have good strength to 600°F and are corrosion resistant.

The hydraulic cylinder body is made of Ti-6Al-4V alloy. The bore is dry lubricated with a molybdenum disulfide compound. The bore is expected to be rubbed only by the Teflon dynamic seal (Figure 45), but if the 17-7PH stainless steel piston head touches the bore, the dry lube reduces any scoring tendency. The continuous presence of hydraulic fluid will also act as a lubricant.

The interior parts of the hydraulic cylinder assembly are made of 17-7PH stainless steel because of its increased strength, hardness, and stiffness.

The dynamic seals are of Teflon because of its low friction and ability to tolerate higher pressures. The static seals are Buna "N" O-rings with Teflon backup rings to increase the pressure capability.

The 17-7PH stainless steel piston rod is chromium plated in case the Teflon chevron seals fail to prevent contact of the rod with the adapter (Figure 45), also of 17-7PH stainless steel.

The scrapers (Figure 45) are of copper alloy to prevent scoring of the piston rod.

The shaft seal bellows (Figure 35) are constructed of Type 321 stainless steel. This material was selected because it is softer and more conformable than Rene' 41 bellows when internally pressurized. One end of the bellows bears against an L605 cobalt-base alloy washer. This material combination can rub without developing high friction or galling.

The edges of the butterfly blades are flame sprayed with Stellite 6, a cobalt-base carbide-containing alloy, to minimize friction and wear of the blades against the Rene' 41 seal.

The H. I. Thompson A-100 insulation has proved to be satisfactory for similar environments in the past. The Solami C foil covering of Type 321 stainless steel is a highly conformable corrugated sheet that has performed satisfactorily for similar applications.

5.10 DEVᵢ LOPMENT TESTING

Development testing falls into two categories. The first is the development required to obtain adequate performance. The second is the development that, although not mandatory, probably will yield improved performance of the diverter.

5.10.1 Development Testing To Ensure Adequate Performance

There appears to be only one test in this category. This test is the development of the optimum shape and location of the blade relative to the seal required to minimize leakage.

To achieve a good seal from one valve assembly to the next without repeated fit-up problems, good reproducibility will be required of:

- The cylindrical seal shape and location relative to the valve body and flanges

- The location of the bearing in the valve body

- The shape of the sealing edge of the blade and its location relative to the shaft

To obtain a good seal, a development program will be required to establish the optimum nominal shape of the sealing edge of the blade relative to the flexible sealing element. It is expected that the development program will be required only once. Sufficiently accurate reproducibility should ensure good sealing on subsequent valves.

The development program will proceed in the following steps:

1. The cylindrical seal will be installed as nearly as feasible to its nominal size, shape, and location in a complete valve body.

2. The sealing edge of the blade would be ground as accurately as feasible to its nominal size and shape relative to its shaft center lines. Probably, this is a cylindrical intersection when viewed parallel to the axis of the cylindrical seal.

3. The assembled valve with the blade in the closed position will be pressurized to operating pressure, or slightly above, while at room temperature. Simple feeler gage measurements will indicate the relative effect resulting from pressure if leakage occurs. It will be desirable to experiment with different closing torques on the blade, including the probable aerodynamic torque.

4. Using the gap measurement of Step 3, any change in the nominal shape of the blade sealing edge judged desirable can be achieved either by grinding or by building up and grinding the edge smooth.

87

5. The blade will be tried again and Steps 3 and 4 will be repeated, as necessary, to obtain approximately zero leakage. Several repetitions of this step might be necessary to obtain the desired, nearly zero, leakage.

The shape of the blade established by the preceding steps will serve as a pattern for all subsequent blades.

This development test should include a test of both blades to be sure that both cylindrical seals for the two blades are sufficiently symmetrical to operate with just one blade shape.

It would be desirable during the development test to determine, at least approximately, how much variation in relative shapes could be tolerated without causing a significant leakage. This determination would permit the tolerances to be only as tight as necessary and, therefore, would contribute toward the lowest cost of production units.

Also, it is probably desirable to determine the effect of operating at temperatures and pressures somewhat below the design values. It would be helpful to know how much leakage occurs just after engine start-up as compared to the amount encountered during normal engine operating conditions.

5.10.2 Develop Testing of Probable Value - Not Mandatory

Several development tests appear justified for this second category. The diverter probably could be made and perform without them, but a possibility exists that performance could be improved in some areas by using these tests.

One development test is a flow test of a model, either 0.25 or full scale. Perhaps the full-scale model is indicated. Plaster models of the valve body are required for manufacturing. Fiber glass shapes of the plaster models can be tested. Any desired changes in shape of either the blade or the body can be determined by the flow test. The plaster models would then be modified accordingly.

A flow test model can indicate any area where significant flow separation and its resulting loss occurred. Experimental shape changes with modeling clay could undoubtedly reduce these losses.

As indicated in the actuation system, a flow test to determine the aerodynamic torque on the blade is desirable. Both losses and aerodynamic torque are probably highly dependent on the blade angle of incidence. If the aerodynamic torque is too low to hold the blade against the flexible cylinder for effective sealing, additional torque, such as by the overcenter spring, should be provided.

The optimum shape of the valve body considers the aerodynamic losses and the stability of the valve body under pressure which can affect the sealing. Therefore, a determination of the change in shape under pressure is possibly another development test that should be made.

88

Another potentially valuable test can be accomplished on the unit tested for shape change under pressure. This is a strain study with a photoelastic coating and strain gages. The test can indicate two things:

- Where added weight might be saved by chem-milling or by otherwise thinning parts

- Where additional material might be necessary to prevent long-term creep distortion

The two blades weigh 49.4 pounds and are candidates for weight reduction. A stress and deflection test using a photoelastic coating and strain gages is also indicated for the blade.

Another development test to determine a thermal profile over the diverter, particulariy in areas of sharp thermal gradients, might indicate areas that should be redesigned to prevent cracks resulting from thermal strain cycling. Such a test might also indicate a need for bearing design improvement.

Development testing of bearing materials at higher temperatures might permit a simpler uncooled bearing design.

Development testing is also indicated in the selection of a material with which to flame coat the edge of the blade to minimize friction, wear, and galling. Of the several candidate materials, including several carbide-containing cobalt-base alloys, there is probably one better than the other for use against the Rene' 41 seal.

Development testing might show that the kinetic energy in the closing blade is low enough to prevent damage to the seal even if the actuator does not snub the blade. If this were true, some simplification of the actuator could result. The piston rings, two of the Leechek check valves, two of the Lee Jet orifices, and two O-rings with backups would be removed. The cylinder assembly and the cylinder body (Figure 45) would be shorter and lighter and cost would be reduced.

5.11 WEIGHT

The weight of the diverter valve assembly as shown in Figure 35 is 118.76 pounds

The principal weight groups are:

Valve housing (Figure 36)	(lb)
Duct walls	30.59
Bearing reinforcements	5.26
Bolting flanges	6.37
Vanes	4.53
Insulation and covering	2.69
Housing total	49.44
Butterfly blades (Figure 37) 2 at 24.7	49.40

Actuating mechanism (Figure 35)	(lb)
Hydraulic cylinder	3.44
Shafts	4.42
Cooling fins	4.64
Springs	2.82
Bell cranks	1.20
Linkage assembly	1.04
Studs	.96
Miscellaneous items	1.40
Actuating mechanism total	19.92
Valve assembly total weight	118.76

This weight is as low as can be designed conservatively without development testing. Stress coat and strain gage testing might show where strength and stiffness are good enough to permit some weight removal from the 30.59-pound valve body or from the combined blade weight - 49.44 pounds.

It is estimated that perhaps as much as 10 to 15 pounds might be removed from the assembly by development testing.

If the diverter valve housing were made of a material such as L605 cobalt-base alloy to decrease manufacturing costs and heat-treating problems of Rene' 41, the weight of the body would be increased about 40 pounds.

5.11.1 Scalability of Diverter to Larger Diameters

The diverter design (Figure 35) can be scaled up to considerably larger diameters.

There appear to be no particularly difficult problems introduced by the scale-up. The design approach remains essentially the same. The seal approach, the aerodynamic flow contours, the bearing design, the blade design, and the actuator design are similar.

The weight will increase approximately as the 2.35 ± 0.03 power of the duct diameter. The same relative geometry of the diverter would be maintained. This variation of weight with diameter is shown by the curves of Figure 48.

A description of the way each major weight component of the diverter varies with diameter of the diverter will be given in the following paragraphs. Those components whose weights vary with the duct diameter in the same ratio are grouped together on the curves of Figure 48.

The weight of the walls of the diverter housing is expected to increase nearly as the cube of the diameter. The length, circumference, and wall thickness (to maintain the same hoop stress) each increase as the diameter increases. The thickened areas around the bearing reinforcement will also increase about as the cube of the diameter.

90
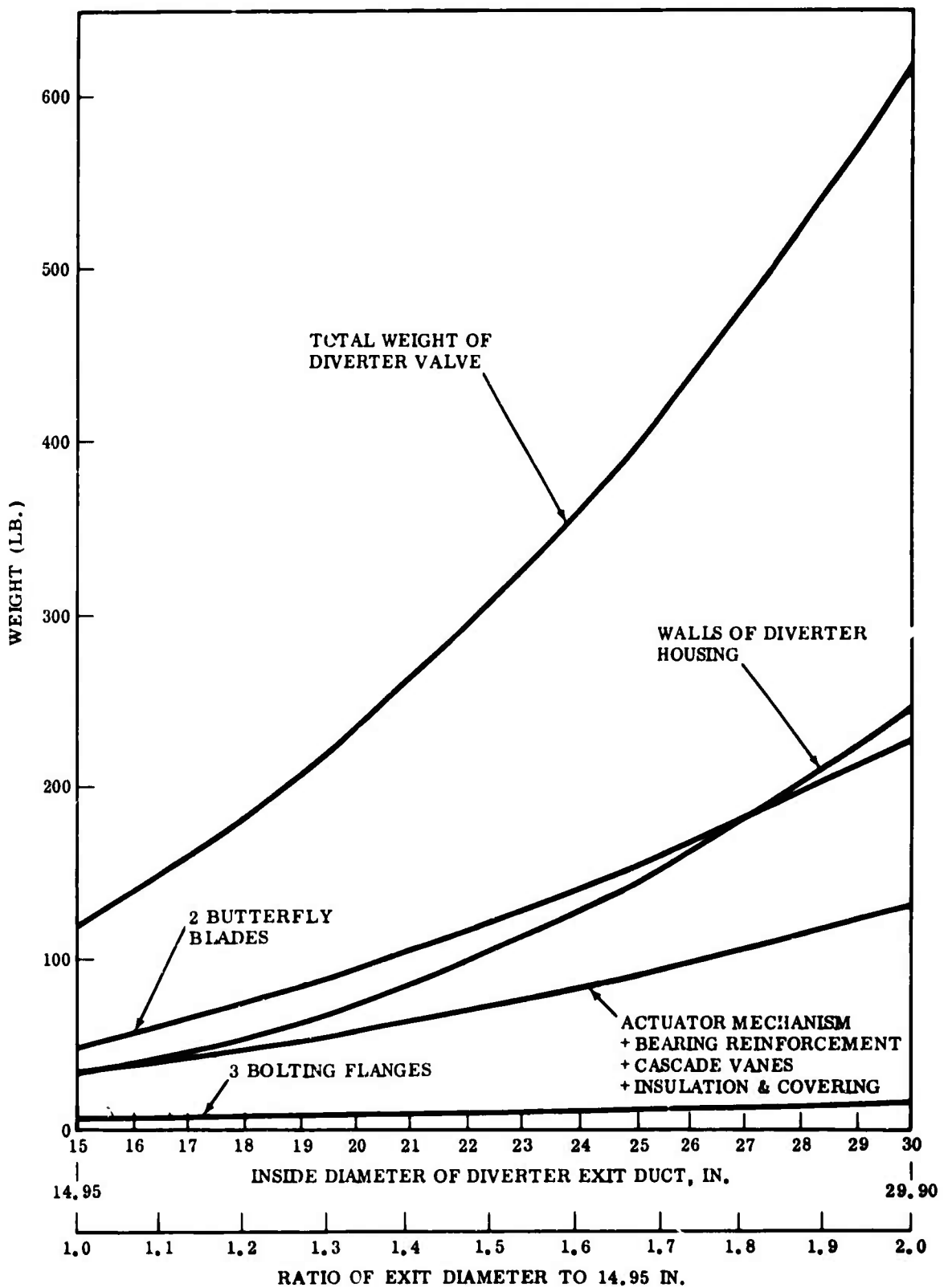
Figure 48. Weight Versus Diverter Exit Diameter and Exit Diameter Ratio
for Diverter Valve and Components.

The butterfly blades are expected to increase in weight approximately as the 2.2 power of the diameter. It is expected that the basic shell thickness of the blade will remain approximately the same. The area of the blade and therefore of the shell of the blade would increase as the square of the diameter. As the blade gets larger, a thinning - as by chemically milling - of some areas of the shell along with thickening of some portions of the edges and stiffeners appears desirable. These changes are expected to keep the average shell thickness about the same.

The shear, torque, and bending loads on the shafts will increase, so the shaft diameters and lengths will increase. As the shaft diameter increases, the inside diameter, wall thickness, and depth of the hubs of the blades will also increase.

Thus, the weight of the blade, including the shell, stiffeners, and hubs, is estimated to vary as the 2.2 power of the duct diameter.

The weight of the vanes will vary as the square of the duct diameter. The sheet metal thickness for the vanes is determined largely by handling considerations, rather than by aerodynamic loading, so it would not be increased. About the same number of vanes would be used, thus increasing the average gap between vanes. To retain about the same gap-to-chord ratio, the chord would have to increase as the diameter increases. The length of the vanes also varies with the diameter; therefore, the weight of the vanes increases as the square of the duct diameter.

The weight of the actuating mechanism, including the hydraulic cylinder, is expected to increase about as the square of the duct diameter. The lengths of nearly every element would increase as the duct diameter increases. The loads will also increase. The weight of some of the actuator elements will vary as the square of the duct diameter varies. The weight of some elements will be greater and some will be less. The total weight is estimated to vary as the square of the duct diameter.

The weight of the bearing reinforcements, including the beams between the bearings, is expected to increase about as the square of the duct diameter. The lengths or diameters of most of the elements would increase about as the duct diameter. The bearing loads and beam loads will increase about as the square of the duct diameter. In most cases the cross-sectional area of the elements will vary about as the duct diameter. The beam will obtain increased strength by an increase in depth rather than an increase in sheet metal gage. Thus the total weight is estimated to vary about as the square of the duct diameter.

The weight of the insulation and covering will vary as the surface area of the diverter body and therefore as the square of the duct diameter. The thickness of the insulation and covering would remain the same.

The weight of the bolting flanges is expected to vary slightly more than directly with the diameter, perhaps about as the 1.3 power of the duct diameter. The circumference of the flanges varies directly as the duct diameter. The bolting leg of the flange would retain about the same cross section, but the leg that is resistance welded to the duct will become heavier as the duct diameter and wall thickness increase.

The weights of all components that are considered to vary as the square of the duct diameter are grouped together on the curve of Figure 48. These components, described in the preceding paragraphs, are the actuating mechanism, the vanes, the bearing reinforcements, and the insulation and covering.

The weights of the other components are shown by individual curves on Figure 48.

5.11.2 Growth Capability to 1600°F

The general design approach of the diverter valve (Figure 35) can be applied to a diverter using 1600°F exhaust gas instead of the 1400°F for which the diverter was designed. The weight would be about 220 pounds. Some possibilities for a weight lower than 220 pounds exist. In any case, several detail changes are required.

The most important characteristic to be considered is the large reduction in creep strength for all of the candidate hot materials when going from 1400° to 1600°F.

The approximate allowable creep rupture stresses and the 0.2-percent creep yield stresses in 1000 hours and elongations are tabulated for three possible materials for the hot parts for both 1400° and 1600°F (Table V).

TABLE V. ELEVATED TEMPERATURE MATERIAL PROPERTIES					
	0.2% creep in 1000 hours		Creep rupture in 1000 hours		(% Elongation)
	(psi)	(psi)	(psi)	(psi)	
Material	1400°F	1600°F	1400°F	1600°F	1400° to 1600°F
Rene' 41 (sheet)	30,000	8000	38,000	13,000	5
L605	8000	3000	24,000	10,000	12 to 30
Inconel 713LC, low iron (vacuum investment casting)	41,000	17,000	60,000	30,000	4 to 10

Other materials have been considered but they have either lower creep strengths or lower elongations than the above tabulated materials.

With the greatly reduced creep strengths, the wall thickness required to carry the hoop load is greatly increased. For a 20.70-inch-diameter duct at 1600°F and 48 psig not to exceed 0.2-percent creep in 1000 hours, the wall thickness would be 0.17 inch for L605, 0.07 inch for Rene' 41, and 0.030 inch for the Inconel 713LC, low iron casting.

Probably the best approach would still be the Rene' 41 material. The material thickness for the 14.95-inch-diameter exit ducts would be 0.05 inch. The 0.05-inch thick Rene' 41 material would also be used for the seal.

Since the bearings would still be cooled to below about $1100^{\circ}F$, the bearing reinforcements would not increase much in weight. The shafts would about double in weight because of their lower allowable stress in critical areas.

The Inconel 713LC, low iron, cast blade material loses more than half its creep yield strength. However, because of probably better distribution of weight, the blades would be expected to about double in weight to about 100 pounds.

The weight of the insulation and actuator mechanism would be expected to remain about the same.

The weight of all components would total about 220 pounds.

Another approach that would require additional design study would be the possibility of casting the diverter housing of Inconel 713LC, low iron material. Since a one-piece vacuum investment cast housing would be quite large, it might be possible to cast the housing in several pieces and electron beam weld them together. Considerable weight could be saved by chemical milling or otherwise thinning noncritical areas. The seals would be electron beam welded in place. The flanges could be integrally cast to save some weight.

The cast housing approach might reduce the 220-pound weight by 20 to 40 pounds. The cast housing would appear more worthwhile with even larger sizes or higher temperatures or pressures.

Once the exact application was known, more weight might be removed from the blades. Because it has not been known which blade will be closed most of the time, both blades have been designed for the 1000-hour life at the full temperature of the gas. Probably one blade is open more than the other in most applications. Also, the closed blade is likely to have a mean temperature slightly below the gas temperature because of a cooler environment on the unpressurized side of the blade much of the time. A 50° or $100^{\circ}F$ reduction in mean temperature of the blade would increase the allowable stress and permit a lower weight.

Another approach that might be feasible in some applications would be to cool portions of the pressurized shell by blowing cooling air between the shell and an external shroud. One problem to be expected with such an approach would be sharper thermal gradients that would tend to cause distortions and decrease the thermal strain cycle life.

VI. PHASE IV - TECHNOLOGY DEMONSTRATION

Fabrication of the major portion of the diverter valve assembly (Figure 35) will involve the use of conventional manufacturing operations and processes currently available (i.e., state of the art). However, the close tolerances of those components necessary to achieve minimum leakage and the forming of components made from Rene' 41 represent difficult fabrication tasks that require the development of a manufacturing process. Normally, the fabrication of prototype hardware is accomplished with soft tooling. However, fabrication of a prototype diverter valve involves Class A tooling for:

- Forming Rene' 41 components

- Machining close-tolerance components used in the hydraulic cylinder assembly (Figure 45) and the valve blade (Figure 37)

- Assembling the components used on the valve housing assembly (Figure 36) to accurately position and locate the machined components, i.e., inlet and outlet flanges and the blade shaft bearing housings

6.1 MANUFACTURING OPERATIONS

The manufacturing operations involved in fabrication of a prototype valve fall into three categories:

- Detail component fabrication

- Buildup of subassemblies

- Assembling of the subassemblies and detail components into the complete diverter valve

6.1.1 Detail Component Fabrication - Major Details Only

Half Stamping - Figure 36

This part will be formed from stage dies with chem-milling required to finalize the various areas of the material thicknesses indicated on the drawing. Tooling required includes

- Interstage form dies

- Weld fixture

- Expander

- Template

This part is considered to be one of the major areas where fabrication difficulties will be encountered and will involve the manufacturing process development as described in paragraph 6.2.

Exhaust Tubes - Figure 36

These parts will be made from sheet stock, rolled and welded into a cylinder and cut at the required angle. It is problematical that the tolerances at the ends which contact the blade can be held; therefore, the development testing described in paragraph 6.2 may be required. Tooling required includes

- Angle cutoff fixture

- An expander to obtain a proper fit in the areas at which resistance welding to the -1 stamping is achieved

Stampings - Figure 36

These parts will be formed from stage dies. Tooling required includes

- Interstage form dies

- Weld fixture

- Expander

- Trim template

Saddle Brace - Figure 36

This part will be made from form dies. Tooling required includes

- Form dies

- Trim template

Flanges - Figure 36

These parts will be made from a flash-welded bar stock forming a rough ring. Parts will be rough machined leaving sufficient stock for final machining after heat treating. Tooling required includes

- Machining fixture

- Drill fixture

Vanes - Figure 36

These parts will be made in three or four stages with inner stage annealing. Tooling required includes

- Form dies

- Trim template

Blade - Figure 37

This part will be made from an investment casting held to very close tolerances. Three-dimension milling will be used to achieve the required contour and radius edges which contact the sealing portions of the tubes (Figure 36). The wearing surfaces will be flame sprayed with Stellite No. 6 and will be given a final three-dimension grinding to achieve the dimensions specified on the drawing. With respect to the close tolerances on this part, the development testing described in paragraph 6.2 may be required. Tooling required includes

- Machining fixture

- Gear shaper fixture

- Inspection fixture

- Casting pattern

Bell Crank - Figures 42 and 43

These parts will be made from investment castings. Tooling required includes

- Mill fixture

- Drill fixture

- Gear shaper fixture

6.1.2 Subassembly Operations

Valve Housing Assembly - Figure 36

The sequence of operations to manufacture this assembly is:

1. Assemble and join the two -1 stampings to form the basic valve body.

2. Attach the -11 flange to the valve body.

3. Attach the -10 flange to the -2 tube.

4. Attach the -2 and -3 tubes to the valve body.

5. Assemble and join the -4 and -5 elbow stampings to complete the elbow.

6. Attach the elbow to the -2 tube.

7. Attach the -10 flange to the elbow.

8. Elox vane slots in elbow.

9. Install vanes in elbow.

10. Attach the -7, -8, and -9 components to the valve body.

11. Rough machine the -9 housing to allow for finish machining after final heat treating.

12. Heat-treat complete valve body assembly in a heat-treating fixture to maintain the relative positions of the end flanges and the -9 housings.

13. Final machine the -9 housing.

14. Install the 51208-14, -15, and -16 (Figure 36) insulation components.

Tooling required includes

- Weld fixture for the -1 stamping

- Final assembly weld fixtures

- Vane elox fixture and electrode

- Heat-treat fixture and muffle

- Drill fixture for the -9 housing

- Sizing expander

Hydraulic Cylinder Subassembly - Figure 45

This subassembly is comprised primarily of machine parts held to close tolerances. Because of the numerous angular holes and special mill operations, these components will require special mill setups and Class A tooling.

Tooling required includes

- Boring bars

- Grinding holders

- Drill jigs

- Mill fixtures

- Heat treat retort

6.1.3 Final Assembly Operations

Valve Assembly Diverter - Figure 3⁻

For the most part, the final assembly will be performed by hand installing parts and subassemblies already finalized in machining. An assembly fixture should be used to keep overall locations of flanges in place while securing cylinder valves and springs. This fixture will also be used as a final inspection fixture.

6.2 MANUFACTURING PROCESS DEVELOPMENT

The major area of processed development required to undertake the fabrication of a prototype diverter valve is the area involved in forming those components made from Rene' 41 material. This material is more difficult to form than the austenitic stainless steels, and because of its great resistance, all forming must be done in the annealed condition. Because of its spring-back and work-hardening characteristics during forming, it is necessary to form in several stages whenever severe forms are required. In such cases, annealing is required between stages. Annealing is accomplished at $1975^{\circ}F$ for 30 minutes, then quenched quickly in oil. Quenching must be completed in 2 seconds to obtain optimum ductility.

Because of the severe formin ; which will be involved in making the stamped components (Figure 36), the possibility exists that they may be more readily formed by a greater number of individual stampings which would then be welded together and subjected to a secondary forming operation.

Another area requiring process development is the fusion welding of Rene' 41 components. In welding Rene' 41, satisfactory welds can only be made by using the proper welding procedures. Recommendations are:

- Material must be properly annealed before welding.

- Good fit-up is absolutely necessary.

- Copper and argon backing should be used to achieve rapid cooling of the weld area.

Gas coverage on both sides is mandatory on all butt joints. Joint edges should be ground to remove burrs before welding. Control of arc length and current is helpful for minimum heat input.

To undertake the development of the processes described above, it is felt that it can be accomplished by fabricating an elbow subassembly consisting of the elbow half stampings with several of the vanes installed. Since the channel section in the stamping (shown in zone B-27 in Figure 36), represents severe forming, it is felt that the elbow stamping could be increased in length so that a representative channel section could be included when the elbow is stamped to establish required interstage forming and annealing processes.

99

All of the processes (i.e., forming, annealing, welding, and heat treating) necessary to produce such an elbow are typical of those encountered in making an entire valve diverter assembly. However, these processes could be accomplished at considerably less cost, since the fabrication of the tooling and fixturing necessary to fabricate a stamping (Figure 36) is involved. If a manufacturing development program for the diverter is required, Solar recommends making only an elbow subassembly in the initial stage of the program.

VII. RECOMMENDATIONS

The following recommendations are based on the results of this study:

- Initiate a manufacturing development program to establish a manufacturing process to use Rene' 41 material in the fabrication of a diverter valve.

- When VTOL vehicle requirements are confirmed, immediately establish necessary design parameters to ensure a more definitive design study program for a complete diverter system.

APPENDIX I
AERODYNAMIC ANALYSIS OF DIVERTER VALVES

An aerodynamic analysis of different diverter valve configurations has been completed and the results are presented in this report.

The main factors considered in order to estimate the aerodynamic quality of each configuration have been: the total pressure losses, the velocity gradient, and the possibility of flow breakaway. Also, as a support to the mechanical approach, the aerodynamic forces acting on the systems and the leakage problems have been considered.

The conditions of the flow entering the diverter valve were based on a mass-flow of 70 lb/sec., a total pressure of 60 psia, and a temperature of 1500°F. It was assumed that the Mach number of the flow entering the system would be about 0.3.

The total pressure loss evaluation includes the skin-friction, turning, contraction and expansion losses. The calculations were made, in general, in accordance with the procedure of SAE Aero-Space Applied Thermodynamics Manual, Section 1. The effects of compressibility have been included.

The two configurations shown in this report are the symmetrical double butterfly type, Figure 49, and the rotating elbow type, Figure 50. The two types are the result of the analysis and comparison of four different diverter valve configurations which were described in the report ER 1806-1 of November 11, 1966. The symmetrical double butterfly type corresponds to the original configuration 3, while the rotating elbow type corresponds to the original configuration 4. Configuration 1 was an asymmetrical double butterfly type, while configuration 2 corresponded to a straight pipe with bellows at the inlet which allow the duct to swing to either side when connecting to the through or the diverted duct.

The losses in the rotating elbow system are due to skin friction and high turning, plus the effect of the strut. The pressure losses in the through-flow position should amount to about 0.87 psi, which corresponds to a loss coefficient $(\Delta P/q)$ of about 0.25. The pressure losses in the diverted-flow position should amount to about 0.56 psi, which corresponds to a loss coefficient of about 0.16. The through-flow position consists of a "Z" bend made up by two reversed 45-degree elbows (the losses are about 50 percent higher than when considering each elbow independently); the diverted flow consists of a 90-degree bend made up by two 45-degree elbows (the losses are about 25 percent lower than when considering each elbow independently). The system has a constant diameter of 16 inches, which corresponds to a Mach number of 0.3. The curvature of the elbows corresponds to an (r/d) of 1.5, which is the minimum required to keep the flow distortion within acceptable values.

The main reasons for the pressure losses in the symmetrical double butterfly system are that the shape basically corresponds to a miter bend with a splitter vane in the second half of the stream-path; that the vane closing one branch presents a discontinuity to the cylindrical shape of the rest of the duct and the resulting corners are a source of vortex losses; and that there is a 15-degree bend at the inlet and a 60-degree bend at the exit of the diverted-flow duct, in an area of much

102
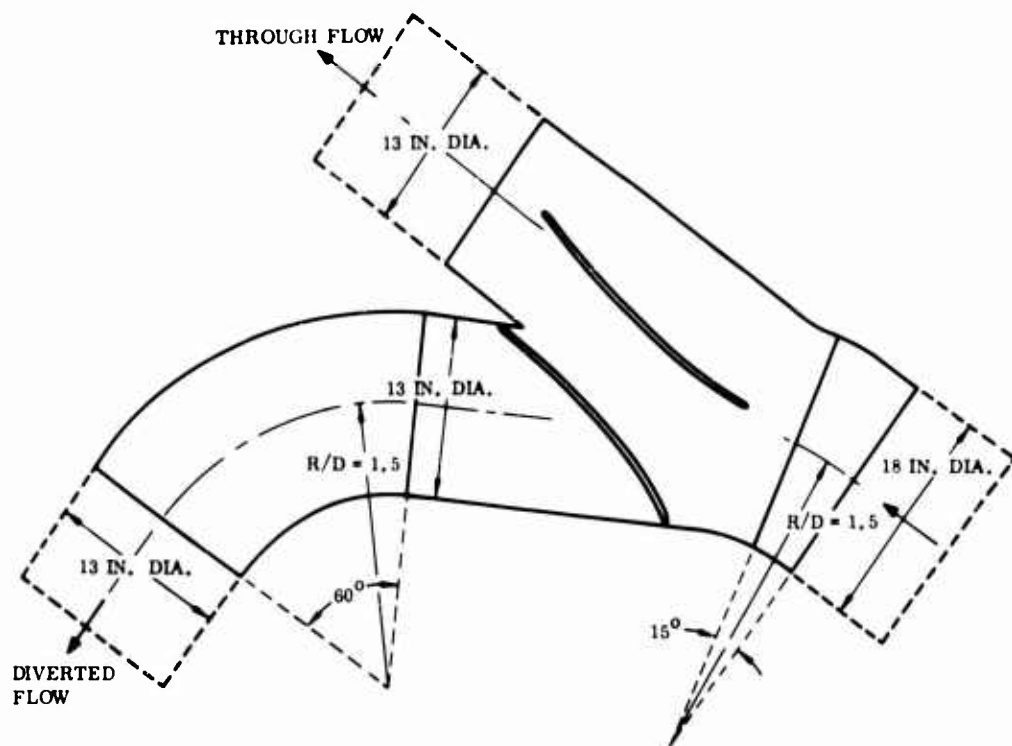
Figure 49. Symmetrical Double Butterfly Type.
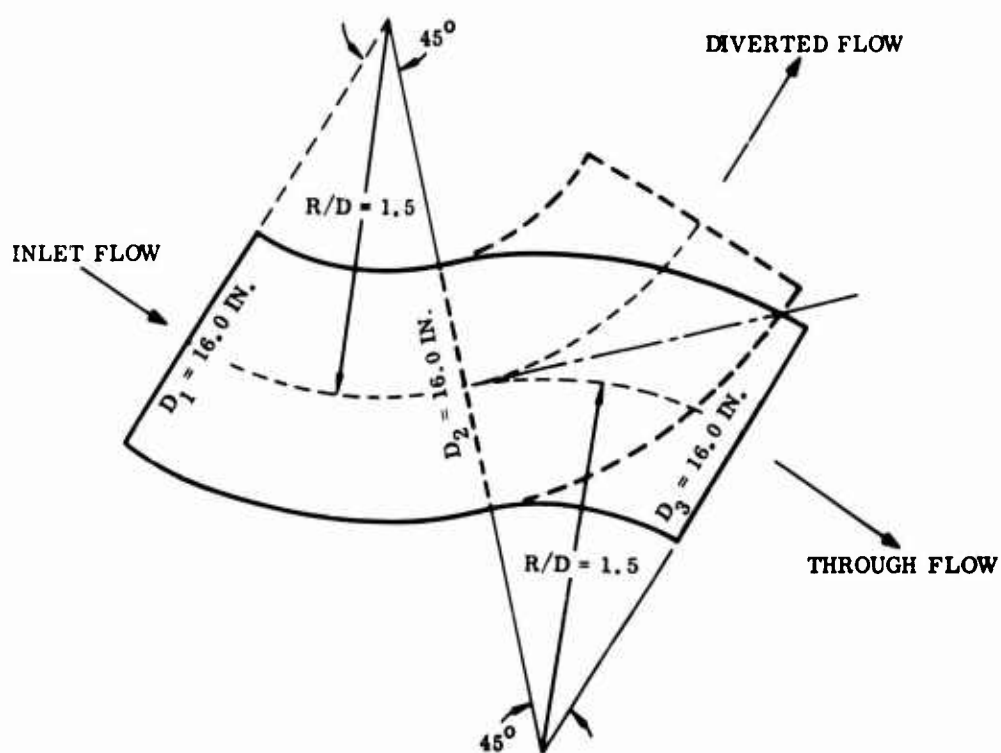
Figure 50. Rotating Elbow Type.

103

higher dynamic pressure than the rest of the system. According to the evaluation, the pressure losses in the through-flow position should amount to about 0.44 psi, which corresponds to a loss coefficient ($\Delta P/q$) of about 0.20. The pressure losses in the diverted-flow position should amount to about 1.38 psi, which corresponds to a loss coefficient of about 0.65. The system has an initial diameter of 18 inches, which corresponds to a Mach number of 0.234, and an exit diameter of 13 inches, which corresponds to a Mach number of 0.5. The velocity profile at the exit, at any of the two positions, is expected to be reasonably good.

The values of pressure losses shown above for the two systems should not be compared directly, as the symmetrical double butterfly type has a lower velocity at the inlet and a much higher velocity at the outlet in comparison to the rotating elbow type. These differences indicate that the symmetrical double butterfly type will require a longer diffuser than the rotating elbow, between the engine and itself (if the Mach number leaving the engine is higher than 0.3) or a steeper angle of diffusion, with corresponding higher losses which should be added to the diverter losses. In regard to the velocity leaving the diverter, if the rotating elbow type would use a contraction in the second elbow, from a diameter of 16.0 inches to a diameter of 13.0 inches, the turning losses will reduce and the total losses in the through-flow position would be 0.77 psi, which corresponds to a loss coefficient of 0.22, while the total losses in the diverted-flow position would reduce to 0.49 psi, which corresponds to a loss coefficient of 0.14.

It should be pointed out that all the bends considered on these configurations have an $r/d = 1.5$. If mechanical considerations permit the use of higher values of r/d, like 3.0, or if a cascade is installed in the bends, the pressure losses would be smaller than shown above. The calculations have not considered the effect of a probable swirl coming out of the engine or the effect of the diffuser upstream of the system, all of which will affect the behavior of the flow through the valve.

In the final analysis the optimum design of the diverter valve will depend on the upstream conditions existing and the downstream conditions required. The inlet diameter of the system should be a consequence of the optimum diffuser design produced upstream of it. An acceleration of the flow through the diverter system to a Mach number of 0.5 would be advantageous in order to reduce the turning losses, but this solution, of course, assumes that there are not additional elements downstream of the diverter valve which will suffer higher losses due to the increased velocity, counterbalancing the gains produced in the diverter. Another question to be considered refers to which of the two ducts (through position or diverted position) should have the minimum pressure losses. Summarizing, the final configuration should be designed as part of an optimized system rather than as a separate entity. The designs analyzed here may, therefore, be scaled or changed in the light of system design information contained in Tables III, IV, VII, and VIII and shown in Figures 49 through 53.

104

TABLE VI. PRELIMINARY SIZING AND FLOW CONDITIONS

Item	Symbol	Units	Value			
Flow	W	lb/sec	70	70	70	70
Total Pressure	P_1	psia	60	60	60	60
Total Temperature	T_1	F	1500	1500	1500	1500
Mach Number	M_{N_1}	-	0.234	0.300	0.400	0.500
Area	A	sq in.	254.47	202.31	157.95	132.92
Diameter	D	in.	18.00	16.05	14.18	13.01
Static Pressure	p_1	psia	57.86	56.54	54.02	50.98
Static Temperature	t_1	F	1482.4	1471.3	1449.6	1422.4
Static Density	ρ	lb/ft^3	0.08048	0.07909	0.07642	0.07317
Velocity	V	ft/sec	492.7	629.9	835.1	1036.4
Dynamic Pressure	q_1	psi	2.14	3.46	5.98	9.02
Reynolds Number	Re	-	2.04×10^6	2.29×10^6	2.61×10^6	2.87×10^6

	Value					
70	70	70	70	70	70	70
60	60	60	60	60	60	60
1500	1500	1500	1400	1400	1400	
0.234	0.302	0.501	0.227	0.294	0.483	
254.5	201.1	132.7	254.5	201.1	132.7	
18.00	16.00	13.00	16.00	16.00	13.00	
57.86	56.50	50.95	57.99	56.67	51.03	
1482.5	1471.0	1422.1	1384.3	1373.8	1331.0	
0.08048	0.07904	0.07313	0.08494	0.08349	0.07772	
492.7	634.0	1038.4	465.8	601.5	976.6	
2.14	3.50	9.05	2.01	3.33	8.47	
2.04×10^6	2.30×10^6	2.88×10^6	2.10×10^6	2.38×10^6	2.96×10^6	

DIVERTED-FLOW POSITION

F = 1940 lb
Fx = 1371 lb ⎫ WHEN CONSIDERING THE
Fy = 1371 lb ⎬ DYNAMIC PRESSURE ONLY
T = 4695 lb-ft ⎭

THROUGH-FLOW POSITION

F = 0
Fx = 0   ⎫ WHEN CONSIDERING THE
Fy = 0   ⎬ DYNAMIC PRESSURE ONLY
T = -1616 lb-ft ⎭

WHEN CONSIDERING THE DYNAMIC PRESSURE PLUS THE
RELATIVE STATIC PRESSURE (AMBIENT PRESSURE OUTSIDE
THE WALLS, 14.70 PSI)

DIVERTED-FLOW POSITION	THROUGH-FLOW POSITION
F = 13907 lb	F = 0
Fx = 9835 lb	Fx = 0
Fy = 9835 lb	Fy = 0
T = 25,654 lb-ft	T = 11,614 lb-ft

Figure 51. Rotating Bend Type Diverter Valve;
Aerodynamic Forces on the Bend.

DIVERTED-FLOW POSITION

F = 4479 lb
Fx = 1371 lb ⎫ WHEN CONSIDERING THE
Fy = 4264 lb ⎬ DYNAMIC PRESSURE ONLY
T = 11,121 lb-ft ⎭

THROUGH-FLOW POSITION

F = 2893
Fx = 2893   ⎫ WHEN CONSIDERING
Fy = 0   ⎬ THE DYNAMIC PRESSURE ONLY
T = 5028 lb-ft ⎭

WHEN CONSIDERING THE DYNAMIC PRESSURE PLUS THE
RELATIVE STATIC PRESSURE (AMBIENT PRESSURE OUTSIDE
THE DUCTS: 14.70 PSI)

DIVERTED-FLOW POSITION	THROUGH-FLOW POSITION
F = 11,529 lb	F = 2820 lb
Fx = 9835 lb	Fx = 2820 lb
Fy = 6015 lb	Fy = 0
T = 15,689 lb-ft	T = 7093 lb-ft

Figure 52. Rotating Bend Type Diverter Valve;
Aerodynamic Forces on the System.

107

2.90 IN.

**INTERSECTION OF STRUT
CENTER LINE AND
BEND INSIDE WALL**

$q = 3.46$ lb/in^2.

PROJECTED AREA

DISTRIBUTED LOAD

16.35 IN.

4.87 IN.

21.22 IN.
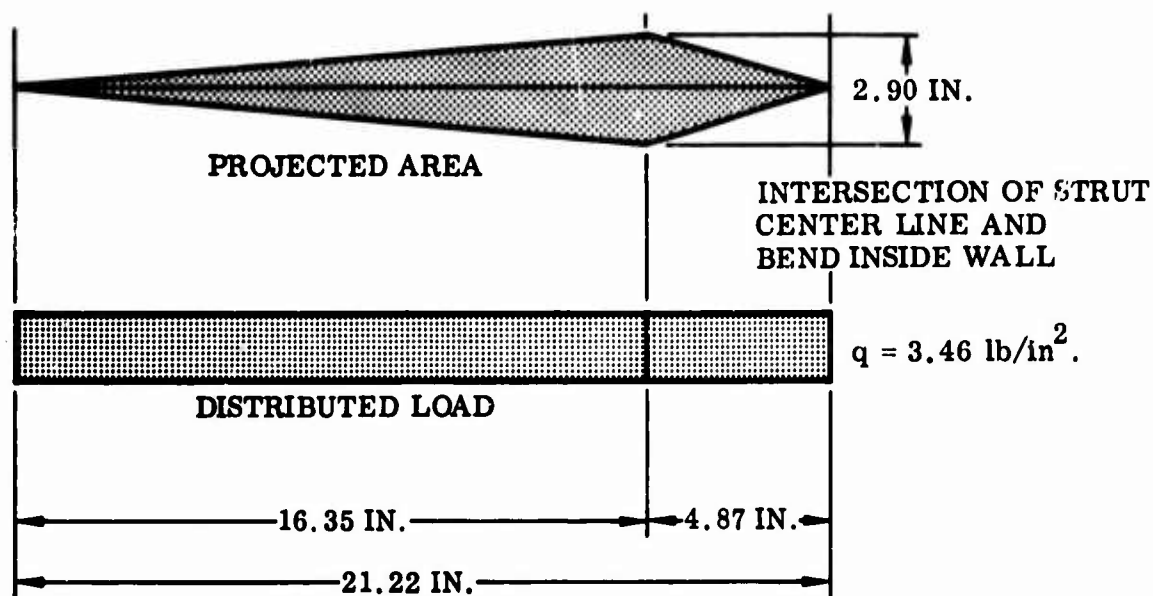
Figure 53.   Rotating Elbow Type Diverter Valve; Maxi-
mum Aerodynamic Load Acting on Strut.

DIVERTED FLOW

THROUGH
FLOW

DIVERTED-FLOW POSITION

F = 2493 lb
Fx = 1071 lb
Fy = 2250 lb

WHEN CONSIDERING THE
DYNAMIC PRESSURE ONLY

THROUGH-FLOW POSITION

F = 1181 lb
Fx = 1181 lb
Fy = 0

WHEN CONSIDERING THE
DYNAMIC PRESSURE ONLY

**WHEN CONSIDERING THE DYNAMIC PRESSURE PLUS THE
RELATIVE STATIC,PRESSURE (AMBIENT PRESSURE OUTSIDE
THE DUCTS: 14.70 PSI)**

DIVERTED-FLOW POSITION   **THROUGH-FLOW POSITION**

F = 12,833 lb F = 5617 lb
Fx = 11,476 lb Fx = 5617 lb
Fy = 5859 lb Fy = 0

INLET FLOW

Figure 54.   Symmetrical Double Butterfly Type Diverter
Valve; Aerodynamic Forces on the Bend.

108

DIVERTED FLOW

THROUGH FLOW

F_x F F_y

DIVERTED-FLOW POSITION

F = 4396 lb
F_x = 1071 lb   WHEN CONSIDERING
F_y = 4264 lb   THE DYNAMIC PRESSURE ONLY

THROUGH-FLOW POSITION

F = 3193 lb   WHEN CONSIDERING
F_x = 3193 lb   THE DYNAMIC PRESSURE ONLY
F_y = 0

WHEN CONSIDERING THE DYNAMIC PRESSURE PLUS THE
RELATIVE STATIC PRESSURE (AMBIENT PRESSURE OUTSIDE
THE DUCTS: 14.70 PSI)

DIVERTED-FLOW POSITION   THROUGH-FLOW POSITION

F = 12957 lb F = 5461 lb
F_x = 11476 lb F_x = 5461 lb
F_y = 6015 lb F_y = 0

INLET FLOW

Figure 55.   Symmetrical Double Butterfly Type Diverter
Valve; Aerodynamic Forces on the System.

109

APPENDIX II
DIVERTER VALVE STRESS ANALYSIS

BLADE (Figure 37)

The blade analysis model for geometry, loading, and beam support is shown below. The loading is for the closed blade position consisting of a 48-psig uniform pressure load. A simple support at each bearing is assumed. Two conditions of bending are considered, and then superposed:

1. Cantilever action of each blade half with fixed end at section V-V (zero slope change at V-V).

2. Beam bending between simple supports at each bearing.
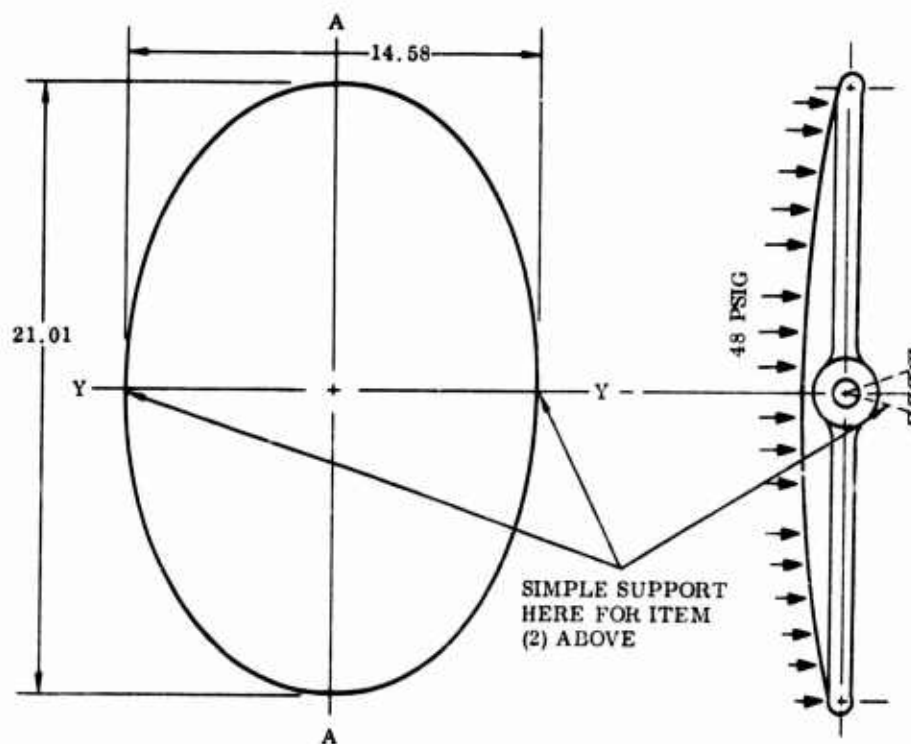
This approach is not considered exactly rigorous but errs on the conservative side. Because of the variable section modulus, the computation is performed on digital computer using Solar program no. 134. Output gives shear, moment, slope, and deflection at each input station. Each input station has a discrete load equivalent to the total pressure on an area assigned to each station.

Section properties are computed for each of the letter sections A-A through S-S and V-V shown in Figure 37. These are summarized below.

CANTILEVER BENDING ANALYSIS

SECOND AREA MOMENT (Sections J-J through S-S and V-V)
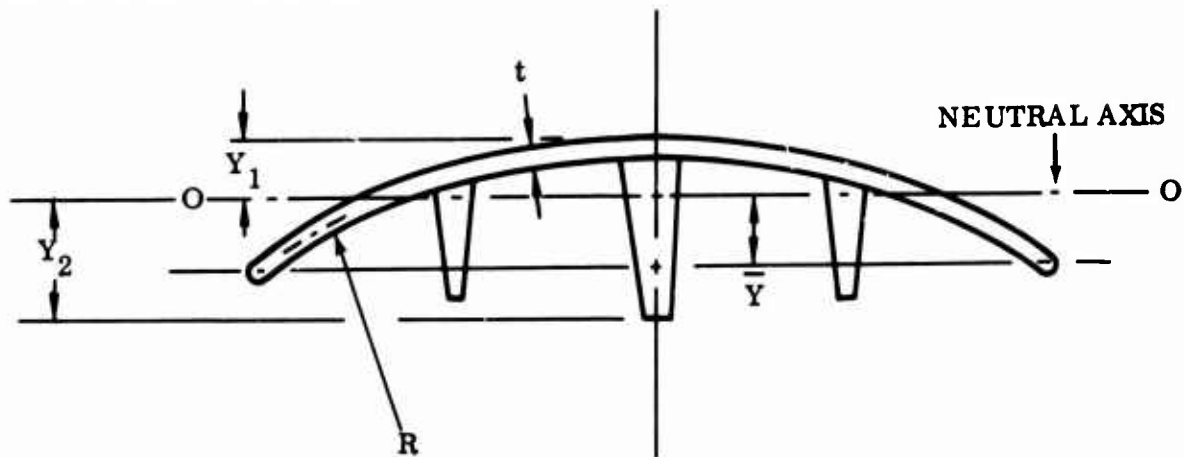
CANTILEVER BENDING LOAD SUMMARY

The assumed discrete load (pressure x local area equivalent) distribution and station location are shown below.

LOAD W_i (lb)

0	0	405	770	1000	985	710	611	611	386	386	100

EI_0 * ($lb\text{-}in.^2$)	2500	80.0	34.60	16.15	13.44	11.00	10.15	8.32	5.10	1.84	0.46
Δ_i (in.)	2.0	0.58	0.58	1.15	1.15	1.15	1.15	1.15	1.15	1.15	0.52
STA.	1	2	3	4	5	6	7	8	9	10	11 12

* E = 23.09 psi at 1400°F
x 10^6

111
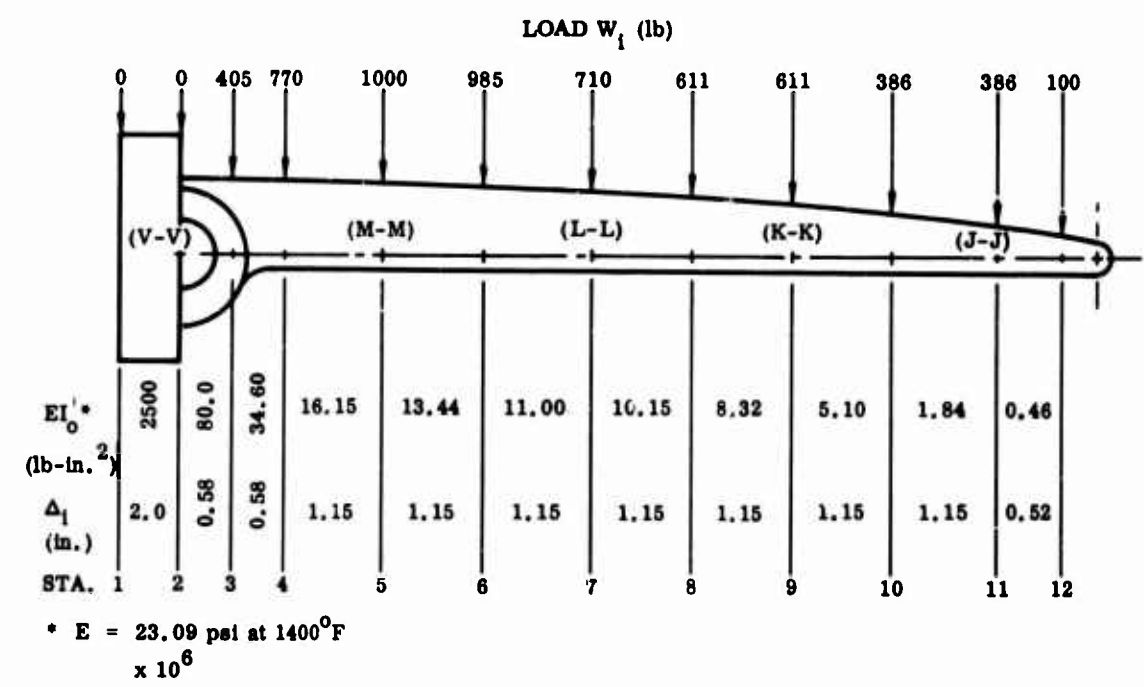
Station	I_0 (In.^{4})	$\bar{Y}$ (In.)	Y_1 (In.)	$\dfrac{I_0}{\bar{Y}}$	$\dfrac{I_0}{Y_1}$
J-J	0.0095	0.114	0.169	0.083	0.056
K-K	0.361	0.281	0.319	1.29	1.13
L-L	0.450	0.456	0.461	0.98	0.97
M-M	0.597	0.672	0.561	0.89	1.06
V-V	3.487	3.267	1.265	13.00	2.75
N-N	0.812	0.979	0.662	-	-
P-P	0.698	0.885	0.637	-	-
R-R	0.350	0.605	0.565	-	-
S-S	0.049	0.302	0.272	-	-
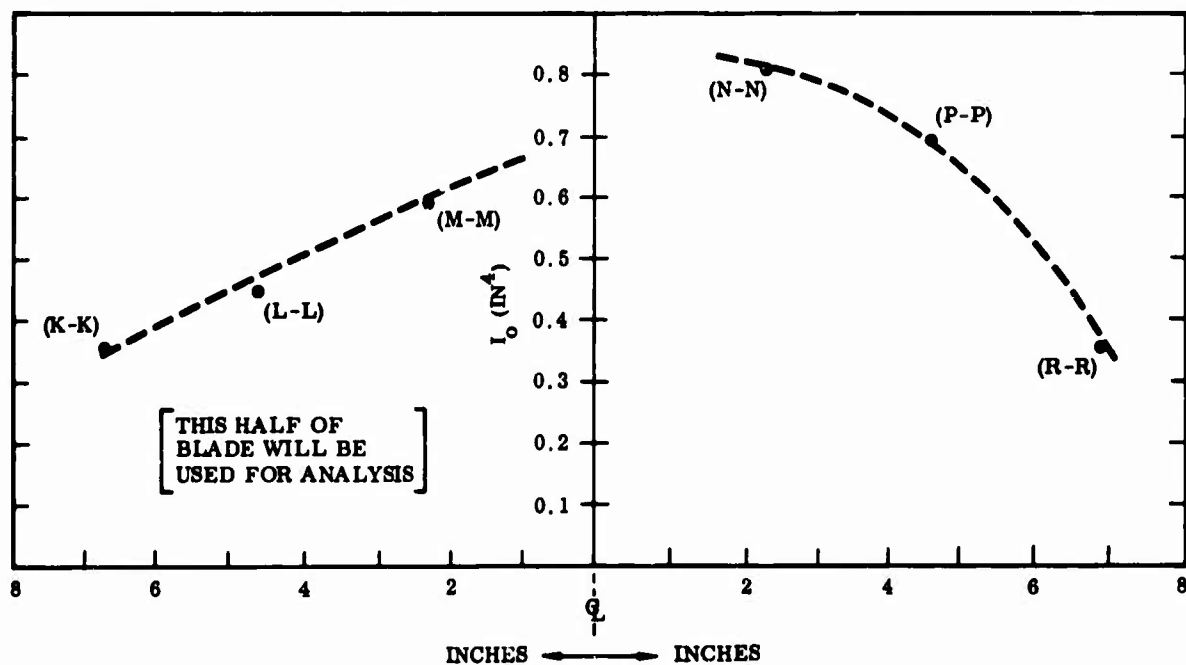
RESULTS - CANTILEVER BENDING ANALYSIS

The IBM 360 output sheet is contained in Table VIII. Shear stresses are seen to be negligible. The results are shown graphically on page 115.

The critical bending stresses are considered to be at the sealing edge and at the pressure side of the blade (see pages 111 and 112 for section properties).

$$\text{Bending Stress} = f_b = \frac{MY}{I_0} = M/Z, \quad Z = \frac{I_0}{Y}$$

Station Number	M (In.-Lb)	I_0 (In.^{4})	Y_1 (In.)	$\overline{Y}$ (In.)	$\dfrac{I_0}{Y_1}$	$\dfrac{I_0}{\overline{Y}}$	f_b at Seal Edge (psi)	f_b at Pressure Surface (psi)
2 (V-V)	25,442	3.48	1.26	0.26	2.75	13.3	-	9,250
3	22,012	0.68	*0.64	*0.82	1.06	0.83	-	20,800
4	18,816	0.64	*0.62	*0.77	1.03	0.83	-	18,300
5 (M-M)	13,309	0.597	0.56	0.67	1.07	0.89	-15,000	12,400
7 (L-L)	5,727	0.450	0.46	0.46	0.98	0.98	Neg.	5,850

*Conservatively estimated values ∴ actual stress less than calculated value shown.

SIMPLE SUPPORT BENDING ANALYSIS

SECOND AREA MOMENT (Sections A-A through H-H, Figure 37)

CALCULATION SCHEMATIC FOR SECTIONS A-A THROUGH H-H (SHADED PORTION OMITTED FOR SECTIONS A-A, A'-A', AND B-B)
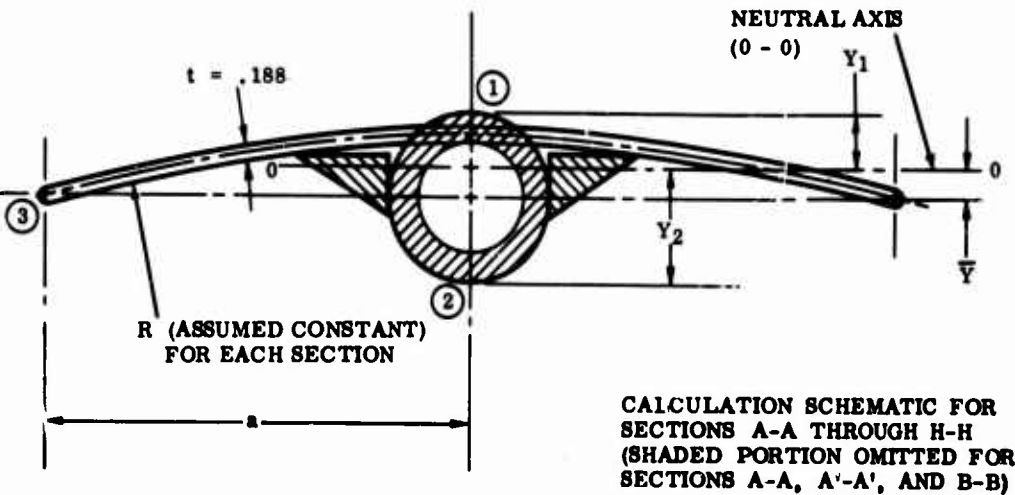
TABLE VIII. CANTILEVER BENDING ANALYSIS

R1=12721.121   R2=-18685.121

Station Number	Weight	EIX10E-6	Delta	X	Shear	Moment	Slope	Deflection
1	0.00	2500.00	2.00	0.00	0.0	0.0	0.00015901	0.0
2	0.00	80.00	0.57	2.00	-12721.12	-25442.24	-0.00015901	0.0
3	405.00	34.60	0.57	2.57	5964.00	-22012.94	-0.00043336	-0.00017031
4	770.00	16.15	1.15	3.15	5559.00	-18816.52	-0.00095124	-0.00056838
5	1000.00	13.44	1.15	4.30	4789.00	-13309.17	-0.00219058	-0.00237492
6	985.00	11.00	1.15	5.45	3789.00	-8951.82	-0.00322791	-0.00549055
7	710.00	10.15	1.15	6.60	2804.00	-5727.22	-0.00402030	-0.00965826
8	611.00	8.32	1.15	7.75	2094.00	-3319.12	-0.00457413	-0.01460005
9	611.00	5.10	1.15	8.90	1483.00	-1613.67	-0.00498544	-0.02009680
10	386.00	1.84	1.15	10.05	872.00	-610.87	-0.00535827	-0.02604443
11	386.00	0.46	0.52	11.20	486.00	-51.97	-0.00561413	-0.03235356
12	100.00	0.0	0.00	11.72	100.00	0.03	-0.00564350	-0.03523054
13	0.00	1.00	0.00	11.72	0.00	0.03	-0.00564350	-0.03528054

IHC2171

114
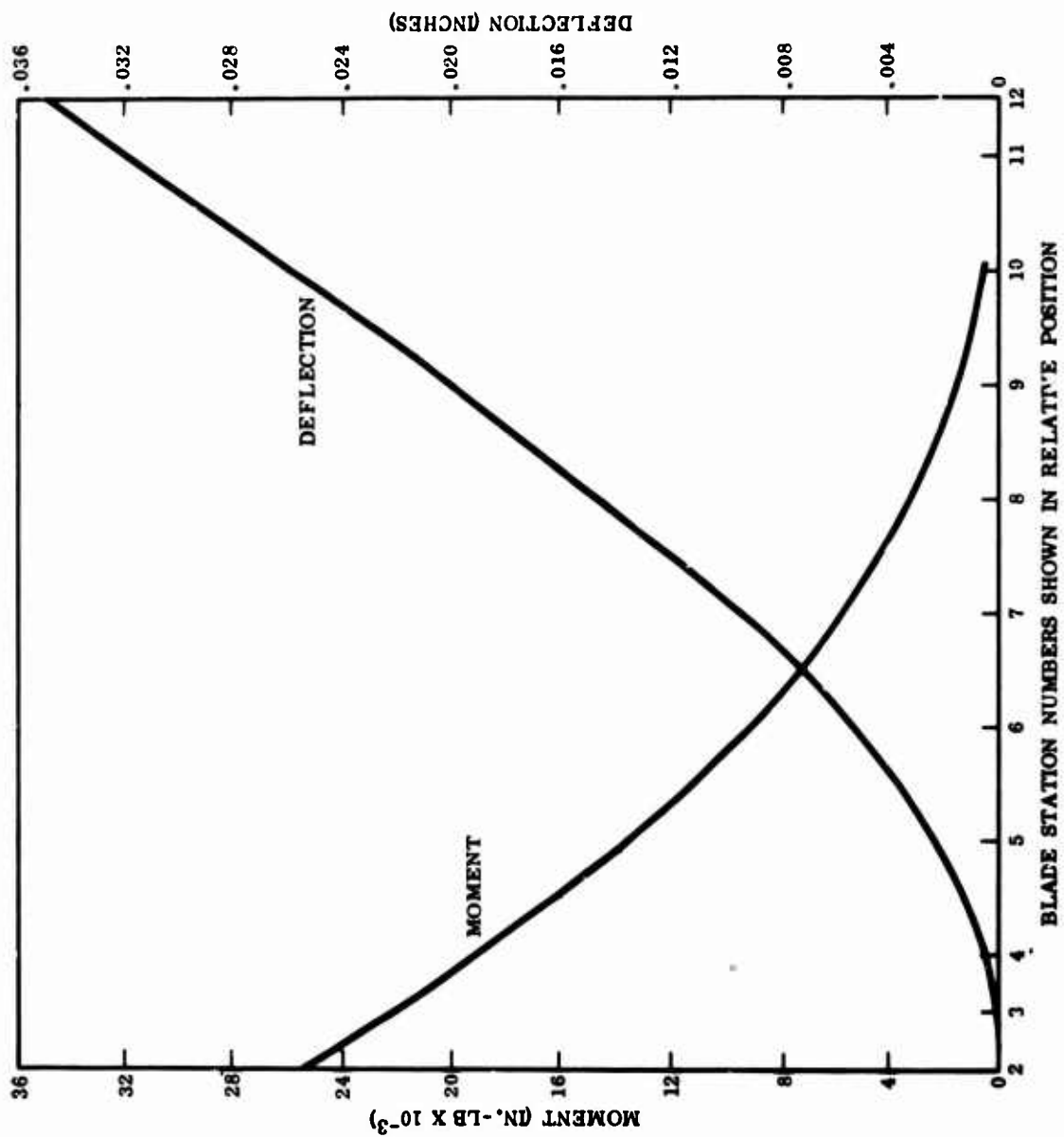
Figure 56. Bending Moment and Deflection vs. Blade Station For Pressure Loaded Cantilever Assumption.

115

Station	a (In.)	R (In.)	$\overline{Y}$ (In.)	I_0 (In.^{4})
A-A	10.50	37.50	1.000	0.803
A'-A'	10.35	38.96	0.931	0.686
B-B	9.68	39.00	0.812	0.487
D-D	9.05	39.00	0.678	0.562
E-E	8.34	39.09	0.599	0.568
F-F	7.30	39.15	0.458	0.730
G-G	6.00	40.10	0.210	0.632
H-H	4.00	40.25	0.053	0.638

SIMPLE SUPPORT BENDING LOAD SUMMARY
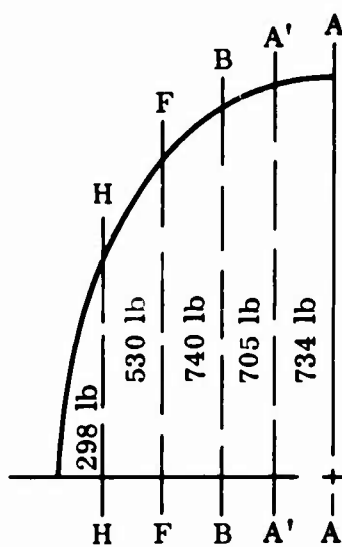
The assumed equivalent discrete load distribution and station location are shown below

LOAD (W) IN.-LB

	100	298	400	507	509	582	1445	1439	1468

¢ SYM.

SIMPLE
SUPPORT

EI_o
$(E = 23.09)$
$\times 10^6$

14.0	14.7	16.9	13.1	13.0	12.0	15.8	18.5

Δ_i
(INCHES
BETWEEN
STATIONS)

0.6	0.75	0.75	0.75	0.75	0.85	1.44	1.44

STATION	1	2	3	4	5	6	7	8	9

(DWG REF)		(H-H)	(G-G)	(F-F)	(E-E)	(D-D)	(B-B)	(A'-A')	(A-A)

117
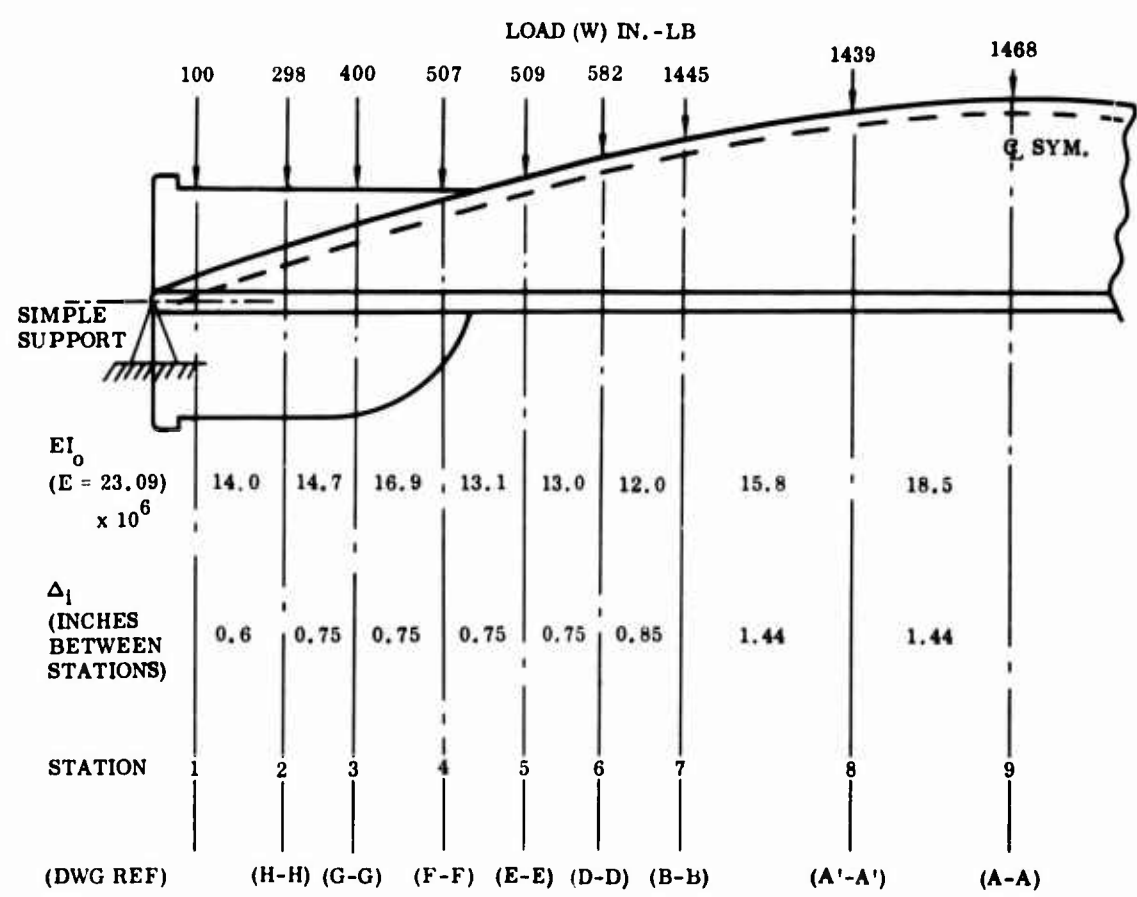
The IBM 360 output sheet for blade bending between simple supports is contained in Table IX.

Direct shear stresses are seen to be negligible by examination.

Bending moment and deflection results are summarized graphically on page 120.

Bending stress calculations are tabulated on the next page for points 1 , 2 , and 3 (see schematic on page 113).

$$\text{Bending Stress} = f_b = \frac{MY}{I_0} = \frac{M}{Z}$$

$$Z = \frac{I_0}{Y}$$

Station	M (in.-lb)	I_0	Y_1	Y_2	$\bar{Y}$	z_1	z_2	$\bar{z}$	f_b ① $= \frac{M}{Z_1}$	f_b ② $= \frac{M}{Z_2}$	f_b ③ $= \frac{M}{\bar{Z}}$
A-A	25,615	0.803	0.532	-	1.00	1.51	-	0.803	17,000	-	32,000
A'-A'	24,558	0.686	0.569	-	0.931	1.20	-	0.735	20,500	-	33,500
B-B	21,429	0.487	0.588	-	0.812	0.83	-	0.600	25,800	-	35,700
D-D	18,354	0.562	0.520	0.870	0.678	1.08	0.646	0.830	17,000	28,400	22,200
E-E	15,204	0.568	0.420	1.370	0.599	1.35	0.414	0.950	11,300	36,800	16,000
F-F	11,672	0.730	0.555	1.410	0.458	1.31	0.517	1.590	8,900	22,600	7,350
G-G	7,760	0.630	0.800	1.200	0.210	0.785	0.525	3.00	9,900	14,800	2,580
H-H	3,548	0.638	1.000	1.000	0.053	0.638	0.638	12.70	Negligible		-

118

TABLE IX. BEAM DEFLECTION PROGRAM DIVERTER VALVE BENDING WITH SIMPLE SUPPORT AT EACH SPLINE

RJ= -6014.008   R2= -6013.992

| Station Number	Weight	EIX10E-6	Delta	X	Shear	Moment	Slope	Deflection
1	100.00	14.00	0.60	0.00	0.00	0.00	-0.00798711	0.00
2	298.00	14.70	0.75	0.60	5914.01	3548.40	-0.00791469	-0.00477054
3	400.00	16.90	0.75	1.35	5616.01	7760.41	-0.00765197	-0.01060803
4	507.00	13.10	0.75	2.10	5216.01	11672.41	-0.00714564	-0.01615714
5	509.00	13.00	0.75	2.85	4709.01	15204.16	-0.00637292	-0.02122660
6	582.00	12.00	0.85	3.60	4200.01	18354.17	-0.00536078	-0.02562674
7	1445.00	15.80	1.44	4.45	3618.01	21429.47	-0.00413431	-0.02966215
8	1439.00	18.50	1.44	5.89	2173.01	24558.60	-0.00220199	-0.03422429
9	1468.00	18.50	1.44	7.33	734.01	25615.57	-0.00024927	-0.03598920
10	1439.00	15.80	1.44	8.77	-733.99	24558.62	0.00186679	-0.03482457
11	1445.00	12.00	0.85	10.21	-2172.99	21429.51	0.00427168	-0.03040487
12	582.00	13.00	0.75	11.06	-3617.99	18354.21	0.00563068	-0.02619636
13	509.00	13.10	0.75	11.81	-4199.99	15204.22	0.00659536	-0.02161163
14	507.00	16.90	0.75	12.56	-4708.99	11672.47	0.00728960	-0.01640481
15	400.00	14.70	0.75	13.31	-5215.99	7760.48	0.00774657	-0.01076627
16	298.00	14.00	0.60	14.06	-5615.99	3548.48	0.00803959	-0.00484645
17	100.00	0.00	0.00	14.66	-5913.99	0.09	0.00811565	0.00000006
18	0.00	1.00	0.00	14.66	0.00	0.09	0.00811565	0.000000006

IHC2171

119
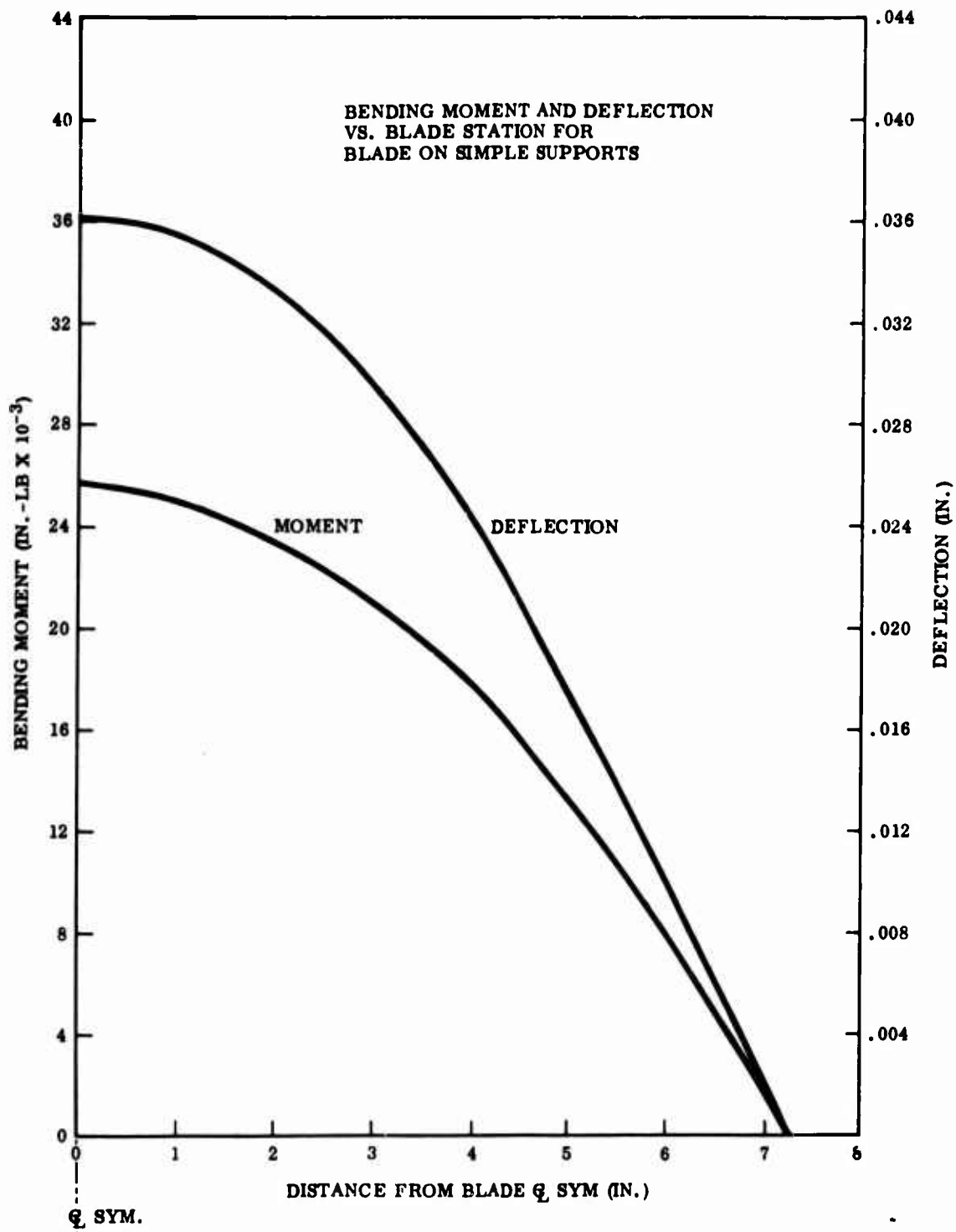
Figure 57.   Bending Moment and Deflection vs. Blade Station
For Blade on Simple Supports.

120

BLADE STRESS SUMMARY

The blade material is alloy 713 LC with controlled low iron content for maximum creep strength.

The following are typical properties (from Ref. 6):

Uniaxial tension stress for 0.2% creep
in 1000 hours at 1400°F ....= 41,000 psi

F_{ty} at 1400°F ....= 108,000 psi

F_{ty} at room temperature ....= 106,000 psi

The individual computed stresses are all well within the target creep limit. Due to the complex nature of blade shape, curvature, and section variation, calculation of an equivalent stress creep analysis is impractical. The following three factors also favor a conservative stress condition:

- At the computed condition of maximum stress (closed position), the blade temperature will be less than 1400°F (estimated between 1300°F and 1350°F).

- The existence of a combined stress resulting in localized creep will soon cause stress redistribution to a more favorable condition.

- During the 1000-hour operation, each blade will only experience a portion of this time at the maximum stress condition.

HOUSING (Figure 36)

Only the maximum membrane stresses will be calculated. The localized discontinuity and "bulging" stresses for noncircular shape should be determined experimentally for accurate determination.

Housing material = Rene' 41 with following properties (Ref. 1):

Uniaxial tension stress for 0.2% creep
in 1000 hours at 1400°F ....= 30,000 psi

F_{ty} at 1400°F ....= 104,000 psi

F_{ty} at room temperature ....= 130,000 psi

HALF STAMPING (Figure 36)

At Section F-F (Figure 36)

$$f = \frac{pR}{t} = \frac{48 \times 22.08}{.090} \doteq 11,800 \text{ psi (where } t = .090)$$
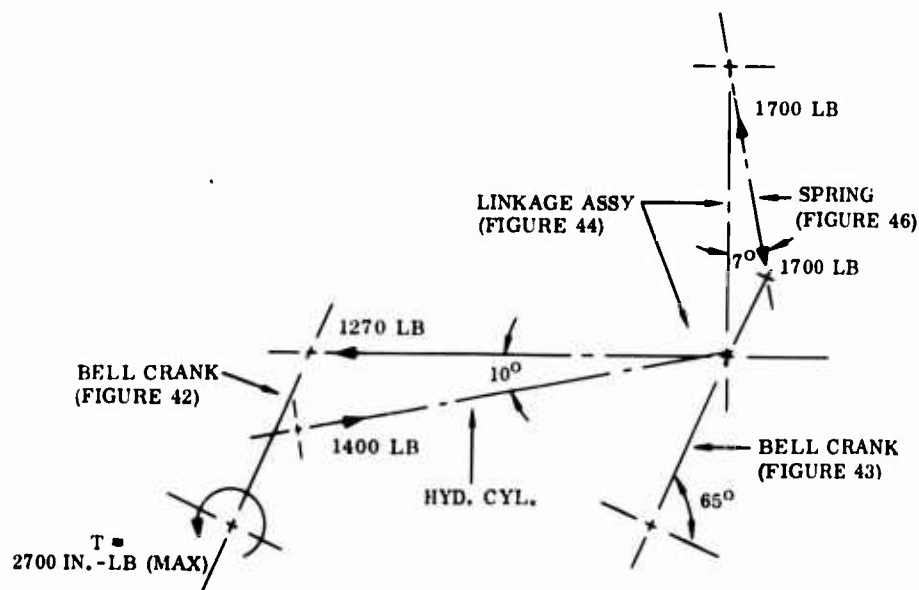
At Section E-E (Figure 36)

$$f = \frac{pR}{t} = \frac{48 \times 14.78}{.030} = 23,600 \text{ psi (where } t = .030)$$

The above value of 23,600 will be approximately the maximum membrane stress in housing shell, and is well below the creep limit.

ACTUATOR LINKAGE

The maximum loads are shown in the schematic below for the moment the actuation cycle begins (negligible load components not shown).

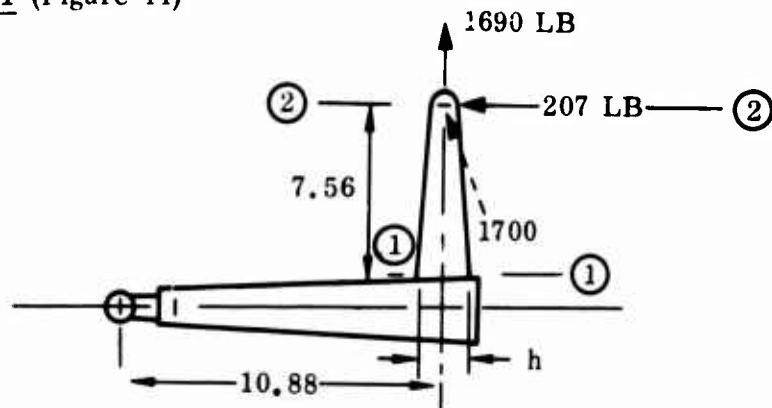Linkage Material = Ti-6Al-4V

Working Temp = 600°F

Properties (Ref 1):

$$F_y = 120 \text{ ksi} \times 67\% = 80 \text{ ksi}$$

$$F_u = 130 \text{ ksi} \times 74\% = 96.5 \text{ ksi}$$

122

Stress Range for Life > 10,000 cycles = 80,000 psi (Ref. 3)

LINKAGE ASSY (Figure 44)

At Section ① - ①

$$A = Z \times .093 \times 1.22 = 0.227 \text{ in.}^2$$

$$Z = \frac{Ah}{6} = \frac{0.227 \times 1.22}{6} = 0.046 \text{ in.}^3$$

$$M = 207 \times 7.56 = 1565 \text{ in.-lb}$$

$$f_b = \frac{M}{Z} = \frac{1565}{0.046} = \underline{34,000 \text{ psi}}$$

$$f_t = \frac{P}{A} = \frac{1690}{0.227} = \underline{7,450 \text{ psi}}$$

$$\text{Max } f = f_b + f_t = 41,650 \text{ psi}$$

$$\text{M.S.} = \frac{80}{41.65} - 1 = \underline{+0.92}$$

At Section ② -- ②

Check for lug strength

$$\text{(Ref 2) } P_{all} = K_{bry} A_{br} F_y = 1.8 \times .027 \times 80 \times 10^3$$

$$= 3,900 \text{ lb}$$

$$\frac{R_0}{2R_i} = \frac{.24}{.125} = 2.0 \qquad \text{M.S.} = \frac{3,900}{845} - 1 = \underline{3.6}$$

$$\therefore K_{bry} = 1.8 \qquad A_{br} = .250 \times .093 = .027$$

123

SPRINGS (Figure 46)

$$\text{Material} = 17\text{-}7 \text{ CH } 900$$

Properties:

Wire Dia	F_y
.225 ~ .306	242 ksi
.306 ~ .44	235 ksi

$$E = 28 \times 10^6 \text{ psi}$$

$$\mu = 0.28$$

$$G = 10.9 \times 10^6 \text{ psi}$$

(All design equations from Ref. 4)

SPRING P/N 51217

$$D_w = .375 \qquad O\,D = 2.0 \qquad D_m = 2-.375 = 1.625$$

$$C = \frac{D_m}{D_w} = \frac{1.625}{.375} = 4.33$$

$$K_a = 1.37$$

$$F = 1095 \sim 1165 \qquad N_C = 13.5$$

$$\text{Yield Strength} = 235 \times .95 = 223 \text{ ksi}$$

$$\text{Yield Strength in Shear} = 223 \times .65 = 145 \text{ ksi}$$

$$S_S = Ka\,\frac{8FD_m}{\pi D_w^{\ 3}} = 1.37 \times \frac{8 \times 1165 \times 1.625}{\pi\,(.375)^3} = 125,000 \text{ psi}$$

$$\delta = \frac{8FD_m^{\ 3}N_c}{G\,D_w^{\ 4}} = \frac{8 \times 1165 \times 1.625^3 \times 13.5}{10.9 \times 10^6\,(.375)^4} = 2.5$$

$$\text{Compressed length under 1165 lb} = 6 \text{ in.}$$

$$\text{Free length} = 6 + 2.5 = 8.5$$

124

$$k = \frac{F}{\delta} = \frac{1165}{2.5} = 466 \text{ ib/in.}$$

Minimum space for spring $= 8.2 - (1.9 + .34 + .2)$

$$= 8.2 - 2.44 = 5.76$$

$$\delta_{max} = 8.5 - 5.76 = 2.74$$

$$F_{max} = -466 \times 2.74 = 1280 \text{ lb}$$

$$(S_s)_{max} = 125,000 \times \frac{1280}{1165} = 137,500 \text{ psi}$$

$$M.S. = \frac{145}{137} - 1 = +\underline{.05}$$

SPRING 51217-1

$$D_w = .25 \qquad OD = 1.19 \qquad D_m = 1.19 - .25 = .94$$

$$C = \frac{.94}{.25} = 3.76 \qquad K_a = 1.43$$

$$F = 494 \sim 534 \text{ lb} \qquad N_C = 17$$

Yield strength $= 242 \times .95 = 230 \text{ ksi}$

Yield strength in shear $= 230 \times .65 = 150 \text{ ksi}$

$$S_S = 1.43 \times \frac{8 \times 534 \times .94}{\pi (.25)^3} = 117,000 \text{ psi}$$

$$\delta = \frac{8 \times 534 \times (.94)^3 \times 17}{10.9 \times 10^6 (.25)^4} = 1.42$$

Compressed length under 534 lb $= 5.28$

Free length $= 5.28 + 1.42 = 6.7$

$$K = \frac{534}{1.42} = 376 \text{ lb/in.}$$

Minimum space for spring $= 5.76 - (.36 + .36) = 5.04$

$$\delta_{max} = 6.7 - 5.04 = 1.66$$

$$F_{max} = 376 \times 1.66 = 624 \text{ lb}$$

$$(S_S)_{max} = 117,000 \times \frac{624}{534} = 137,000 \text{ psi}$$

$$M.S. = \frac{150}{137} - 1 = +\underline{.09}$$

Maximum shear stresses in both springs are below the yield strength in shear of the material.

BELL CRANK LONG AND BELL CRANK SHORT (Figures 43 and 42)

These items are considered adequate by inspection.

HYDRAULIC CYLINDER ASSY (Figure 45)

CYLINDER (Figure 45)

$$\text{Working Pressure} = 3000 \text{ psi}$$

$$\text{Proof Pressure} = 1.5 \times 3000 = 4500 \text{ psi}$$

$$\text{Burst Pressure} = 2.0 \times 3000 = 6000 \text{ psi}$$

$$\text{Temp} = 600^{\circ}F$$

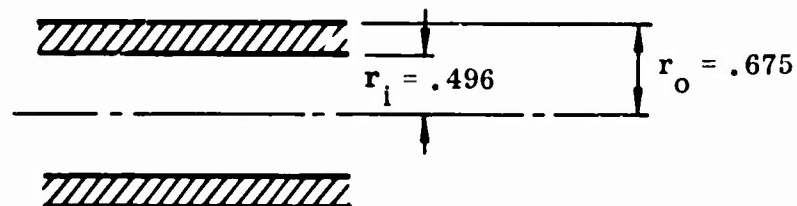$$\text{Material} = 6 \text{ Al } 4V \text{ Titanium}$$

Material properties at $600^{\circ}F$ (Ref. 1):

$$F_y = 120 \text{ ksi} \times 67\% = 80 \text{ ksi}$$

$$F_u = 130 \text{ ksi} \times 74\% = 96.5 \text{ ksi}$$

Estimated stress range for life > 10,000 cycles = 80,000 psi (Ref. 3).

MAXIMUM HOOP STRESS

126

Using Lame's solution for thick cylinders,

$$f_t = p \frac{r_o{}^2 + r_i{}^2}{r_o{}^2 - r_i{}^2} = p \frac{0.636}{0.144} = 4.43 \, p$$

$$f_t = 4.43 \times 3000 = 13{,}250 \text{ psi}$$

$$\text{M.S.} = \frac{80}{13.25} - 1 = \underline{+\,5.05 \text{ at working pressure}}$$

$$f_t = 4.43 \times 4500 = 20{,}000 \text{ psi}$$

$$\text{M.S.} = \frac{80}{20} - 1 = \underline{+3.00 \text{ at proof pressure}}$$

$$f_t = 4.43 \times 6000 = 26{,}600 \text{ psi}$$

$$\text{M.S.} = \frac{46.5}{26.6} - 1 = \underline{+\,2.60 \text{ at burst pressure}}$$

LUG END
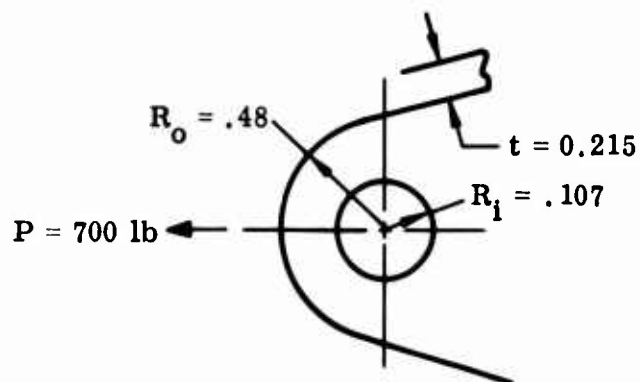
From Ref. 2,

$$P_{allowable} = K_{bry} \, A_{br} \, F_y$$

$$K_{bry} = \text{(From Figure 14, Ref. 2)}$$

$$A_{br} = \text{Projected area} = 2R_i t$$

$$\frac{R_o}{2 R_i} = 1.5 \;\rightarrow\; K_{bry} = 1.5$$

127

$$A_{br} = 2 \times .107 \times .215 = .0675$$

$$M.S. = \frac{8100}{700} - 1 = \underline{+ 10.6}$$

$$P_{all} = 1.5 \times .0675 \times 80 \times 10^3 = 8100 \text{ lb}$$

SHAFT (Figure 38)

The shaft load schematic is shown below. The total blade pressure force reacted at each bearing is

$$F_t = \text{blade area} \times 48 \text{ psig}/2$$

$$= \frac{\pi \times 10.50 \times 7.28 \times 48}{2} = 5750 \text{ lb}$$

5750 LB

.34

1.95

①

T = 2700 IN.-LB

①

.95

1.61

$R_1 = 5750 \times 1.61/_{2.56}$

$R_2 = \frac{5750}{2.56} \times .95 = 2140 \text{ LB}$

= 3610 LB

3430 IN.-LB MAX.

M

S
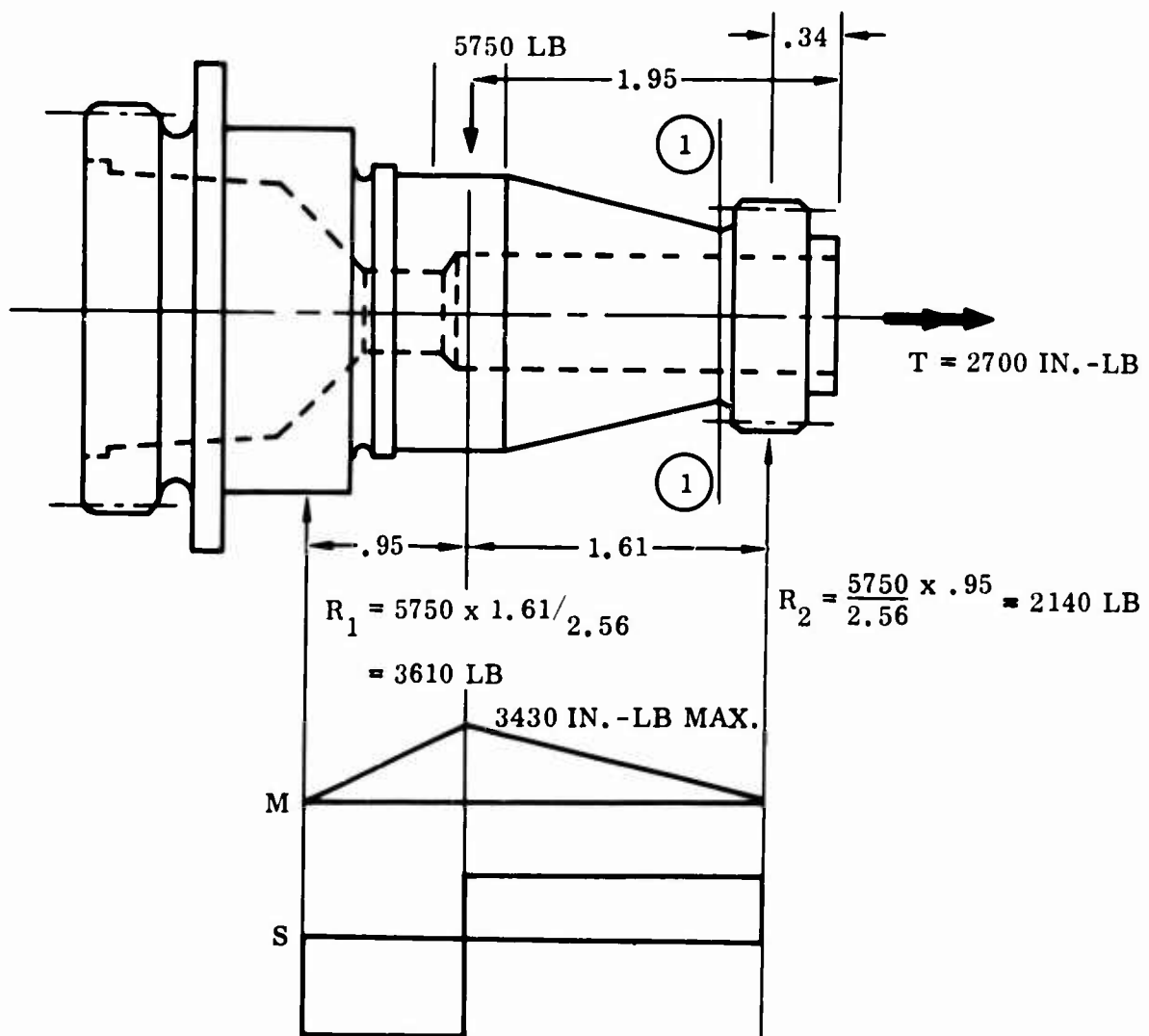
At point of maximum moment, equivalent moment and torque are

$$M' = \frac{1}{2}(M + \sqrt{M^2 + T^2}) = \frac{1}{2}(3430 + \sqrt{3430^2 + 2700^2}) = 3915 \text{ in.-lb}$$

$$T' = \sqrt{M^2 + T^2} = \sqrt{3430^2 + 2700^2} = 4400 \text{ in.-lb}$$

$$I = .049(1.4^4 - .60^4) = 3.70 \text{ in.}^4$$

$$I_p = 2 \times I = 7.40$$

$$f_t = \frac{M R_o}{I} = \frac{39.5 \times .70}{3.70} = \underline{\text{Negligible}}$$

$$f_s = \frac{T' R_o}{I_p} = \frac{4400 \times .70}{7.40} = \underline{\text{Negligible}}$$

At minimum torsion area (① - ①)

$$f_s = \frac{T R_o}{I_p}$$

$$I_p = 2 \times .049(.88^4 - .60^4) = 2 \times .049 \times .470 = .046$$

$$f_s = \frac{2700 \times .44}{.046} = 25,800 \text{ psi}$$

For alloy 713C at 1400°F $\quad \rightarrow \quad$ M.S. $= \dfrac{108}{25.8} - 1 = \underline{\underline{+3.2}}$

Spline at blade end of shaft

From Ref. 5, maximum tooth shear stress is

$$f_s = \frac{4T}{DN F_e t_c} = \frac{4 \times 2700}{1.08 \times 13 \times .39 \times .045}$$

$$= 44,000 \text{ psi}$$

$$\text{M.S.} = \frac{.7 \times 108}{44} - 1 = \underline{\underline{+0.72}}$$

129

and tooth contact compressive stress is

$$f_c = \frac{2T}{DNF_{eh}} \qquad\qquad h \approx \frac{D}{N} \approx \frac{1.08}{13} = .083$$

$$f_c = \frac{2 \times 2700}{1.08 \times 13 \times .39 \times .083} = 11,900 \text{ psi (\underline{Negligible})}$$

LITERATURE CITED

1. MIL-HDBK-5A, METALLIC MATERIALS AND ELEMENTS FOR AERO-SPACE VEHICLE STRUCTURES, February 8, 1966.

2. Melcon, M. A. and Hoblit, F. M., DEVELOPMENTS IN THE ANALYSIS OF LUGS AND SHEAR PINS, Product Engineering, June 1953.

3. ROOM AND ELEVATED TEMPERATURE FATIGUE CHARACTERISTICS OF Ti-6Al-4V, Titanium Metals Corp. of America Titanium Data, December 1957.

4. HANDBOOK OF MECHANICAL SPRING DESIGN, Associated Spring Corp, Bristol Conn., 1964.

5. Dudley, D. W., WHEN SPLINES NEED STRESS CONTROL, Product Engineering, December 23, 1957.

6. ALLOY 713C TECHNICAL DATA, International Nickel Company, August 1963.

APPENDIX III
DIVERTER VALVE AERODYNAMIC ANALYSIS

The main factors considered in estimating the aerodynamic quality of the diverter valve have been: the total pressure losses, the velocity gradient, and the possibility of flow breakaway. Also, as a support to the mechanical design, the aerodynamic forces acting on the system and the leakage problems have been analyzed.

The conditions of the flow entering the diverter valve were based on a mass flow of 70 lb/sec, a total absolute pressure of 60 psia, and a temperature of 1400°F. The diameter of the inlet section is 20.70 inches, while the diameter of the outlet section is 14.95 inches. The Mach number of the flow entering the system is about 0.17, while the Mach number of the flow leaving the system is about 0.35.

The total pressure loss evaluation includes the skin-friction, turning, contraction and expansion losses. The calculations were made, in general, in accordance with the procedure of SAE Aero-Space Applied Thermodynamics Manual, Section 1. The effects of compressibility have been included. The system was split into a number of portions and each one was related to a typical case for which pressure loss coefficient data are available. The overall pressure loss is obtained as the sum of all the partial losses. The analyses of the system in the through-flow and in the diverted-flow positions are made independently. The procedure of analysis is similar, since the two positions are symmetrical, with the exception that the diverted-flow position has, additionally, a 60-degree vaned bend.

In either of the two positions (through flow or diverted flow), when one butterfly valve is open and the other one closed, the valve in the open position in effect subdivides the system into two channels. The butterfly valve in the closed position makes a sharp 44-degree angle with the upstream duct direction, while the butterfly valve in the open position receives the flow at zero incidence and smoothly turns it 15 degrees. One of the two channels is defined by the surfaces of the two butterfly valves and the casing wall, while the other channel is defined by one surface of the open butterfly valve and the casing. In the diverted-flow position, the two channels lead to the entrance of the 60-degree vaned elbow.

The predicted total pressure loss in the through-flow position amounts to about 0.26 psi, which corresponds to 22 percent of the inlet dynamic head or 0.4 percent of the inlet total pressure.

The predicted total pressure loss in the diverted-flow position amounts to about 0.79 psi, which corresponds to 69 percent of the inlet dynamic head or 1.3 percent of the inlet total pressure.

The calculations have not considered the effect of a probable swirl coming out of the engine or the effect of the diffuser upstream of the system, all of which will affect the behavior of the flow through the valve.

The cross section of the two channels in each position presents corners due to the discontinuity of the vanes to the conical shape of the main duct. These corners are a source of vortex losses. Also, there is a discontinuity in one of the channels

132

due to the boss, which produces contraction and expansion losses and wakes. The accelerated flow whould minimize this effect.

The velocity gradient of the flow leaving the system is expected to be small, especially in the through-flow position, where the flow is required to turn only 15 degrees. The diverted-flow position requires an additional 60-degree turn, which is a source of high losses and high velocity gradient when the radius of curvature of the turn is small. In order to minimize those problems and at the same time to use as small a space as possible, a bend of small radius of curvature with airfoil cascade has been adopted.

Although this diverter valve is expected to produce acceptable losses with small velocity gradient and no flow breakaway, the irregular internal shape of the system makes it desirable to have a scale model flow test that will evaluate the pressure losses and indicate if further refinements of valve body and blade contour are required.

Annex A contains the calculations for the pressure loss analysis.

Annex B contains the analysis of the aerodynamic forces acting on the diverter valve and the torque produced on the flange at the entrance of the system.

Annex C contains the study of the torque characteristics of the butterfly valve.

Annex D presents the analysis of the aerodynamic forces acting on each one of the cascade vanes at the 60-degree bend.

Table X presents the sizing and flow conditions of the diverter valve.

Annex E presents the analysis of gas leakage through the valve seat and shaft hub. The results predict a very negligible amount of leakage.

TABLE X SIZING AND FLOW CONDITIONS					
	Symbol	Formula	Units	Through Flow Value	Diverted Flow Value
1	W	Data	lb/sec	70	-
2	P_1	Data	psia	60	-
3	T_1	Data	°F	1400	-
4	γair	Data	-	1.330	-
5	γ.01 fuel/air	Data	-	1.322	-
6	γ	Adopted	-	1.33	-

	Symbol	Formula	Units	Through Flow Value	Diverted Flow Value
7	D_1	Adopted	in.	20.70	–
8	D_2	Adopted	in.	14.95	–
9	T_1	③ + 460	°R	1860	–
10	$\sqrt{T_1}$	⑨$^{1/2}$	–	43.1277	–
11	A_1	π ⑦^2/4	sq in.	336.536	–
12	$W\sqrt{T_1}/A_1,\ P_1$	① ⑩ / ⑪ ②	–	0.14951	–
13	Mn_1	From Compr. Flow Relations, for ⑫	–	0.170	–
14	$(P/p)_1$	From Compr. Flow Relations, for ⑫	–	1.0193	–
15	$(T/t)_1$	From Compr. Flow Relations, for ⑫	–	1.00475	–
16	$(\rho t/\rho s)_1$	From Compr. Flow Relations, for ⑫	–	1.0145	–
17	$(V/\sqrt{T})_1$	From Compr. Flow Relations, for ⑫	–	8.08	–
18	p_1	②/ ⑭	psia	58.86	–
19	q_1	②- ⑱	psi	1.14	–
20	t	⑨/ ⑮	°R	1851.2	–
21	t	⑳ – 460	°F	1391.2	–
22	ρt	144②/53.3⑨	lb/cu ft	0.08715	–
23	ρs	㉒ / ⑯	lb/cu ft	0.08590	–
24	μ	From map CR-3500 for 21	lb/hr ft	.1020	–
25	μ	㉔ /3600	lb/sec ft	28.33 x 10^{-6}	–

TABLE X - Continued

134

		TABLE X - Continued			

	Symbol	Formula	Units	Through Flow Value	Diverted Flow Value
26	ν	(25) / (23)	ft^2/sec	3.298×10^{-4}	-
27	V_1	(10) , (17)	ft/sec	348.5	-
28	Re	(27) (7)/12 (26)	-	1.82×10^6	-
29	A_2	π(8)^2/4	sq in.	175.5389	-
30	P_{12}/q_1	Assumed	-	0.22	0.69
31	ΔP_{12}	(19) x (30)	psi	0.25	0.79
32	P_2	(2) - (31)	psia	59.75	59.21
33	$W\sqrt{T_2}/A_2$, P_2	(1) (10) / (29) (32)	-	0.28783	0.29046
34	Mn_2	From Compr. Flow Relations, for (33)	-	0.344	0.347
35	$(V/\sqrt{T})_2$	From Compr. Flow Relations, for (33)	-	16.277	16.417
36	$(P/p)_2$	From Compr. Flow Relations, for (33)	-	1.0809	1.0827
37	p_2	(32) / (36)	psia	55.28	54.69
38	q_2	(32) - (37)	psi	4.47	4.52
39	V_2	(10) , (35)	ft/sec.	702.0	708.0

ANNEX A
CALCULATIONS FOR THE PRESSURE LOSS ANALYSIS

I. DIVERTED-FLOW POSITION

The diverted-flow butterfly valve (in open position) divides the flow passage into two channels. One of the two channels is defined by the surfaces of the butterfly valves and the casing wall. That channel is the upper channel. The other channel is defined by one surface of the butterfly valve in the open position and the casing. It is the lower channel. The two channels lead to the entrance of the 60-degree vaned elbow.

Partial Losses

Upper channel

1. Initial turning:

Since the configuration is unusual, it is related to different typical cases and the results are compared.

   a. Miter bend of circular section

   Since the turning angle of the channel outer wall is about 44 degrees, and of the inner wall (the most critical wall in regard to turning losses) is 15 degrees without sharp corner, the shape could be considered as a 15-degree miter bend of circular section, in which case the pressure loss coefficient would be

   $$K_T = 0.09 \quad \text{(SAE, Sec. 1, Figure 1A-15)}$$

   b. Miter bend of square section

   Using data for square miter bends, from SAE, Sec. 1, Figure 1A-21,

   $$K_T = 0.05 \quad (15^o \text{ miter})$$

   $$K_T = 0.09 \quad (21^o \text{ miter})$$

   c. Square miter with a round inner wall

   Considering the round inner wall,

   $$K_{T44} = 0.66 \quad K_{T90} = 0.66 \times 0.14$$

   $$K_T = 0.09 \quad \text{(SAE, Sec. 1, Figures 1A-16 and 1A-11)}$$

136

d. Sudden contraction and turning

Considering this configuration to be similar in the same way to one-half of a sudden contracting channel, the 44-degree turn will be one of the round corners of the contraction. The parameters required are

$$r/d_2 = 12/2 \times 9.3 \approx 0.65$$

$$A_2/A_1 \approx 9.3/12 = 0.775$$

$$K_{Tcontr.} = 0.04 \quad \text{(SAE, Sec. 1, Figure 1A-39)}$$

Additionally, there is a smooth 15-degree turn. The parameters required in order to use data from SAE, Sec. 1, Figure 1A-10 and 11 are

$$r/d \approx 2$$

$$Re \approx 2 \times 10^6$$

$$K_{T15} = 0.24 \, K_{T90} = 0.24 \times 0.085 \approx 0.02$$

$$K_T = K_{Tcontr.} + \frac{K_{T15}}{(A_2/A_1)^2}$$

$$K_T = 0.04 \cdot \frac{0.02}{(0.775)^2} = 0.04 + 0.03$$

$$\underline{K_T = 0.07}$$

Considering the answers from a., b., c., and d., the selected conservative value is

$$\underline{K_{T1} = 0.09}$$

The corresponding total pressure loss is

$$P_1 = q_1 \times K_{T1}$$

$$P_1 = 1.14 \times 0.09$$

$$\underline{\underline{P_1 = 0.103 \text{ psi}}}$$

2. <u>Channel skin-friction losses</u>:

Cross-sectional area of the upper channel is

$$A \approx 7.0 \times 15.0 = 105 \text{ sq in.}$$

Wetted perimeter of the upper channel is

$$W_p \approx 2(7.0 + 15.0) = 2 \times 22.0 = 44 \text{ in.}$$

Hydraulic radius is

$$r_{hyd.} = \frac{A}{W_p}$$

$$r_{hyd.} = \frac{105}{44} = 2.39$$

$$\underline{r_{hyd.} = 2.4 \text{ in.}}$$

Passage length is

$$\underline{L \approx 22.0 \text{ in.}}$$

<u>Friction factor</u>:

Considering a roughness $\epsilon = .000005$ (drawn tubing), the relative roughness ϵ/D will vary between 0.000003 and 0.00001 (for D of 20 inches through 6 inches). From SAE, Sec. 1, Figure 1A-4, for an Re of 2×10^6 and ϵ/D of 0.00001,

$$\underline{4_f = 0.010}$$

The corresponding loss coefficient is

$$K_{T2} = \frac{f. L}{r_{hyd}}$$

$$K_{T2} = \frac{0.010 \times 22.0}{4 \times 2.4} = 0.023$$

$$\underline{K_{T2} = 0.023}$$

The average dynamic head in the channel is about the same as the outlet dynamic head q_2.

The corresponding total pressure loss is

$$P_2 = q \times K_{T2}$$

$$P_2 = 4.47 \times 0.023 = 0.1028$$

$$\underline{P_2 = 0.103 \text{ psi}}$$

$$\Delta P_1 + \Delta P_2 = 0.103 + 0.103$$

$$\underline{\Delta P_1 + \Delta P_2 = 0.206 \text{ psi}}$$

Lower channel:

1. Initial turning:

If the pressure loss were evaluated for the lower channel, the loss coefficient corresponding to a 15-degree circular bend with an r/d of 1.4 would be

$$K_{T15} = 0.24 \, K_{T90} = 0.23 \times 0.12 = 0.028$$

$$\underline{K_{T1} = 0.028}$$

$$P_1' = q_1 \times K_{T1}$$

$$P_1' = 1.14 \times 0.028 = 0.032$$

$$\underline{P_1' = 0.032 \text{ psi}}$$

However, there is another source of losses in the lower channel, which is the contraction and expansion due to the valve boss

2. Contraction and expansion due to the valve boss:

The effect of the valve boss affects about two-thirds of the flow passing through the lower channel.

The contraction produced by the boss corresponds to an area ratio of about 0.85. The radius of curvature of the corner is

$$r/d_2 \approx 1.0/2 \times 5.5 = 0.09$$

$$K_{Tcontr.} = 0.010 \text{ (SAE} = \text{Sec. 1, Figure 1A-39)}$$

139

The expansion following the contraction should produce an additional loss coefficient:

$$K_{Texp.} = 0.022 \text{ (SAE = Sec. 1, Figure 1A-38)}$$

The total loss coefficient would then be

$$K_{T3} = K_{Tcontr.} + \frac{K_{Texp.}}{(Ar)^2}$$

$$K_{T3} = 0.010 + \frac{0.022}{(0.85)^2} = 0.010 + 0.030$$

$$\underline{\underline{K_{T3} = 0.040}}$$

Since the affected flow amounts to only two-thirds of the total flow in the channel,

$$P_3 = 2/3 \, q \times K_{T3}$$

$$P_3 = 2/3 \times 4.47 \times 0.040 = 0.119$$

$$\underline{\underline{P_3 = 0.119 \text{ psi}}}$$

This amount is somewhat conservative; therefore, it can be regarded as including the additional skin friction due to the ribs of the valve.

$$\Delta P_1 + \Delta P_2 + \Delta P_3 = 0.032 + 0.103 + 0.119$$

$$\underline{\underline{\Delta P_1 + \Delta P_2 + \Delta P_3 = 0.254 \text{ psi}}}$$

3. Bend with a cascade of vanes:

In order to reduce to a minimum the losses in the 60-degree turn at the exit of the diverted position, while using the minimum space possible, a cascade of turning vanes has been used. The expected pressure loss coefficient (considering that the upstream flow is an accelerated one and, therefore, that it will have a thin boundary layer) is expected to be of the order of 10 to 14 percent of the dynamic head entering the bend.

$$\underline{K_{T4} = 0.12}$$

$$P_4 = q_2 \times K_{T4}$$

140

$$P_4 = 4.47 \times 0.12 = 0.536$$

$$P_4 = 0.536 \text{ psi}$$

Overall total pressure losses in the diverted branch:

a. Considering the upper channel,

$$\Sigma P_u = \Delta P_1 + \Delta P_2 + \Delta P_4$$

$$\Sigma P_u = 0.103 + 0.103 + 0.536$$

$$\Sigma P_u = 0.742 \text{ psi}$$

b. Considering the lower channel,

$$\Sigma P_L = \Delta P_1 + \Delta P_2 + \Delta P_3 + \Delta P_4$$

$$\Sigma P_L = 0.03 + 0.103 + 0.119 + 0.536$$

$$\Sigma P_L = 0.790 \text{ psi}$$

$$\Sigma \Delta P_1 = 0.790 \text{ psi}$$

$$\Sigma \Delta P_1 / P = 0.790/60 = 0.013$$

$$\Sigma \Delta P_1 / P = 1.3\%$$

$$\Sigma \Delta P_1 / q_1 = 0.790/1.14 = 0.693$$
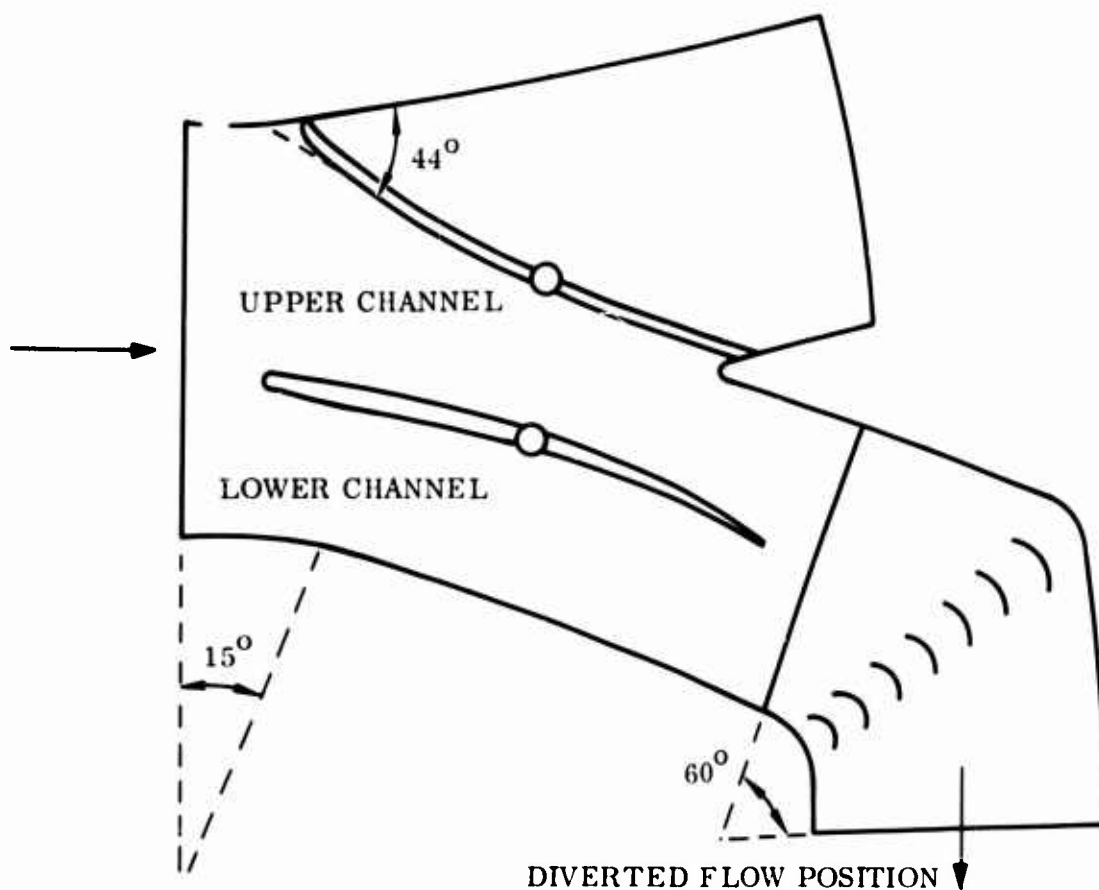
$$\Sigma \Delta P_1 / q_1 = 0.69$$

II. THROUGH-FLOW POSITION

The configuration in this case is identical to the one of the diverted branch, with the exception that it lacks the 60-degree vaned bend. Therefore, the overall pressure losses, similarly to case I, would be

1. Considering the upper channel,

$$\Sigma \Delta P_u = \Delta P_1 + \Delta P_2$$

141

UPPER CHANNEL

LOWER CHANNEL

44°

15°

60°

DIVERTED FLOW POSITION ▼

$$\Sigma \Delta P_u = 0.103 + 0.103$$

$$\underline{\underline{\Sigma \Delta P_u = 0.206 \text{ psi}}}$$

2. Considering the lower channel,

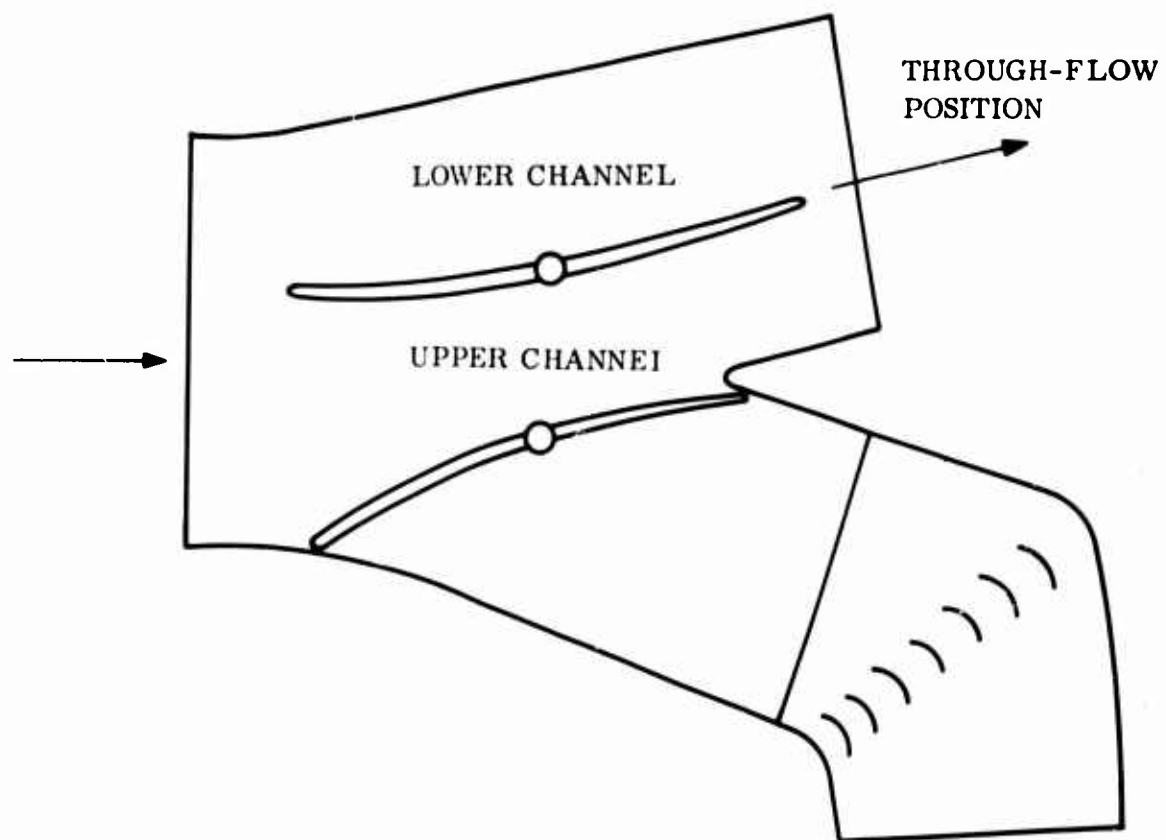$$\Sigma \Delta P_L = \Delta P_1 + \Delta P_2 + \Delta P_3$$

$$\Sigma \Delta P_L = 0.032 + 0.103 + 0.119$$

$$\underline{\underline{\Sigma \Delta P_L = 0.254 \text{ psi}}}$$

$$\underline{\underline{\Sigma \Delta P_{II} = 0.254 \text{ psi}}}$$

$$\Sigma \Delta P_{II}/P = 0.254/60 = 0.004$$

$$\underline{\underline{\Sigma \Delta P_{II}/P = 0.4\%}}$$

142

$$\Sigma \Delta P_{II}/q_1 \ = \ 0.254/1.14 \ = \ 0.223$$

$$\underline{\underline{\Sigma \Delta P_{II}/q_1 \ = \ 0.22}}$$

ANNEX B
ANALYSIS OF THE AERODYNAMIC FORCES ACTING ON THE DIVERTER VALVE AND THE TORQUE PRODUCED ON THE FLANGE AT THE ENTRANCE OF THE SYSTEM

CONDITIONS AT THE NOZZLE

Mach number: $\qquad M_N = 1.000$

Specific heat ratio: $\qquad \gamma = 1.33$

Mass flow: $\qquad M = 70$ lb/sec

Total pressure: $\qquad P = 60$ psia

Total temperature: $\qquad T = 1400^{\circ}F = 1860^{\circ}R$

From compressible flow relations, for M_N and γ,

$$M\sqrt{T/A.P} = 0.5228$$
$$P/\rho = 1.8506$$
$$V/\sqrt{T} = 44.2643$$

Nozzle area:

$$A = \frac{M\sqrt{T/P}}{(M\sqrt{T/A.P})}$$

$$A = \frac{70\sqrt{1860/60}}{0.5228} = \frac{70 \times 43.1277}{60 \times 0,5228} = 96.24$$

$$\underline{A = 96.24 \text{ sq. in.}}$$

Nozzle diameter:

$$D = \sqrt{4A/\pi}$$

$$D = \sqrt{4 \times 96.24/\pi} = \sqrt{122.54} = 11.070$$

$$\underline{D = 11.07 \text{ in.}}$$

Absolute static pressure:

$$p = P/(P/p)$$

$$p = 60/1.8506 = 32.42$$

$$\underline{p = 32.42 \text{ psia}}$$

Flow velocity at the nozzle:

$$V = \sqrt{T} \times (V/\sqrt{T})$$

$$V = \sqrt{1860} \times 44.2643 = 43.1277 \times 44.2643 = 1909.2$$

$$\underline{V = 1909.0 \text{ ft/sec}}$$

AERODYNAMIC FORCES ACTING ON THE DIVERTER VALVE

$$\begin{cases} F_x = P_1 \cdot A_1 - P_2 \cdot A_2 \cdot \cos\theta + \dfrac{M}{g}(V_1 - V_2 \cdot \cos\theta) - P_{atm}(A_1 - A_2 \cdot \cos\theta) \\[2mm] F_y = P_2 \cdot A_2 \cdot \sin\theta + \dfrac{M}{g} \cdot V_2 \cdot \sin\theta - P_{atm} A_2 \cdot \sin\theta \end{cases}$$

or

$P_{1\,relative}$
$$\begin{cases} F_x = P_{1\,rel.} \cdot A_1 - P_{2\,rel.} \cdot A_2 \cdot \cos\theta + \dfrac{M}{g}(V_1 - V_2 \cdot \cos\theta) \\[2mm] F_y = P_{2\,rel.} \cdot A_2 \cdot \sin\theta + \dfrac{M}{g} \cdot V_2 \cdot \sin\theta \end{cases}$$

$$P_{1\,rel.} = P_1 - P_{atm} = 58.86 - 14.70 = 44.16$$

P_1

$$\underline{P_{1\,rel.} = 44.16 \text{ psi}}$$

$$\underline{A_1 = 336.54 \text{ sq in.}}$$

$$\underline{V_1 = 348.5 \text{ ft/sec}}$$

$P_{1\,rel.}$

$$P_{2\,rel.} = P_2 - P_{atm} = P_{nozzle} - P_{atm} = 32.42 - 14.70 = 17.72$$
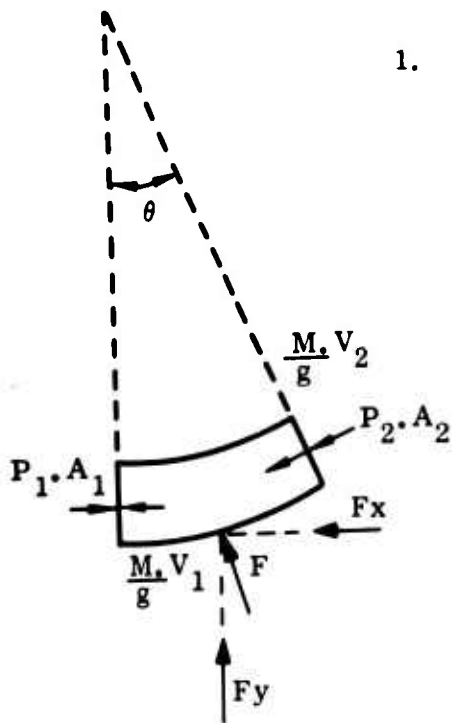
$$\underline{P_{2\,rel.} = 17.72 \text{ psi}}$$

$$\underline{A_2 = 96.24 \text{ sq in.}}$$

$$\underline{V_2 = 1909.0 \text{ ft/sec}}$$

$$\underline{M = 70 \text{ lb/sec}}$$

$$P_{1\,rel.} \times A_1 = 44.16 \times 336.54 = 14,861.6$$

$$P_{2\,rel.} \times A_2 = 17.72 \times 96.24 = 1705.4$$

145

1. **Through-Flow Position**

$\theta = 15^{\circ}$

$\sin \theta = 0.2588$

$\cos \theta = 0.9659$

$F_x = 14861.6 - 1705.4 \times 0.9659 +$

$\qquad \dfrac{70}{32.17} (348.5 = 1909.0 \times 0.9659)$

$F_x = 14861.6 - 1647.2 + \dfrac{70}{32.17} (348.5 - 1843.9)$

$F_x = 14861.6 - 1647.2 - 3253.9$

$\underline{F_x = 9960.5 \text{ lb}}$

$F_y = 1705.4 \times 0.2588 + \dfrac{70}{32.17} \times 1909.0 \times 0.2588$

$F_y = 441.4 + 1075.0$

$\underline{F_y = 1516.4 \text{ lb}}$

$F = \sqrt{F_x^2 + F_y^2}$

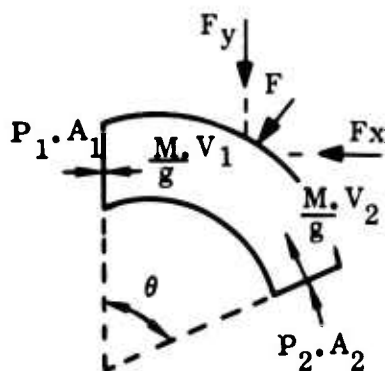$F = \sqrt{(9960.5)^2 + (1516.4)^2} = \sqrt{99211560 + 2299469}$

$F = \sqrt{101511029}$

$\underline{F = 10,075 \text{ lb}}$

2. **Diverted-Flow Position**

$\theta = 75^{\circ}$

$\sin \theta = 0.9659$

$\cos \theta = 0.2588$

146

$$F_x = 14861.6 - 1705.4 \times 0.2588 + \frac{70}{32.17}\ (348.5 - 1909.0 \times 0.2588)$$

$$F_x = 14861.6 - 441.4 + \frac{70}{32.17}\ (348.5 - 494.0)$$

$$F_x = 14861.6 - 441.4 - 316.6$$

$$\underline{F_x = 14103.6\ \text{lb}}$$

$$F_y = 1705.4 \times 0.9659 + \frac{70}{32.17} \times 1909.0 \times 0.9659$$

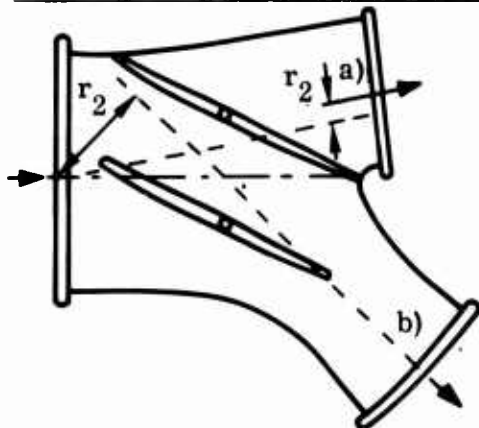$$F_y = 1647.2 + 4012.2$$

$$\underline{F_y = 5659.4\ \text{lb}}$$

$$F = \sqrt{F_x^{\ 2} + F_y^{\ 2}}$$

$$F = \sqrt{(14103.6)^2 + (5659.4)^2} = \sqrt{198911533 + 32028808}$$

$$F = \sqrt{230940341}$$

$$\underline{F = 15,196\ \text{lb}}$$

TORQUE ACTING ON THE DIVERTER VALVE

$$T = \left(p_{2\ \text{rel.}} \times A_2 + \frac{M}{g} \cdot V_2\right) \cdot r_2$$

$$P_{2\ \text{rel.}} \times A_2 = 1705.4\ \text{lb}$$

$$M \cdot V_2/g = 70 \times 1909.0/32.17 = 4153.9\ \text{lb}$$

1. **Through-Flow Position**

$$r_2 = 2.05\ \text{in.}$$

$$T = (1705.4 + 4153.9) \times 2.05 - 5859.3 \times 2.05$$

$$T = 12012\ \text{lb-in.}$$

$$\underline{T = 1001\ \text{ft/lb}}$$

147

2. **Diverter-Flow Position**

r_2 = 22.2 in.

T = (1705.4 + 4153.9) x 22.2 = 5859.3 x 22.2

T = 130,075 lb-in.

T = 10,840 ft/lb

ANNEX C
STUDY OF THE TORQUE CHARACTERISTICS OF THE BUTTERFLY VALVE

To determine the torque characteristics of the butterfly valves (Table XI) being used in the diverter valve system, actual test data of a lenticular butterfly valve of 0.125 thickness/diameter ratio tested at an air pressure ratio of 4/1 has been used on this analysis. The test data are presented in the Memorandum No. M. 304: "Torque and Flow Characteristics of a Butterfly Valve Operating at Pressure Ratios Above the Critical," by A.H. Robinson, of the National Gas Turbine establishment, July 1957.

According to this reference, and assuming that the butterfly valve of the diverter system is equivalent to a valve in a pipe of constant diameter equal to the exit diameter of the former (15 inches) or the initial diameter of the former (20.7 inches), the torque will be given in Figure 58. The nondimensional torque is shown in Figure 59, which is based on Figure 4 of the above-mentioned reference. It is felt that the analogy, although it is only approximately correct, should give sufficient accuracy.

The following conclusions of the above-mentioned reference are included in order to clarify the torque characteristics of the butterfly valve.

The general form of the pressure profile over the upstream face of the valve is shown by the shaded area of Figure 59. Except at low pressure ratios and large valve angles, the flow will break away as shown from the edges of the disc, resulting in a fairly even pressure distribution over the downstream face. The closing torque will thus increase with pressure ratio until the valve begins to choke, whereupon the downstream face pressure distribution will begin to oppose this closing torque. The resultant torque will consequently drop until the shock system is clear of the valve disc, when further increase of pressure ratio will not affect the pressure distribution over the valve.

At low pressure ratios, the closing torque on the valve is highest when the valve is 15° to 20° from the fully open position and rises with pressure ratio reaching a maximum shortly before the valve is passing maximum mass-flow. If the opening angle does not exceed 40°, the torque characteristic remains constant with further increase of pressure ratio. At greater valve openings, however, the torque characteristic falls as the pressure ratio is increased beyond the critical and reaches a minimum value which may be as low as half the maximum value.
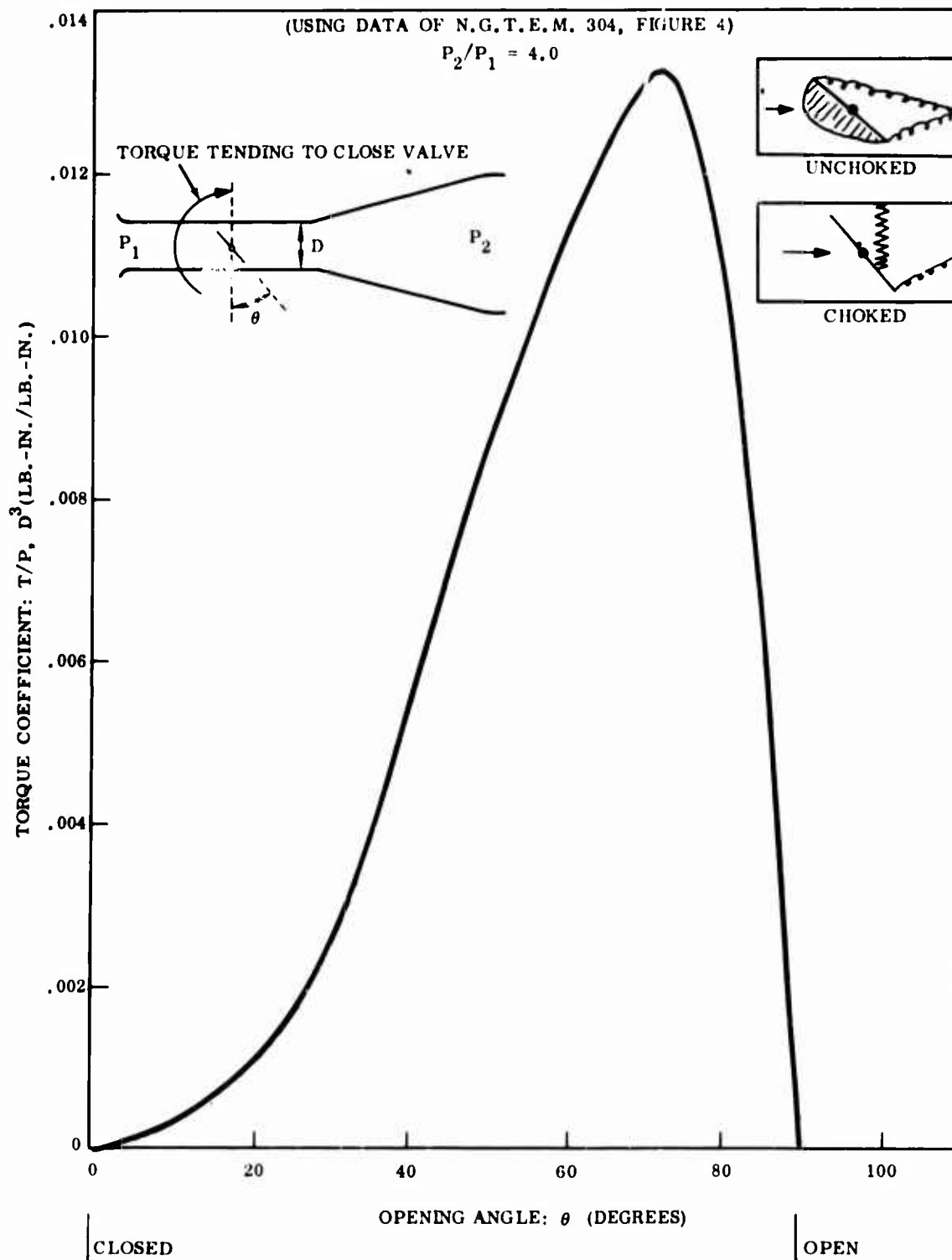
149

Figure 58. Torque Characteristics of a Butterfly Valve in a Pipe.

150

TABLE XI. DIVERTER VALVE TORQUE CHARACTERISTICS OF BUTTERFLY VALVE

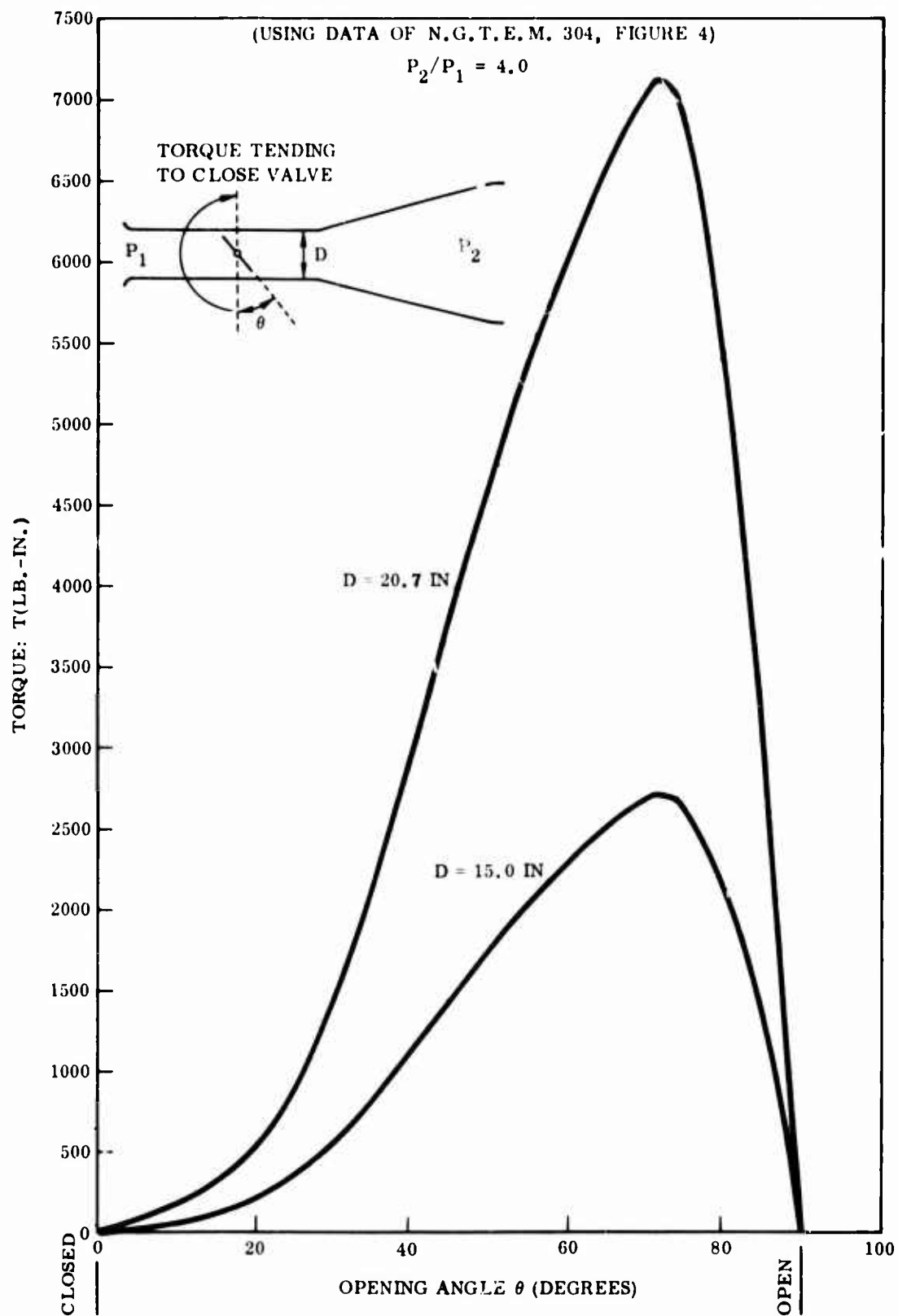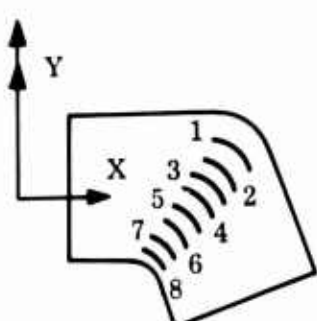| Opening Angle θ (deg)	Pressure Ratio P_2/P_1	Torque Coefficient $P_1 \cdot D^3$	Inlet Pressure P_1 (psia)	Torque/ D^3 (psi)	Pipe Diameter D (in.)		D^3 (cu in.)		Torque (lb in.)	Torque (lb in.)
10	4.0	0.0003	60.00	0.018	15.0	20.7	3375	8870	60.8	159.7
20	4.0	0.0010	60.00	0.060	15.0	20.7	3375	8870	202.5	532.2
30	4.0	0.0026	60.00	0.156	15.0	20.7	3375	8870	526.5	1383.7
40	4.0	0.0054	60.00	0.324	15.0	20.7	3375	8870	1093/5	2873.9
50	4.0	0.0086	60.00	0.516	15.0	20.7	3375	8870	1741.5	4576.9
60	4.0	0.0113	60.00	0.678	15.0	20.7	3375	8870	2288.2	6013.9
70	4.0	0.0132	60.00	0.792	15.0	20.7	3375	8870	2673.0	7025.0
75	4.0	0.0130	60.00	0.780	15.0	20.7	3375	8870	2632.5	6918.6
80	4.0	0.0106	60.00	0.636	15.0	20.7	3375	8870	2146.5	5641.3

Figure 59. Torque Coefficient Characteristics of a Butterfly Valve in a Pipe.

ANNEX D
ANALYSIS OF THE AERODYNAMIC FORCES ACTING ON EACH ONE OF
THE CASCADE VANES AT THE 60-DEGREE BEND

Since the static pressure and velocity at inlet and outlet sections of the channels between vanes have the same valves, the aerodynamic force acting on the cascade vanes is given by

$$\begin{cases} F_x = \dfrac{M}{g} \cdot V (1 - \cos \theta) \\[2mm] F_y = \dfrac{M}{g} \cdot V \cdot \sin \theta \end{cases}$$

$$M = 70 \text{ lb/sec}$$

$$V = 708.0 \text{ ft/sec}$$

$$\theta = 60^{\circ}$$

$$\therefore \sin \theta = 0.8660$$

$$\cos \theta = 0.5000$$

$$F_{x_t} = \frac{70}{32.17} \times 708.0 (1-0.5000) = 770.3$$

$$\underline{F_{x_t} = 770.3 \text{ lb}}$$

$$F_{y_t} = \frac{70}{32.17} \times 708.0 \times 0.8660 = 1334.1$$

$$\underline{F_{y_t} = 1334.1 \text{ lb}}$$

$$F = \sqrt{F_x{}^2 + F_y{}^2}$$

$$F_t = \sqrt{(770.3)^2 + (1334.1)^2} = \sqrt{593362 + 1779823} = \sqrt{2373185}$$

$$\underline{F_t = 1540.5 \text{ lb}} \qquad \text{(total force on the cascade)}$$

The cascade vanes are distributed in such a way that their span is smallest near the inner wall of the bend (where the flow requires more guidance to prevent separation and where the end-wall effect (three-dimensional loss) is more critical due to small aspect ratio). Considering the vane near the outer wall (highest span) as No. 1 and the one near the inner wall as No. 8, the vane resisting the highest
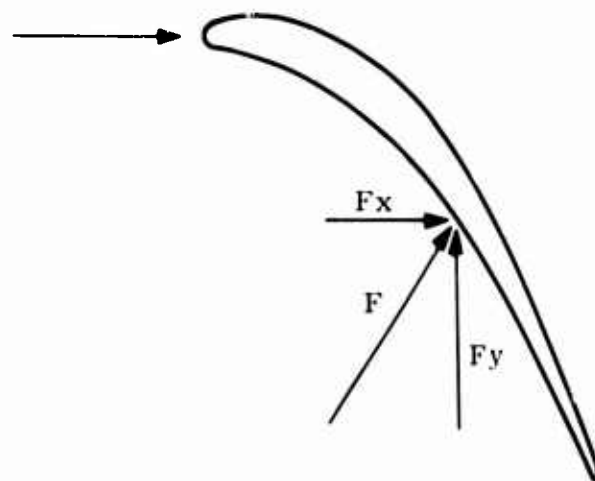
aerodynamic force is Vane No. 3, with a flow between Vanes No. 3 and No. 4 amounting to about 1/6 of the total flow.

$$\therefore F_x = 128.4 \text{ lb}$$

$$F_y = 222.4 \text{ lb}$$

$$F = 256.8 \text{ lb}$$

The height of Vane No. 3 is about 14 inches.

ANNEX E
ANALYSIS OF GAS LEAKAGE THROUGH THE VALVE SEAT
AND SHAFT HUB

Gas leakage through valve seat:

The valve seat has an elliptical shape with a perimeter equivalent to a circumference of 21-inch diameter. Assuming a clearance of 0.001 inch, the leakage area would be

$$A = \pi . D . c$$

$$A = \pi \times 21.0 \times 0.001 = 0.0660$$

$$\underline{A = 0.0660 \text{ sq in.}}$$

$$T = 1860^{\circ}R \quad \therefore \sqrt{T} = 44.2643$$

$$\Delta P = P - P_{amb.} = 60.0 - 15.0 = 45.0 \text{ psi}$$

The maximum amount of flow that can leak through that clearance is given by

$$M_L . \sqrt{T}/A . \Delta P = 0.5228 \quad (M_N = 1.0 : \gamma = 1.33)$$

$$M_L = 0.5228 A . \Delta P/\sqrt{T}$$

$$M_L = 0.5228 \times 0.0660 \times 45.0/44.2643$$

$$\underline{M_L = 0.035 \text{ lb/sec}}$$

$$M_L/M = 0.035/70.0 = 0.0005$$

$$\underline{M_L = 0.05\% M}$$

Assuming a clearance of 0.005 in. (which is very improbable),

$$\underline{M_L = 0.25\% M}$$

Gas leakage through shaft hub:

Assuming that the 1.81-in.-dimater hub has a clearance of 0.001 in., the two leakage areas of each valve would be

$$A = 2\pi \cdot D \cdot c$$

$$A = 2\pi \times 1.81 \times 0.001 = 0.0114$$

$$\underline{A = 0.0114 \text{ sq in.}}$$

considering the two valves.

$$\underline{A = 0.0228 \text{ sq in.}}$$

The maximum amount of flow that can leak through the clearance is given by

$$M_L \cdot \sqrt{T}/A \cdot \Delta P = 0.5228 \qquad (M_N = 1.0 : \gamma = 1.33)$$

$$\sqrt{T} = \sqrt{1860} = 44.2643$$

$$\Delta P = 45.0 \text{ psi}$$

$$M_L = 0.5228 \ A. \ \Delta P/\sqrt{T}$$

$$M_L = 0.5228 \times 0.0228 \times 45.0/44.2643 = 0.0121$$

$$\underline{M_L = 0.012 \text{ lb/sec}}$$

$$M_L/M = 0.012/70.0 = 0.0002$$

$$\underline{\underline{M_L = 0.02\% \ M}}$$

Assuming a clearance of 0.005 in. (which is very improbable)

$$\underline{\underline{M_L = 0.1\% \ M}}$$

DOCUMENT CONTROL DATA - R & D

(Security classification of title, body of abstract and indexing annotation must be entered when the overall report is classified)

1. ORIGINATING ACTIVITY (Corporate author)	2a. REPORT SECURITY CLASSIFICATION
SOLAR DIVISION OF INTERNATIONAL HARVESTER COMPANY	UNCLASSIFIED
	2b. GROUP

3. REPORT TITLE

Preliminary Design of an Advanced Exhaust Gas Diverter

4. DESCRIPTIVE NOTES (Type of report and inclusive dates)

FINAL REPORT

5. AUTHOR(S) (First name, middle initial, last name)

ALBERT MIERLOT

6. REPORT DATE	7a. TOTAL NO. OF PAGES	7b. NO. OF REFS
DECEMBER 1967	167	NONE

8a. CONTRACT OR GRANT NO.	9a. ORIGINATOR'S REPORT NUMBER(S)
DA 44-177-AMC-433(T)	
b. PROJECT NO.	USAAVLABS Technical Report 67-69
c. TASK 1M121401D14415	9b. OTHER REPORT NO(S) (Any other numbers that may be assigned this report)
d.	ER 1856

10. DISTRIBUTION STATEMENT

This document has been approved for public release and sale; its distribution is unlimited.

11. SUPPLEMENTARY NOTES	12. SPONSORING MILITARY ACTIVITY
	U.S. Army Aviation Materiel Laboratories Fort Eustis, Virginia

13. ABSTRACT

The report contains results of a design study program for an advanced device for the diversion of high energy gas generator turbine discharge gases. Numerous concepts of such devices were initiated during the preliminary period. Evaluation of these concepts resulted in the selection of two design approaches for further design studies. One design, a basic butterfly valve, embodies significant improvements over the current type. The second design represents a unique concept which uses a rotating elbow enclosed within a housing to achieve gas flow diversion. An analysis and comparison of the two designs brought about the selection of the butterfly approach for the preparation of a final design and for the preparation of manufacturing drawings. A manufacturing plan describing the processes and methods which would be required to fabricate a prototype version of the butterfly valve is included.

DD FORM **1473** REPLACES DD FORM 1473, 1 JAN 64, WHICH IS OBSOLETE FOR ARMY USE.

14. KEY WORDS	LINK A		LINK B		LINK C	
	ROLE	WT	ROLE	WT	ROLE	WT
Preliminary Design						
Exhaust Gas						
Diverter						
Turbine Discharge Gas						
Gas Flow Diversion						
Butterfly Valve						